

# *CHAPTER-4*

## *BIOAVAILABILITY ENHANCEMENT OF DIACEREIN*

## **CHAPTER 4: BIOAVAILABILITY ENHANCEMENT OF DIACEREIN**

This chapter of the thesis has been aimed to the bioavailability enhancement of poorly water soluble drug Diacerein. This chapter has been divided into two parts which are as following:

**Part-1:** Formulation of Diacerein nanosuspension

**Part-2:** Formulation of Diacerein inclusion complex with cyclodextrins

### **4.1 Materials:**

DAR was obtained as gift sample from Wockhardt Research Centre, Aurangabad, India. Rhein standard was purchased from Sigma-Aldrich, India. Marketed formulation "Dycerin", (Diacerein IP 50 mg, Glenmark Pharmaceuticals Ltd., Mumbai, India) was purchased from local pharmacy.

Yttrium stabilized-Zirconium oxide beads were obtained as gift sample from Lupin Pharmaceuticals Ltd, Pune, India. Poloxamer 188 (Lutrol F68) and Poloxamer 407 (Lutrol F127) were kindly gifted by Dr. Reddy's Laboratories Ltd. Hyderabad, Andhra Pradesh, India. Sodium Lauryl Sulfate (SLS), Polyvinylpyrrolidone Kollidone® 30 (PVP K30), Tween 20 and Tween 80 were purchased from S.D. Fine Chemicals, Mumbai, India. Lactose, sucrose, trehalose and mannitol were purchased from Himedia, Mumbai, India.  $\beta$ -Cyclodextrin ( $\beta$ -CD) and Methyl- $\beta$ -Cyclodextrin (M- $\beta$ -CD) were purchased from Himedia Laboratories Pvt. Ltd., Mumbai. Hydroxy propyl - $\beta$ -Cyclodextrin (HP- $\beta$ -CD) was obtained as a gift sample from Sun Pharma Advance Research Company, Vadodara.  $\gamma$ -Cyclodextrin ( $\gamma$ -CD) was procured as a gift sample from Roquette Pharma, U.S.A.

Acetonitrile (HPLC Grade) and Methanol (HPLC Grade) were procured from Merck Chemicals, Mumbai, India. Dimethylsulfoxide (HPLC grade), Orthophosphoric acid (HPLC Grade), Glacial Acetic Acid (HPLC Grade), Ethyl Acetate (HPLC Grade) and Perchloric acid (HPLC Grade) were purchased from Spectrochem Chemicals (Mumbai, India). Potassium dihydrogen phosphate (AR grade), Sodium dihydrogen phosphate (AR grade), Ammonium acetate (AR grade), HCl (AR grade) and Sodium hydroxide (AR grade) were purchased from S.D. Fine Chemicals, Mumbai, India.

Caco-2 cell lines were purchased from NCCS, Pune, India. Dulbecco's Modified Eagle's medium (DMEM), Fetal Bovine Serum (FBS), sodium pyruvate, sodium bicarbonate, penicillin-streptomycin solution, Trypsin-EDTA solution, Hank's balanced salt solution (HBSS) and phosphate buffered saline (PBS) were purchased from Himedia, Mumbai, India. Lucifer yellow and MTT (3-(4,5-dimethylthiazolyl-2)-2,5-diphenyltetrazolium

bromide) dye were purchased from Sigma Aldrich INDIA, Bangluru, India. 12-well Transwell inserts were purchased from Nunc, Denmark. 96-well plates were purchased from Coster, Corning, USA.

Purified HPLC grade water was obtained by filtering double distilled water through nylon filter paper 0.22  $\mu\text{m}$  pore size and 47 mm diameter (Millipore, Bangalore, India).

#### **4.2 Instruments:**

1. Weighing balance (AX120, Shimadzu, Japan)
2. Bath Sonicator
3. High speed magnetic stirrer (Remi, MS500, Remi equipments Pvt. Ltd., Mumbai, India)
4. Centrifuge (3K 30 Sigma Laboratory Centrifuge, Osterode, Germany)
5. pH meter (LABINDIA Analyticals Instrument Pvt. Ltd., Mumbai, India)
6. Spinix MC-01 Vortex Shaker (Tarsons Products Pvt. Ltd. New Delhi, India)
7. Rotospin Test tube Rotator (Tarsons Products Pvt. Ltd. New Delhi, India)
8. Quartz Double Distillation Unit
9. Dissolution Test Apparatus-Basket type USP (VEEGO Instruments, Mumbai, India)
10. UV-visible Spectrophotometer (UV-1700, Shimadzu, Japan)
11. Spectrofluorimeter (RF-5301, Shimadzu, Japan)
12. High Performance Liquid Chromatography (Shimadzu, Japan)
13. Particle Size Analyzer (Malvern Zetasizer Nano ZS 90, Malvern Instruments, UK)
14. Laser Diffraction Particle Size Analyzer (Malvern Mastersizer-2000, UK)
15. Lyophilizer (Heto Dry Winner, Vaccubrand, Denmark)
16. Differential Scanning Calorimeter (DSC-60-A, Shimadzu, Japan)
17. X-ray Diffractometer (XRD, X-Pert-PRO, PANalytical, Netherland)
18. Bruker ALPHA FTIR Spectrometer (Bruker Optics, Germany)
19. Scanning Electron Microscope (SEM, JSM-6060, JEOL Ltd., Tokoyo, Japan)
20. Transmission Electron Microscope (TEM, PHILIPS, Technai 20, Japan)
21. Micro Plate Multi Detection Instrument (680-XR, Bio-Rad Laboratories, France)

### 4.3 Part-1: Formulation of Diacerein Nanosuspension

#### 4.3.1 Introduction

This part of the project has been aimed to develop NS of DAR using media milling technology and to investigate its effects on oral bioavailability of DAR in developed formulation as compared to plain drug and marketed formulation. Different stabilizers and surfactants including PVP K30, poloxamers (188 and 407), SLS and polysorbates were tried in an effort to develop stable Diacerein nanosuspension (DAR-NS). In this study, factorial design based on response surface method was adopted to optimize formulation parameters for preparation of an efficient DAR-NS. A 3<sup>3</sup> full factorial design was employed to evaluate the combined effect of the selected variables on the particle size of prepared DAR-NS.

The prepared aqueous NS was converted to the solid state using freeze drying technique (Lyophilization) with subsequent addition of cryoprotectant in order to produce a physically stable DAR-NS. Different cryoprotectants used in the study were lactose, sucrose, trehalose and mannitol. The mean particle size (MPS), polydispersity index (PDI) and zeta potential were investigated, prior and post to lyophilization of prepared NS. Saturation solubility and *in vitro* dissolution studies were performed as per the pharmacopoeial protocol. Lyophilized DAR-NS was further characterized for its physical properties by Differential Scanning Calorimetry (DSC), X-ray Diffraction (XRD) Study, Scanning Electron Microscopy (SEM) and Transmission Electron Microscopy (TEM). The chemical stability of DAR-NS was evaluated by assessing the percentage of DAR in the formulations stored at 5°C±3°C (refrigerator) and at room temperature for a period of six months. The physical stability DAR-NS was checked by analysing the particle size and zeta potential of same stored sample. *In vitro* cytotoxicity (MTT Assay) and *in vitro* gastro-intestinal permeability studies of DAR-NS were performed using Caco-2 cell line model. *In vivo* pharmacokinetic study of DAR-NS was performed in rabbits to assess the oral bioavailability of optimized formulations and compared with standard API and marketed formulation (Dycerin) of DAR.

#### 4.3.2 Development of DAR-NS formulation

DAR-NS was prepared by media milling technique<sup>1,2</sup>. Media milling was carried out in a glass vial containing drug, stabilizer, aqueous medium and milling beads. Zirconium oxide beads were used as milling media and water was used as an aqueous medium. NS was prepared by transferring exactly weighed portion of stabilizer/surfactant in a 20 ml

flat bottom A-grade glass vial previously containing 5 ml double distilled water and sonicated to dissolve the content. A weighed quantity of DAR was incorporated to the stabilizer solution and sonicated for 5 minutes to disperse the drug in the medium. Then magnetic stirring bar (22 x 8 mm) and weighed quantity of zirconium oxide beads were added in the dispersion and comminution was carried out on a high speed magnetic stirrer at 2000 rpm for a particular period of time. The outcome of this milling process was nanonization of DAR and thus producing the DAR-NS. In prepared NS, suitable cryoprotectant was added in definite ratio and stirred to solublize. The resulting mixture was lyophilized (Heto Dry Winner, Vaccubrand, Denmark) to get the physically stable solid NS.

A plain drug suspension was also prepared by simply dispersing the DAR and surfactant/stabilizer in double distilled water at the same proportion as was used for the DAR-NS formulation. This DAR suspension was compared with DAR-NS for particle size of drug particles.

#### **4.3.2.1 Preliminary optimization of formulation parameters**

In preliminary optimization, the various parameters influencing the formulation of nanosuspension were selected and optimized. Parameters were optimized by varying one parameter at a time, while keeping other constant, so that the effect of selected parameters could be optimized. The parameters studied were type and ratio of milling beads, volume of milling beads and very importantly type of excipients (different surfactants/polymeric stabilizers were used). Each batch was repeated thrice (n=3) for confirmation of repeatability. The parameters were optimized to minimum mean particle size and PDI.

##### **4.3.2.1.1 Type and ratio of milling beads**

To study the effect of material and size of milling beads on nanosuspension formation, Yttrium stabilized-Zirconium oxide beads and glass beads of two different size ranges (i.e. small and large) were tried. Small size beads were having diameter in the range of 0.4 to 0.5 mm whereas large size beads were in between 1.4 to 1.6 mm. Different ratios of beads varied from 0:100 to 100:0 for small: large size range beads were also tried to evaluate the effect of size of milling media on size reduction of DAR. Concentration of DAR (10% w/v), Poloxamer 407 concentration (1% w/v), volume of milling beads (100% w/v) and milling time at 15 hours were kept constant in this trial.

#### 4.3.2.1.2 Volume of milling beads

Trial batches were prepared with different volumes of small sized zirconium oxide milling beads at 80% w/v, 100% w/v and 120% w/v. DAR concentration (10% w/v), Poloxamer 407 concentration (1% w/v) and milling time at 15 hours were kept constant in this trial.

#### 4.3.2.1.3 Selection of excipients

Trial batches were prepared with different surfactants/polymeric stabilizers (Tween 20, Tween 80, poloxamer 188, poloxamer 407, PVP K30 and SLS). Concentration of all excipients was fixed at 1% w/v. DAR concentration (10% w/v), volume of small sized zirconium oxide beads (100% w/v) and milling time at 15 hours were kept constant in this trial. Key properties of each excipient are summarized in Table 4.1.

**Table 4.1** Relevant properties and chemical formula of excipients tried to prepare a stabilized Nanosuspension.

Name	Category	Average Molecular Weight (g/mol)	Chemical Formula
Tween 20	Non-ionic surfactant	1227.54 g/mol	$C_{58}H_{114}O_{26}$
Tween 80	Non-ionic surfactant	1310 g/mol	$C_{64}H_{124}O_{26}$
Poloxamer 188 (Pluronic® F68)	Non-ionic triblock copolymer	7680-9510 g/mol	$HO(C_2H_4O)_a(C_3H_6O)_b(C_2H_4O)_aH$ (a=80, b=27)
Poloxamer 407 (Pluronic® F127)	Non-ionic triblock copolymer	9840-14600 g/mol	$HO(C_2H_4O)_a(C_3H_6O)_b(C_2H_4O)_aH$ (a=101, b=56)
Polyvinylpyrrolidone (PVP K30)	Non-ionic Polymer	35,000-51,000 g/mol	$(-CH(NCH_2CH_2CH_2CO)CH_2-)_n$
Sodium Lauryl Sulphate (SLS)	Anionic surfactant	288.37 g/mol	$NaC_{12}H_{25}SO_4$

#### 4.3.2.2 Optimization of key parameters by Factorial Design

Various formulation and process variables relating to effectiveness and usefulness should be optimized simultaneously when developing pharmaceutical formulations. In case of traditional method of optimization, combined effects of the independent variables are not considered. The difficulties in optimizing a pharmaceutical formulation are due to the difficulty in understanding the real relationship between dependent and independent responses. Factorial design has often been applied to optimize the formulation variables with basic need of understanding of interaction of independent variables<sup>3</sup>.

#### 4.3.2.2.1 Selection of independent and dependent variables and structure of design

As per the preliminary experiments, stabilizer concentration ( $X_1$ ), drug concentration ( $X_2$ ) and milling time ( $X_3$ ) were selected as independent variables whereas particle size (PS) and saturation solubility (SS) were selected as dependent variables (responses). A three factorial three level  $3^3$  randomized full factorial design was performed for optimization of DAR-NS formulation. In this design, three factors were evaluated, each at 3 levels (i.e. -1, 0, +1), and experimental trials were performed at all 27 possible combinations with three replicates. Replicate experimental runs were carried out in complete randomized manner. Other factors such as type of stabilizer (poloxamer 407), type of milling beads (small sized  $ZrO_2$  beads), volume of milling beads (100%w/v) and dispersing media (double distilled water, 5 ml) were kept constant for all the experiments.

A multilinear stepwise regression analysis was performed using Microsoft Excel software. The full models were used to plot two dimension contour plots for both PS and SS. All the statistical operations were carried out by Design Expert (version 8.0.7.1, statease, Inc. Minneapolis, USA). Table 4.2 and Table 4.3 summarize experimental batches studied, their factor combinations, and the translation of the coded levels to the experimental units employed during the study.

**Table 4.2** Coded translation of formulation variables of  $3^3$  full factorial design for DAR-NS.

Independent Variables		Design Level		
Uncoded	Coded	Low (-1)	Middle (0)	High (+1)
Poloxamer 407 Concentration (%w/v)	$X_1$	1	2	3
DAR Concentration (%w/v)	$X_2$	10	20	30
Milling Time (Hrs.)	$X_3$	8	16	24

**Table 4.3** Layout of factor combinations for DAR-NS using 3<sup>3</sup> full factorial designs (coded values).

Batch No.	X <sub>1</sub>	X <sub>2</sub>	X <sub>3</sub>
B1	-1	-1	-1
B2	-1	-1	0
B3	-1	-1	+1
B4	-1	0	-1
B5	-1	0	0
B6	-1	0	+1
B7	-1	+1	-1
B8	-1	+1	0
B9	-1	+1	+1
B10	0	-1	-1
B11	0	-1	0
B12	0	-1	+1
B13	0	0	-1
B14	0	0	0
B15	0	0	+1
B16	0	+1	-1
B17	0	+1	0
B18	0	+1	+1
B19	+1	-1	-1
B20	+1	-1	0
B21	+1	-1	+1
B22	+1	0	-1
B23	+1	0	0
B24	+1	0	+1
B25	+1	+1	-1
B26	+1	+1	0
B27	+1	+1	+1

#### 4.3.2.2.2 Optimization Data Analysis

Various RSM (Response Surface Methodology) computations for the current optimization study were performed employing Design Expert® software. Polynomial models including interaction and quadratic terms were generated for the response variable using multiple regression analysis (MRA) approach. The dependent response was measured for each trial and then either simple linear equation (Eq. 4.1), or interactive equation (Eq. 4.2) or quadratic model (Eq. 4.3) was fitted by carrying out MRA and F-statistic to identify statistically significant terms.

$$Y = b_0 + b_1X_1 + b_2X_2 + b_3X_3 \tag{Eq. 4.1}$$

$$Y = b_0 + b_1X_1 + b_2X_2 + b_3X_3 + b_{12}X_1X_2 + b_{13}X_1X_3 + b_{23}X_2X_3 + b_{123}X_1X_2X_3 \tag{Eq. 4.2}$$

$$Y = b_0 + b_1X_1 + b_2X_2 + b_3X_3 + b_{12}X_1X_2 + b_{13}X_1X_3 + b_{23}X_2X_3 + b_{11}X_1^2 + b_{22}X_2^2 + b_{33}X_3^2 + b_{123}X_1X_2X_3 \tag{Eq. 4.3}$$

Where  $b_0$  is the intercept representing the arithmetic average of all quantitative outcomes of 27 runs;  $b_1, b_2, b_3$  are linear coefficients;  $b_{12}, b_{13}, b_{23}, b_{123}$  are the interaction coefficients; and  $b_{11}, b_{22}, b_{33}$  are quadratic coefficients computed from the observed experimental values of response  $Y$ ; and  $X_1, X_2$  and  $X_3$  are the coded levels of the independent variable(s). The terms  $X_1X_2, X_1X_3$  and  $X_2X_3$  represents the interaction terms whereas  $X_1^2, X_2^2$  and  $X_3^2$  quadratic terms, respectively. The main effects ( $X_1, X_2$  and  $X_3$ ) represent the average result of changing one factor at a time from its low to high value. The interaction terms ( $X_1X_2X_3$ ) show how the response changes when three factors are simultaneously changed. The polynomial terms ( $X_1^2, X_2^2$  and  $X_3^2$ ) are included to investigate nonlinearity. The polynomial equation was used to draw conclusions after considering the magnitude of coefficients and the mathematical sign it carries, i.e., positive or negative. A positive sign signifies a synergistic effect, whereas a negative sign stands for an antagonistic effect<sup>4-6</sup>.

Statistical validity of the polynomials was established on the basis of ANOVA provision in the Design Expert<sup>®</sup> 8 software. Level of significance was considered at  $p < 0.05$ . The best fitting mathematical model was selected based on the comparisons of several statistical parameters including the standard deviation (SD), multiple correlation coefficient or R-Square ( $R^2$ ), adjusted multiple correlation coefficient (adjusted  $R^2$ ), predicted multiple correlation coefficient (predicted  $R^2$ ) and the predicted residual sum of squares (PRESS), provided by the software. F-value and sequential p-value were also compared to select the best fitted model for analysis of responses. Among them, PRESS indicates how well the model fits the data, and for the chosen model it should be small relative to the other models under consideration<sup>5</sup>. A full model (FM) equation was established after putting the values of regression coefficients of responses PS ( $Y_1$ ) and SS ( $Y_2$ ) in the respective equation for selected polynomial model. Significance of the model was determined by applying analysis of variance (ANOVA) and significance of each coefficient was estimated by Student's 't' test and p-value. Non-significant terms ( $p < 0.0500$ ) were neglected from the FM equation and a reduced model (RM) was generated to facilitate the optimization process. Also, the 3-D response surface graphs and the 2-D contour plots were plotted by keeping least significant independent variable constant and varying other two independent variables, to establish a relationship between dependent and independent variables using Design Expert<sup>®</sup> 8 software. F-statistic was applied on the results of ANOVA of FM and RM to check

whether the non-significant terms can be omitted or not from the FM<sup>7</sup>, using Design Expert<sup>®</sup> 8 and Microsoft Excel 2007. For simultaneous optimization of PS and SS, desirability was calculated using Design Expert<sup>®</sup> 8 software. A check point analysis was performed to confirm the utility of multiple regression analysis and established contour plots in the preparation of DAR-NS. Results of desirability criteria, check point analysis, and normalized error were considered to select the formulation with lowest PS and highest SS.

#### **4.3.2.2.3 Contour Plots**

Contour plots are diagrammatic representation of the values of the responses that help in explaining the relationship between independent and dependent variables. Two dimensional contour plots were established between two independent variables ( $X_1$  vs  $X_2$ ,  $X_1$  vs  $X_3$  and  $X_2$  vs) at fixed level (either -1 or 0 or +1) of third independent variable ( $X_1$ /  $X_2$ /  $X_3$ ) for responses  $Y_1$  (PS) and  $Y_2$  (SS).

#### **4.3.2.2.4 Response Surface Plots**

To understand the main effect and the interaction effects of two variables, response surface plots were used as a function of two factors at a time maintaining all other factors at fixed levels<sup>8,9</sup>. These plots were obtained by calculating the values taken by one factor where the other varies (from -1 to +1 for instance) with constraint of a given response value. The yield values for different levels of variables can also be predicted from the respective response surface plots.

#### **4.3.2.2.5 Check Point Analysis**

A check point analysis was performed to confirm the utility of the established contour plots and reduced polynomial equation in the preparation of NSs. Values of independent variables ( $X_2$  and  $X_3$ ) were taken from three check points on contour plots plotted at fixed levels of -1, 0 and +1 of  $X_1$  and the values of responses  $Y_1$  (PS) and  $Y_2$  (SS) were calculated by substituting the values in the reduced polynomial equation. DAR-NS was prepared experimentally by taking the amounts of the independent variables ( $X_2$  and  $X_3$ ). Each batch was prepared three times and mean values were determined. Difference in the predicted and mean values of experimentally obtained responses  $Y_1$  and  $Y_2$  was compared by using student's 't' test.

#### **4.3.2.2.6 Desirability Criteria**

For simultaneous optimization of responses  $Y_1$  (PS) and  $Y_2$  (SS), desirability function (multi-response optimization technique) was applied and total desirability was

calculated using Design Expert® 8 software. The desirability lies between 0 and 1 and it represents the closeness of a response to its ideal value. The total desirability is defined as a geometric mean of the individual desirability for PS and SS<sup>10,11</sup>.

$$D = \sqrt{d_{PS} \times d_{SS}}$$

Where, D is the total desirability,  $d_{PS}$  and  $d_{SS}$  are individual desirability for PS and SS, respectively. If both the quality characteristics reach their ideal values, the individual desirability is 1 for both. Consequently, the total desirability is also 1. Our optimization criteria included PS of less than 250 nm and maximum SS with minimum concentration of surfactant, high concentration of drug and low stirring time.

#### **4.3.2.2.7 Normalized Error Determination**

The quantitative relationship established by MRA was confirmed by evaluating experimentally prepared DAR-NS. PS and SS predicted from the MRA were compared with those generated from prepared batches of check point analysis using normalized error (NE). The equation of NE is expressed as follows:

$$NE = \sqrt{\sum \left[ \frac{(R_{pred} - R_{obs})}{R_{obs}} \right]^2}$$

where,  $R_{pred}$  and  $R_{obs}$  represents predicted and observed response, respectively.

#### **4.3.2.3 Preparation of optimized DAR-NS**

After studying the effect of independent variables on the responses, the levels of these variables that give the optimum response were determined. Optimization was performed to find out the levels of independent variables ( $X_1$ ,  $X_2$  and  $X_3$ ) that would yield a minimum value of PS and maximum value of SS using Design-Expert 8.0 software. For confirmation, fresh formulations were prepared in triplicate at the optimum levels of independent variables and the resultant DAR-NS were evaluated for responses and compared with the theoretical values.

#### **4.3.2.4 Freeze drying of DAR-NS**

The optimized DAR-NS formulation was freeze dried using lyophilizer (Heto Dry Winner, Vaccubrand, Denmark). Various cryoprotectants (i.e Sucrose, Trehalose dihydrate and Mannitol) at different ratio to the total solid content of NS (i.e. 1:1% w/w, 1:2% w/w, 1:3% w/w and 1:4% w/w) were tried. The selection of type and ratio of cryoprotectant was based on the minimum increment in particle size. 5 ml of each DAR-NS sample with respective concentrations of cryoprotectant was rapidly frozen at -70°C

and lyophilized for 24 hours under vacuum condition.

### **4.3.3 Characterization of DAR-NS**

#### **4.3.3.1 Particle size determination**

The particle size (PS) and polydispersity index (PDI) of prepared DAR-NS were measured using Malvern Zetasizer Nano ZS 90 (Malvern Instruments, Worcestershire, UK), which follows principle of LASER Diffraction (LD) or also called Photon correlation spectroscopy (PCS). Photon correlation spectroscopy is based on the measurement of the Brownian motion of particles. Samples were suitably diluted with double distilled water before measurement, to avoid multiple scattering and to achieve the count rate of 200-400 kbps. Detection was carried out at a scattering angle of 90°; sample temperature was set at 25°C and 12-17 runs of 30 s were performed on each sample. Six replicates of each sample were measured. The average particle size and PDI were observed and standard deviations were calculated.

Particle size of plain DAR suspension was determined using Laser diffraction particle size analyzer (Malvern Mastersizer-2000, UK).

#### **4.3.3.2 Zeta potential**

Typically the electric surface charge is quantified as the so called zeta potential, indicating the physical stability of a colloidal system. The zeta potential is determined by measuring the electrophoretic particle velocity ( $\mu\text{m}/\text{sec}$ ) in an electrical field<sup>12</sup>. Zeta potential distribution was measured using a Malvern Zetasizer Nano ZS 90 (Malvern Instrument, UK). Each sample was suitably diluted with filtered distilled water and placed in a disposable zeta cell. Zeta limits ranged from -200 to +200 mV. The electrophoretic mobility ( $\mu\text{m}/\text{sec}$ ) was converted to zeta potential by in-built software using Helmholtz-Smoluchowski equation. In order to obtain a nanosuspension exhibiting good physical stability (stabilized by electrostatic repulsion), a minimum zeta potential of  $\pm 30$  mV is required. Six replicates of each sample were measured. The mean zeta potential and standard deviation was calculated.

#### **4.3.3.3 Differential Scanning Calorimetry (DSC) Analysis**

The lyophilized DAR-NS, physical mixture, plain drug, poloxamer 407 and trehalose were investigated for their thermal properties and physical state using Differential Scanning Calorimeter (DSC 60-A, Shimadzu, Japan). Accurately weighed samples (4-7 mg) were placed in hermetically sealed aluminium pans and empty pan was used as a reference. Heating scans by heat runs for each sample was set from 30 °C to 300 °C at

10°C min<sup>-1</sup> in a nitrogen atmosphere.

#### **4.3.3.4 X-Ray Diffraction (XRD) Study**

The crystallinity analysis of lyophilized DAR-NS, physical mixture and plain DAR was carried out using X-Ray Diffractometer (X-Pert-PRO, PANalytical, Netherland). The samples were mounted on a sample holder and XRD patterns were recorded in the range of  $3^\circ < 2\theta < 50^\circ$  at the speed of 5° min<sup>-1</sup>.

#### **4.3.3.5 Morphological analysis by TEM and SEM**

Morphological investigations of optimized DAR-NS was carried out by using Transmission Electron Microscopy (TEM). A drop of DAR-NS was placed on a coated carbon grid (300 mesh, 3 mm) and air dried. The grid was then examined immediately under Transmission Electron microscope (Philips, Technai 20, Japan). The electron micrographs were obtained after magnifications. The physical characteristics of the particles observed by TEM were determined using selected area diffraction (SAD) technique. The measurement conditions were  $\lambda = 0.0251 \text{ \AA}$  radiation generated at 200 kV as X-ray source with camera length of 100 cm. The morphology of the standard DAR particles and lyophilized DAR-NS powder was observed under a Scanning Electron Microscope 205 (SEM, JSM-6060, JEOL Ltd. Tokyo, Japan). The samples were mounted directly onto the SEM sample holder using double-sided sticking carbon tape and subjected to conductive platinum coating. Sample images were recorded at the required magnification at the acceleration voltage of 10 kV.

#### **4.3.3.6 Percentage drug content in DAR-NS**

Accurately weighed lyophilized DAR-NS powder (equivalent to 25 mg of DAR) was transferred in a 25 ml volumetric flask and 5 ml DMSO was added. Content was sonicated to dissolve and volume was made up to the mark with diluent. The sample solution was centrifuged at 15,000 rpm for 10 minutes (Sigma centrifuge, Osterode, Germany) and supernatant was filtered with 0.22  $\mu\text{m}$  pore size disposable filter (Millipore India, Bangalore). Filtrate was suitably diluted with diluent to get the sample concentration at 10  $\mu\text{g/ml}$ . Standard solution of DAR (10  $\mu\text{g/ml}$ ) was also prepared and both the solutions were injected into the HPLC system (Shimadzu, Japan). (For instrumentation, chromatographic conditions and method refer Section 3.1.3) Each determination was performed in triplicate, chromatograms were recorded and average % content of DAR in the formulation and standard deviation was calculated.

#### 4.3.3.7 Estimation of saturation solubility

The saturation solubility of standard DAR and DAR-NS formulation were determined by adding excess of material in a 15ml screw capped tube and 10 ml double distilled water was added. The resulting solutions were placed on mechanical shaker for 48 hours at 25°C. After equilibrium was reached, the dispersion was centrifuged at 15,000 rpm for 10 minutes (Sigma centrifuge, Osterode, Germany) to sediment the undissolved drug. Then supernatant was withdrawn and filtered with 0.22 µm pore size disposable filter (Millipore India, Bangalore). The content of dissolved DAR was analyzed by UV spectrophotometer (UV 1700, Shimadzu, Japan) at 257 nm after suitable dilution with methanol. Six replicates of each sample were measured and saturation solubility with SD was calculated.

#### 4.3.3.8 *In vitro* dissolution study

*In vitro* release studies of lyophilized DAR-NS, marketed formulation (Dycerin, Label claim-50mg) and plain DAR were carried out in different dissolution mediums (i.e. Distilled water, Phosphate Buffer pH-6.8, Acetate Buffer pH-4.5 and 0.1N HCl) using USP dissolution apparatus II (paddle method). Dissolution studies were carried out using hard gelatin capsules (Size 0) filled with an accurately weighed quantity of lyophilized DAR-NS (equivalent to 50 mg of DAR). The experiments were performed on 900mL media at 37°C at a rotation speed of 75 rpm. At preselected time intervals, 5 mL samples were withdrawn, filtered immediately and replaced with 5 mL of pre-thermostated fresh dissolution medium. Quantitative determination was performed by UV spectrophotometer at 257 nm. Dissolution tests were performed in triplicate and graph of percent cumulative drug release vs time was plotted. Dissolution profiles were further evaluated on the basis of Dissolution efficiency (DE), Dissolution percentage at 5 min and 60 min (DP<sub>5</sub> and DP<sub>60</sub>), time required to release 50% and 90% of drug (t<sub>50</sub> and t<sub>90</sub>), Mean dissolution time (MDT) and Area under curve (AUC). The DDSolver, an Excel add-in software package, which is designed to analyze data obtained from dissolution experiments was used to calculate different dissolution parameters<sup>13</sup>.

#### 4.3.3.9 Stability Studies

Stability studies of lyophilized DAR-NS was carried out at 5°C±3°C (refrigerator) and at room temperature (RT) for a period of 6 months. Periodically, samples were withdrawn at 1<sup>st</sup>, 2<sup>nd</sup>, 3<sup>rd</sup> and 6<sup>th</sup> month and subjected to examined for chemical and physical stability. Chemical stability was determined by assessing the percentage content of DAR

in stored formulations while physical stability was evaluated by measuring mean particle size (PS), PDI and zeta potential (ZP) of the same.

#### **4.3.4 Cell Line Studies of DAR and its formulations using Caco-2 cell line model**

Human *in vivo* studies are often presumed to serve as the “gold standard” to assess product bioequivalence (BE), permeability and toxicity of solid oral dosage forms. However, when this general assumption is revisited, it appears that *in vitro* studies are sometimes better than *in vivo* in assessing the BE, permeability and toxicity of solid oral dosage forms. Reason for *in vitro* studies to serve as better method are that *in vitro* studies: (a) reduces cost, (b) more directly assess product performance and (c) offer benefits interms of ethical considerations<sup>14</sup>. So at early stage of development, cell cultures are usually preferred to whole animal studies. Prediction of *in vivo* absorption based on *in vitro* methodology may help to reduce the volume of essential clinical investigations. As a tool for *in vitro* studies, cell monolayers have been widely used for for evaluating the cellular uptake and cytotoxicity of drug delivery systems. They present many advantages, including easy to culture and studies can be performed within a controlled environment. In many cases a significant correlation between the studies performed on *in vitro* cell monolayers and *in vivo* human studies has been observed. Hence, *in vitro* studies can be used as predictive tools for estimating the fate and activity of the delivery system in the actual human body<sup>15</sup>. Easy handling, reproducible experimental conditions, and a lack of inter individual variability led to establishment of cell culture models in many labs. Among the numerous techniques available for the prediction of intestinal permeability, the Caco-2 cell line has been extensively used and characterized as a model of the intestinal barrier<sup>16-20</sup>. Caco-2 cell line was established from a moderately well differentiated human colon adenocarcinoma obtained from a 72-year-old patient<sup>21</sup>. Caco-2 cells differentiate spontaneously in culture and exhibit structural and functional differentiation patterns characteristic of mature enterocytes with well established tight junctions and brush border membrane as well as to express several membrane transporters and metabolizing enzymes, allowing the measurement of functional permeability (both passive diffusion and active transport)<sup>22,23</sup>. Consequently, this assay is widely accepted by both the pharmaceutical industry and regulatory agencies since the permeability determined using Caco-2 cells correlates well with oral absorption in humans<sup>19,24,25</sup>.

#### 4.3.4.1 Cell Culture

Caco-2 cells (NCCS, Pune, India) of passages in between 40-45 were used for *in vitro* cytotoxicity study and *in vitro* permeability study experiments. Caco-2 cells were cultured in 25cm<sup>2</sup> tissue culture flasks. Dulbecco's MEM medium with 1.5mM/Litre glutamine, supplemented with 20% FBS, 1mM sodium pyruvate, 1.5gm/Litre of sodium bicarbonate and 1% penicillin-streptomycin solution was used as culture medium. Cells were cultured as a monolayer in an incubator which was set at 37°C in a humidified atmosphere of ~85% relative humidity and ~5% CO<sub>2</sub> and medium was replenished every alternate day<sup>26,27</sup>.

#### 4.3.4.2 *In vitro* Cell Cytotoxicity Studies (MTT Assay)

Measurement of cell viability and proliferation forms the basis for numerous *in vitro* assays of a cell population's response to external factors. An MTT assay was used to assess the cytotoxicity of the free drug as well as the control and the developed formulation. The reduction of tetrazolium salts is now widely accepted as a reliable way to examine cytotoxicity. The yellow tetrazolium MTT (3-(4,5-dimethylthiazolyl-2)-2,5-diphenyltetrazolium bromide) assay is based on conversion of yellow water soluble tetrazolium dye (a tetrazole) to a water insoluble purple formazan by living cells. The MTT dye is reduced by metabolically active cells, in part by the action of dehydrogenase enzymes, to generate reducing equivalents such as NADH and NADPH. The amount of formazan generated is directly proportional to the number of viable cells. The intensity of resulting intracellular water insoluble purple formazan is directly proportional to the number of viable cells and can be quantified by spectrophotometric means (usually between 500-600nm). The MTT Assay measures the cell proliferation rate and conversely, when metabolic events lead to apoptosis or necrosis, the reduction in cell viability. The MTT Reagent yields low background absorbance values in the absence of cells. For each cell type the linear relationship between cell number and signal produced is established, thus allowing an accurate quantification of changes in the rate of cell proliferation<sup>28-36</sup>. Fig. 4.1 showing the conversion of yellow tetrazolium dye to purple formazan in the mitochondria of living cells<sup>35</sup>.

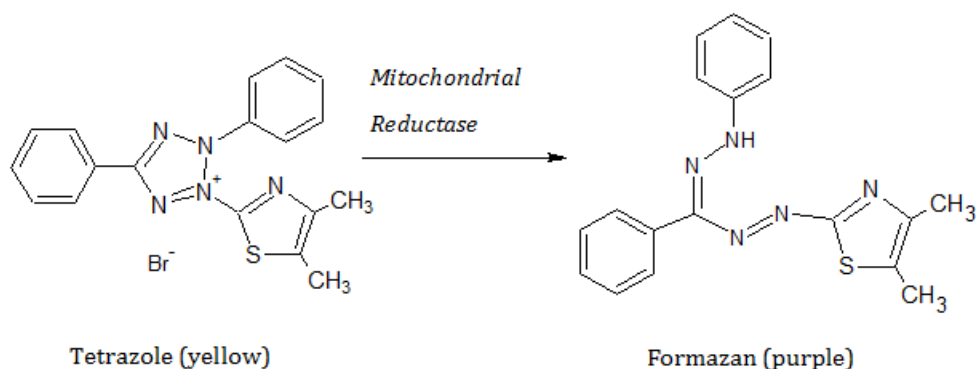


**Fig. 4.1** Reduction of yellow Tetrazole into purple Formazan.

### Experiment

MTT stock solution (1 mg/ml) was prepared by dissolving accurately weighed 10 mg of MTT reagent powder with 10 ml phosphate buffered saline (PBS) in an amber colored 10 ml volumetric flask. The stock solution was stored in dark place at 4°C till the further use.

The *in vitro* cytotoxicity of DAR-NS and plain DAR was evaluated for Caco-2 cells using MTT assay. The cells were cultured in 96-well plates (prelabelled as 4 hour, 24 hour and 48 hour) at a seeding density of  $1.0 \times 10^4$  cells/well for 48 hours. Samples were dissolved in DMSO and different dilutions were made with DMEM culture medium so that the concentration of DMSO did not exceed more than 1% v/v in any diluted sample. Experiments were initiated by replacing the culture medium in each of 96 well of each plate with 100µl of sample solutions (0.1, 1, 10, 100, 250, 500 & 1000 µg/ml) and incubated at 37°C in ~85% relative humidity and ~5% CO<sub>2</sub> environment. After 4 hour of incubation, prelabelled 4 hour-96 well plate was removed from incubator into laminar flow hood area, sample solution was discarded and 100µl of MTT reagent (1 mg/ml) in phosphate buffered saline (PBS) was added aseptically. The plate was again incubated at 37°C in ~5% CO<sub>2</sub> environment for another 4 hours. At the end of incubation period, medium was removed carefully and intracellular formazan was solubilized with 100µl DMSO by agitating cells on orbital shaker for 15 mins. Absorbance was measured at 590 nm with a reference filter of 620 nm using Micro plate multi detection instrument (680-XR, Bio-Rad Laboratories, France). The medium treated cells were used as controls. Same procedure was followed for 24 hour and 48 hour plates.

### Statistical analysis

All calculations, graph preparations and statistical analysis were performed using

Microsoft Excel. Percentage of cell viability was calculated based on the absorbance measured relative to the absorbance of cells exposed to the negative control. To compare the sensitivity of cells to the DAR and its formulation, IC<sub>50</sub> values (concentration of the drug that leads to 50% inhibition in cell proliferation) were calculated.

#### 4.3.4.3 *In vitro* cell permeability assessment of DAR-NS

Drug discovery scientists use many techniques when evaluating the intestinal permeability of drug candidates during the drug selection process<sup>37-44</sup>. The most pervasive preclinical methodologies currently used throughout the industry are: *in vitro* methods, for example, animal tissue-based Ussing chamber or membrane vesicles; cell-based assay systems such as Caco-2 cells and Mardin-Darby canine kidney (MDCK); artificial lipid-based systems such as parallel artificial membrane permeability assay (PAMPA) or immobilized artificial membranes (IAM); *in vivo* methods (whole animal pharmacokinetic studies); *in situ* methods (single-pass perfusion); and *in silico* (computer-aided drug design) methods.

Among these, the Caco-2 cell model has been the most extensively characterized and useful cell model in the field of drug permeability study<sup>18-20,26,27,33,36</sup>. Because the permeation characteristics of drugs across Caco-2 cell monolayers correlates with their human intestinal mucosa permeation characteristics, it has been suggested that Caco-2 cells can be perfectly used to predict the oral absorption of drugs in humans. Caco-2 cells grown on permeable filters (Fig. 4.2) have, therefore, become the “golden standard” for *in vitro* prediction of intestinal drug permeability and absorption<sup>45,46</sup>.

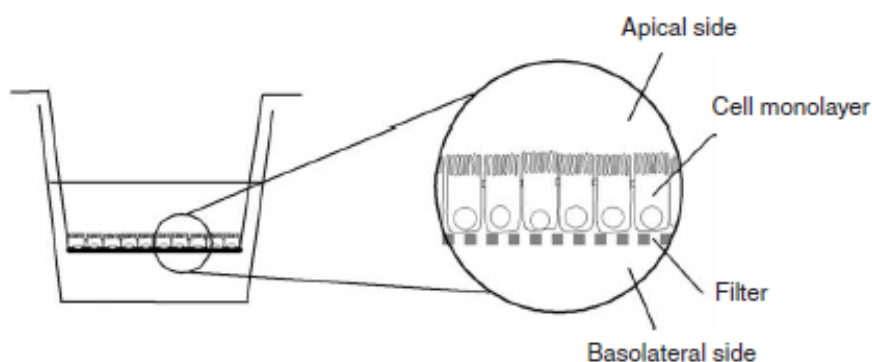


**Fig. 4.2** Diagram of a Caco-2 monolayer grown on a permeable filter.

## Experiment

Caco-2 cell passages in between 40-45, cultured in 12 well cell culture inserts (pore size-0.4µm, diameter-12/18 mm, area-1.13 cm<sup>2</sup>, Product code 12565009, NUNC™, Roskilde, Denmark), were used for *in vitro* permeability assessment of DAR-NS and plain DAR after 21 days post seeding. Prior to the experiment, the inserts were washed twice and equilibrated for 30 mins with pre-warmed transport medium (Hank's balanced salt solution-HBSS containing 25 mM of HEPES, pH-7.4). Accurate quantity of samples were dispersed in transport medium to prepare the solutions having DAR concentration at 250 µg/ml and sonicated. The integrity of the monolayers were checked by monitoring the permeability of paracellular leakage marker (Lucifer Yellow) across the monolayer. Quantification of Lucifer yellow was performed using a Spectrofluorimeter using excitation wavelength at 485 nm and emission wavelength at 530 nm. The cell monolayers were considered tight enough for the transport experiment enough when the apparent permeability coefficient ( $P_{app}$ ) for Lucifer Yellow was less than  $0.5 \times 10^{-6}$  cm/s. All Transport studies were conducted aseptically at 37°C in an atmosphere of ~85% relative humidity and ~5% CO<sub>2</sub>. The 150 µl of transport buffer containing 250 µg/ml test compounds was added to the apical side while the basolateral side of the inserts contained 1.5 ml of transport medium. After the 30, 60, 120, 180, 240 and 480 mins of incubation, aliquot of 100 µl was withdrawn from the receiver chamber and was immediately replenished with an equal volume of pre-warmed transport medium. The samples were stored at -20°C until analyzed. The concentration of the test compounds in the transport medium were analyzed using developed RP-HPLC method as described in Section 3.1.4. The apical to basolateral permeability coefficient ( $P_{app}$  in cm/sec) was calculated according to following equation:

$$P_{app} = \frac{dQ/dt}{A \times C_0 \times 60}$$

where, dQ/dt (flux) is the amount of drug transported across the monolayer from apical to basolateral compartment as a function of time (mg/min), A is the monolayer membrane surface area (cm<sup>2</sup>) and C<sub>0</sub> is the initial concentration of drug on the apical compartment (mg/ml).

### 4.3.5 Pharmacokinetic evaluation of DAR-NS using *in vivo* animal model

Over the last few decades pharmacokinetics has emerged as an integral part of drug and formulation development, especially when identifying a drug's biological properties. By

pharmacokinetics, one means the application of the kinetics to a 'Pharmakon', the Greek word used to specify drugs and poisons. The term thereby implies the time course and fate of drugs in the body<sup>47</sup>.

The most important property of any non-intravenous dosage form, especially oral formulations, intended to treat a systemic condition, is the ability to deliver the active ingredient to the bloodstream in an amount sufficient to cause the desired response. The property of a dosage form has historically been identified as physiologic availability, biologic availability or bioavailability. Bioavailability (denoted as F and generally expressed as a %F) quantifies the proportion of a drug which is absorbed and available to produce systemic effect<sup>48</sup>.

Oral administration is regarded as the preferred route of drug administration, offering numerous benefits including, convenience, ease of compliance, availability to large population, and cost effectiveness. Thus, oral bioavailability plays an important role for successful therapy by this route. Oral bioavailability depends on number of factors like aqueous solubility, dissolution rate, drug permeability, presystemic metabolism, first pass metabolism and susceptibility to efflux mechanisms. Thus, only in vitro evaluation will not be able to predict exact role of nanosizing approach in improving bioavailability. Hence, to find exact improvement in bioavailability, pharmacokinetic studies must be performed. In these studies, pharmacokinetic behaviors of the prepared DAR-NS, plain drug and marketed formulation were investigated to know the effect and advantages of nanosizing on oral bioavailability of DAR.

The plots of drug plasma concentration vs time were plotted for DAR after oral administration of DAR-NS and compared it with plain DAR and marketed formulation (Dycerin). Non compartmental pharmacokinetic analysis was performed<sup>49</sup>. Various pharmacokinetic parameters were calculated using the computer based statistical package PKsolver add-in for microsoft excel<sup>50</sup>. The calculated parameters are as follows<sup>51</sup>:

**Maximum plasma concentration ( $C_{max}$ ):** It was determined directly from the plasma concentration time profiles.

**Time to maximum plasma concentration ( $T_{max}$ ):** It was determined directly from the plasma concentration time profiles.

**Area under the plasma concentration-time curve from time zero to t ( $AUC_{0-t}$ ):** It was calculated by using trapezoidal rule. According to trapezoidal rule, the area under

the curve from time  $t_i$  to time  $t_{i+1}$  is calculated by following equation:

$$AUC_{(0-t)} = \sum_{i=0}^{n-1} \frac{(t_{i+1} - t_i)}{2} (C_i + C_{i+1})$$

Where,  $C_i$  and  $C_{i+1}$  are the concentrations at the times  $t_i$  and  $t_{i+1}$  respectively and  $n$  is the number of data points.

**Elimination rate constant ( $-K_{elimination}$ ):** It was calculated by using following equation:

$$K_{elimination} = -\text{Slope} \times 2.303$$

**Elimination half life ( $t_{1/2}$ ):** The time required to reduce the plasma concentration to one half its initial value is defined as the half-life. It was determined by following equation:

$$t_{1/2} = \frac{0.693}{K_{elimination}}$$

**Area under the plasma concentration-time curve from time zero to infinity ( $AUC_{0-\infty}$ ):**

The trapezoidal rule written in its full form to calculate the AUC from  $t=0$  to  $t=\infty$  is as follows:

$$AUC_{(0-\infty)} = \sum AUC_{(0-t)} + \frac{C_n}{K_{elimination}}$$

Where,  $C_n$  is the drug plasma concentration at time  $t_n$ .

**Area under moment curve (AUMC):** AUMC is the area under the curve of graph of  $C_n \cdot t$  vs  $t$ . It was calculated using following equation:

$$AUMC = \sum_{i=0}^{n-1} \frac{(t_{i+1} - t_i)}{2} (C_i t_i + C_{i+1} t_{i+1}) + \frac{C_{last} \times t_{last}}{K_{elimination}} + \frac{C_{last}}{K_{elimination}^2}$$

**Mean residence time (MRT):** It was determined by following equation:

$$MRT = \frac{AUMC_{cumulative}}{AUC_{cumulative}}$$

**Relative bioavailability (%F):** Relative bioavailability was measured by comparing the AUC of two tested formulation at the same dose levels using the following equation:

$$\text{Relative Bioavailability (\%F)} = \frac{AUC_{test}}{AUC_{reference}} \times 100$$

#### 4.3.5.1 Animals

The pharmacokinetic study was performed in Albino rabbits (New Zealand variety) (weight-1.7 to 2.0 kg, age-09 to 12 months and either sex). The animals were maintained on a standard diet with free access to water and housed into groups of two. Animals were kept at general environment conditions (i.e. 25°C±2°C temperature and 65%±5% RH) under natural light/dark conditions. Animal handling routines were performed according to Good Laboratory Practice. The research protocol of the animal experimentation was approved by the Committee for the Purpose of Control and Supervision of Experiments on Animals (CPCSEA), Ministry of Environment and Forest, Govt. of India, India and Institutional Animal Ethics Committee (IAEC), Pharmacy Department, The M.S. University of Baroda, Vadodara, India.

#### 4.3.5.2 Experimental: Dosing and sampling

Relative bioavailability of DAR-NS was evaluated by comparing the bioavailability of DAR-NS with bioavailabilities of plain DAR and marketed formulation. The dose of the drug in the rabbits was calculated using following formula based on body surface area (BSA)<sup>52</sup>:

$$\text{Rabbit dose } \left( \frac{\text{mg}}{\text{kg}} \right) = \text{HED} \left( \frac{\text{mg}}{\text{kg}} \right) \times \frac{\text{Human } K_m}{\text{Rabbit } K_m}$$

Where, rabbit weight was considered as 1.8 kg, adult human weight was considered as 60 kg and  $K_m$  factor for adult human and rabbit were 37 and 12 respectively<sup>53</sup>.

The maximum dose of DAR that can be given to a adult human in a single day is 100 mg. So according to the above formula, the dose of DAR for rabbits was calculated to be 5.14 mg/kg. In this study, the DAR dose given to the rabbits is 9.25 mg/1.8 kg rabbit weight.

Animals were divided in three treatment groups and each group contained 6 rabbits. The animals were fasted over night prior to the experiment with free access of water. The DAR-NS, plain DAR and marketed formulation (equivalent to 9.25 mg of DAR) were filled in hard gelatin capsule (Capsugel® #size 5) and administered orally. Blood samples (1.0 ml) were collected through marginal ear vein using fresh sterilized disposable needles and syringes in heparinized tubes at 0, 0.5, 1, 1.5, 2, 2.5, 3, 3.5, 4, 4.5, 8, 12, 24 and 48 hours after administration. Collected blood samples were vortexed for 1 min and centrifuged at 20,000 rpm for 10 mins at 4°C (Ultra-centrifuge, 3K 30 Sigma Laboratory Centrifuge, Osterode, Germany). Separated plasma samples were withdrawn and stored

at -20°C until further processing.

#### 4.3.5.3 Instrumental and statistical analysis:

Collected plasma samples were extracted and analyzed by using developed RP-HPLC method (refer Chapter 3, Section 3.1.5). The drug plasma concentration were determined from the calibration curve. Non-compartmental trapezoidal method was employed to calculate the area under the curve (AUC) of plasma concentration as a function of time (t). All data were reported as mean  $\pm$  SD. The statistical significance of the differences between the groups was tested by one-way ANOVA followed by Bonferroni multiple comparison test.

#### 4.3.6 Result and discussion

##### 4.3.6.1 Development of DAR-NS formulation

##### 4.3.6.1.1 Preliminary optimization of formulation parameters

##### 4.3.6.1.1.1 Type and ratio of milling beads

In this trial 100% w/v glass and zirconium beads were tried to study the effect of bead type on size reduction of DAR by media milling. Zirconium beads were found more effective for nanosizing of DAR in comparison to other type of beads. Particle size of  $327 \pm 19$  nm with PDI at  $0.237 \pm 0.021$  was obtained hence zirconium beads were used for further studies. The results of milling with various types of beads are summarized in Table 4.4.

**Table 4.4** Effect of beads type on MPS and PDI of DAR-NS.

Bead type	MPS $\pm$ SD* (nm)	PDI $\pm$ SD*
Small glass beads	612 $\pm$ 35	0.368 $\pm$ 0.029
Large glass beads	793 $\pm$ 27	0.396 $\pm$ 0.033
<b>Small zirconium beads</b>	<b>327<math>\pm</math>19</b>	<b>0.237<math>\pm</math>0.021</b>
Large zirconium beads	575 $\pm$ 31	0.339 $\pm$ 0.037

\* Data are shown as Mean $\pm$ SD, n=3.

Different ratios of small: large zirconium beads varied from 0:100 to 100:0 were also applied, to study the effect of size of milling media on size reduction of DAR. Volume of beads was maintained at 100 %w/v. When 100% small size beads were used, smaller particle size ( $316 \pm 15$ nm) was observed while increase in percentage of large size beads resulted in higher particle size of DAR. When only large size beads were used, maximum mean particle size ( $582 \pm 29$ nm) was observed. On the basis of observations only small size zirconium beads were selected as milling media. Results are indicated in Table 4.5.

**Table 4.5** Effect of ratio of beads on MPS and PDI of DAR-NS.

Ratio of beads (small : large)	MPS±SD* (nm)	PDI±SD*
0:100	582±29	0.348±0.027
25:75	527±22	0.314±0.025
50:50	456±24	0.272±0.017
75:25	389±18	0.247±0.020
<b>100:0</b>	<b>316±15</b>	<b>0.226±0.019</b>

\* Data are shown as Mean±SD, n=3.

Concentration of DAR (10% w/v), Poloxamer 407 concentration (1% w/v), volume of milling beads (100% w/v) and milling time at 15 hours were kept constant in these trials.

#### 4.3.6.1.1.2 Volume of milling beads

It is an important factor which affects the size reduction of drug in media milling. Optimum volume of milling beads are required for maintaining stirring efficiency. Small size zirconium beads at 100 %w/v gave maximum size reduction and optimum stirring hence this concentration of beads was choosed for further studies. DAR concentration (10% w/v), Poloxamer 407 concentration (1% w/v) and milling time at 15 hours were kept constant in this trial. Observations are presented in Table 4.6.

**Table 4.6** Effect of volume of milling media on MPS and PDI of DAR-NS.

Volume of beads (% w/v)	MPS±SD* (nm)	PDI±SD*
80	412±26	0.279±0.024
<b>100</b>	<b>318±13</b>	<b>0.231±0.012</b>
120	366±19	0.246±0.016

\* Data are shown as Mean±SD, n=3.

#### 4.3.6.1.1.3 Selection of excipients

During the course of optimization, the type of stabilizer was chosen between Tween 20, Tween 80, poloxamer 188, poloxamer 407, PVP K30 and SLS. Concentration of all excipients was fixed at 1% w/v. DAR concentration (10% w/v), volume of small sized zirconium oxide beads (100% w/v) and milling time at 15 hours were kept constant in this trial. Milling was carried out at room temperature. Results of preliminary experiment for selection of excipients are shown in Table 4.7 and Fig. 4.3.

**Table 4.7** Effect of type of stabilizer on MPS and PDI of DAR-NS.

Stabilizer	MPS±SD* (nm)	PDI±SD*
Tween 20	508±25	0.298±0.037
Tween 80	493±16	0.281±0.013
Poloxamer 188	379±19	0.254±0.017
<b>Poloxamer 407</b>	<b>321±11</b>	<b>0.220±0.013</b>
PVP K30	422±24	0.277±0.025
SLS	756±23	0.449±0.044

\* Data are shown as Mean±SD, n=3.

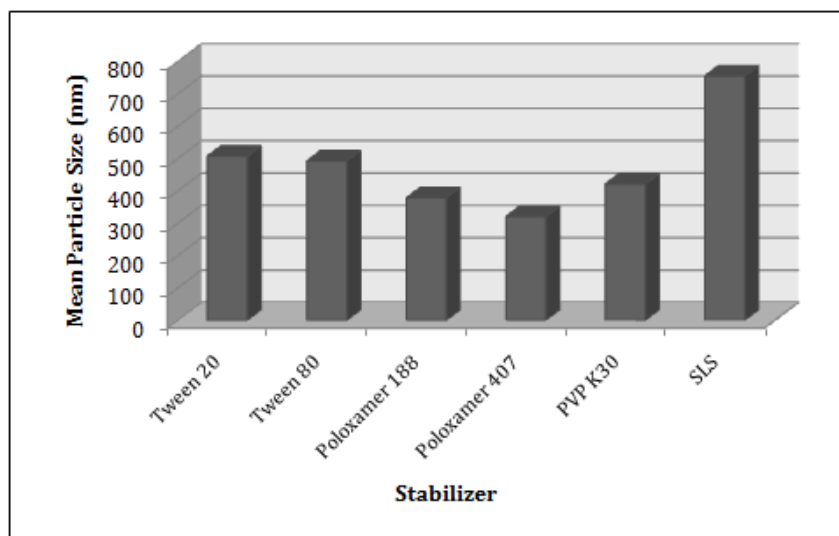


**Fig. 4.3** Graphical representation of stabilizer's effect on mean particle size of DAR-NS.

It was noticed that both the poloxamers contributed efficiently in preparation of NSs with narrow range of particle size and low PDI. Poloxamers are amphiphilic nonionic block polymers consisting of a central polyoxypropylene molecule, which is flanked on both sides by two hydrophilic chains of poly(oxyethylene)<sup>54,55</sup>. Poloxamers have been shown to be quite successful in regard to nanoparticle stabilization<sup>56</sup>. They adsorb strongly onto the surface of hydrophobic nanoparticles via their hydrophobic poly(oxypropylene) centre block<sup>56</sup>. This mode of adsorption leaves the hydrophilic polyoxyethylene side chains in a mobile state because they extend outwards from the particle surface. These side chains provide stability to the particle suspension by a repulsion effect through a steric mechanism of stabilization<sup>57,58</sup>.

Results showed that all the mean particle size in NS stabilized by poloxamer 407 (321±11nm) was significantly smaller than those stabilized by other excipients. Therefore, poloxamer 407 was selected as a stabilizer for further optimization. In this study, poloxamer 407 provided efficient steric stabilization by forming adsorption layers on drug nanoparticles. An important factor of poloxamer 407 was that it formed a

substantial mechanical and thermodynamic barrier at the interface that retards the approach and coalescence of individual particles. The molecular weight of poloxamer 407 is more than poloxamer 188. The molecular weight of a polymer influences the thermodynamic driving force of physical adsorption<sup>59</sup>. Differences in adsorption strength and the thickness of adsorption layers can result from different molecular weights. In particular, polymers of higher molecular weights have less entropy loss related to their freedom of motion, which results in a higher affinity to the drug surface (stronger adsorption and slower desorption)<sup>59</sup>. Therefore, according to the thermodynamic prediction, polymers of higher molecular weights should provide better stabilization.

From this study, it was found that poloxamer 407 gave the lower PDI value ( $0.220 \pm 0.013$ ) compared with the other stabilizers. As per the literature, lower the PDI value, lower will be Ostwald ripening. A PDI value in between 0.1-0.3 indicates a narrow particle size distribution whereas a PDI value greater than 0.3 indicates a very broad size distribution<sup>60,61</sup>.

It could be concluded that the type of stabilizer employed for preparation of NS has significant effect on the particle size and polydispersity value of NS and appeared to be the main reason for efficient formation of nanoparticles and stabilization of the nanosuspension.

#### **4.3.6.1.2 Optimization of key process parameters by Factorial Design**

From the initial studies, various basic process variables (i.e. type and ratio of milling beads, volume of milling beads, selection of excipient) essential for preparation of DAR-NS was optimized and fixed. Other important parameters (independent variables) such as stabilizer concentration ( $X_1$ ), drug concentration ( $X_2$ ) and milling time ( $X_3$ ) were optimized by  $3^3$  factorial design using Design Expert<sup>®</sup> 8 software. Following formulation factors were kept constant during factorial design experiment to study the effect of independent variables on mean particle size of DAR-NS and to avoid design complexity.

Volume of dispersing media (i.e. water)	: 5 ml
Magnetic stirring bar (length × diameter)	: 22 mm × 8 mm
Stirring speed	: 2000 rpm
Type of milling media	: Yttrium stabilized Zirconium oxide beads
Size of milling media	: Small sized (0.4 mm to 0.5 mm diameter)
Volume of milling media	: 100 %w/v (i.e. 5 gm)

Type of stabilizer : Poloxamer 407

By using three factorial three level  $3^3$  randomized full factorial design, 27 possible batches of DAR-NS were prepared with three replicates by media milling technique varying three independent variables, stabilizer concentration ( $X_1$ ), drug concentration ( $X_2$ ) and milling time ( $X_3$ ). The coded values of independent variables ( $X_1$ ,  $X_2$  and  $X_3$ ) and observed, predicted and residual values of both the dependent variables PS ( $Y_1$ ) and SS ( $Y_2$ ) for the 27 combinations are enlisted in Table 4.8. The values of responses for 27 batches showed a wide variation from 185.6 nm to 761.6 nm and 124.5  $\mu\text{g/ml}$  to 545.9  $\mu\text{g/ml}$  for  $Y_1$  and  $Y_2$ , respectively. The ratio of maximum to minimum observed values for  $Y_1$  and  $Y_2$  was 4.10 and 4.38, respectively which are less than 10; therefore any type of transformation was not applied to the obtained values.

Various statistical standards including SD, R-Squared values, predicted residual sum of square (PRESS), F-value and sequential p-value were compared to select the best fitted model for analysis of responses. The model with low SD, higher R-Square value, lower PRESS value, higher F-value and p-values (Prob>F) less than 0.05 was opted for further optimization. The details of above said statistical parameters are summarized in Table 4.9. which clearly suggested the quadratic model for analysis of dependent variables, PS and SS. In quadratic model, the predicted R-Square 0.9502 and 0.9710 are in reasonable agreement with the adjusted R-Square of 0.8123 and 0.8957 for PS and SS, respectively. The higher  $R^2$  values indicate an outstanding relationship among the selected independent variables. In brief, the preferred regression model proved its excellent competency when compared to other models.

**Table 4.8** Combinations of independent variables ( $X_1$ ,  $X_2$  and  $X_3$ ) and observed, predicted and residual values of responses  $Y_1$  and  $Y_2$  as per  $3^3$  full factorial design for formulation of DAR-NS.

Batch No.	Independent Variables (Coded)			Dependent Variables (Responses)					
				Observed Values		Predicted Values		Residual Values	
	$X_1$	$X_2$	$X_3$	$Y_1^*$	$Y_2^*$	$Y_1$	$Y_2$	$Y_1$	$Y_2$
B1	-1	-1	-1	579.3	170.9	572.9	140.0	6.4	30.9
B2	-1	-1	0	487.6	205.7	462.6	226.9	25.0	-21.2
B3	-1	-1	+1	451.5	221.0	452.8	226.5	-1.3	-5.5
B4	-1	0	-1	498.9	201.1	555.1	197.5	-56.2	3.6
B5	-1	0	0	419.4	240.2	430.8	277.8	-11.4	-37.6
B6	-1	0	+1	393.1	248.7	407.1	270.8	-14.0	-22.1
B7	-1	+1	-1	761.6	124.5	737.2	94.2	24.4	30.4
B8	-1	+1	0	632.8	160.6	598.8	167.8	34.0	-7.3
B9	-1	+1	+1	554.2	183.0	561.0	154.2	-6.8	28.7
B10	0	-1	-1	368.4	268.4	349.9	298.2	18.5	-29.8
B11	0	-1	0	216.5	468.3	227.1	437.3	-10.6	31.0
B12	0	-1	+1	199.4	515.4	204.9	489.1	-5.5	22.6
B13	0	0	-1	338.8	295.2	320.3	341.3	18.5	-46.1
B14	0	0	0	202.9	511.7	196.2	454.3	6.7	48.0
B15	0	0	+1	185.6	545.9	172.6	480.1	13.0	45.8
B16	0	+1	-1	472.3	210.1	490.5	223.5	-18.2	-13.4
B17	0	+1	0	337.7	282.9	365.0	310.5	-27.3	-27.6
B18	0	+1	+1	344.8	279.8	340.0	310.3	4.8	-30.4
B19	+1	-1	-1	357.6	283.3	373.8	270.7	-16.2	12.6
B20	+1	-1	0	219.5	462.6	238.6	461.9	-19.1	0.6
B21	+1	-1	+1	206.9	487.7	204.0	565.9	2.9	-41.3
B22	+1	0	-1	359.2	280.0	332.4	299.3	26.8	-9.2
B23	+1	0	0	209.8	482.5	208.5	445.1	1.3	17.4
B24	+1	0	+1	200.3	503.9	185.0	503.6	15.3	0.2
B25	+1	+1	-1	486.7	208.2	490.7	167.0	-4.0	21.1
B26	+1	+1	0	379.5	264.0	378.0	267.4	1.5	-3.5
B27	+1	+1	+1	357.4	282.5	365.8	280.5	-8.4	2.0

$X_1$ : Stabilizer concentration (%w/v),  $X_2$ : Drug concentration (%w/v),  $X_3$ : Milling time (Hours),  $Y_1$ : Particle size (nm) and  $Y_2$ : Saturation solubility (mcg/ml)

\*mean of three replicates, n=3.

**Table 4.9** Fit summary statistics of responses  $Y_1$  and  $Y_2$  as per  $3^3$  full factorial design for formulation of DAR-NS.

Statistical Parameters	Source Model					
	Linear		2FI		Quadratic	
	$Y_1$	$Y_2$	$Y_1$	$Y_2$	$Y_1$	$Y_2$
<b>SD</b>	87.86	86.38	94.21	84.85	25.50	42.29
<b>R-Square</b>	0.6959	0.6149	0.6959	0.6769	0.9811	0.9318
<b>Adjusted R-Square</b>	0.6562	0.5647	0.6047	0.5800	0.9710	0.8957
<b>Predicted R-Square</b>	0.5891	0.4908	0.3697	0.3966	0.9502	0.8123
<b>PRESS</b>	239900	226900	368000	268900	29079	83661
<b>F-value</b>	17.54	12.24	7.63	1.28	85.36	21.17
<b>p-Value Prob&gt;F</b>	<0.05	<0.05	<0.05	<0.05	<0.05	<0.05

A mathematical relationship was established in the form of a polynomial equation (full model) by putting values of regression coefficients (generated by Design Expert® 8) for measured responses PS ( $Y_1$ ) and SS ( $Y_2$ ), separately in Eq. 4.3. Full model (FM) equations for  $Y_1$  and  $Y_2$  are shown below as Eq. 4.4 and 4.5, respectively.

FM for PS.

$$Y_1 = 196.18 - 11.19X_1 + 68.91X_2 - 73.87X_3 + 0.78X_1X_2 + 0.18X_1X_3 - 1.39X_2X_3 + 123.47X_1^2 + 99.87X_2^2 + 50.26X_3^2 + 12.62X_1X_2X_3 \quad \text{Eq. 4.4}$$

FM for SS.

$$Y_2 = 463.69 + 83.27X_1 - 60.43X_2 + 68.11X_3 - 29.12X_1X_2 + 28.86X_1X_3 - 24.91X_2X_3 - 96.95X_1^2 - 85.53X_2^2 - 47.07X_3^2 - 17.30X_1X_2X_3 \quad \text{Eq. 4.5}$$

The above equations represent the quantitative effect of independent variables ( $X_1$ ,  $X_2$  and  $X_3$ ) and their interactions on the responses ( $Y_1$  and  $Y_2$ ). A positive sign indicates a synergistic effect, while a negative sign represents an antagonistic effect. For estimation of significance of the model, the ANOVA was applied. The results of ANOVA for  $Y_1$  and  $Y_2$  were summarized in Table 4.10. Using 5% significance level, a model is considered significant if the p-value (significance probability value) is less than 0.0500. From the p-value presented in Table 4.10, it can be concluded that for responses  $Y_1$  and  $Y_2$ , quadratic models were significant. As shown in the Table 4.10, the model F-values of 93.94 and 23.86 for PS and SS, respectively, also implies that the selected models were significant.

The significance of each coefficient of Eq. 4.4 and Eq. 4.5 were determined by Student's

't' test and p-value, which are enlisted in Table 4.10. The larger the magnitude of 't' value and smaller the p-value, the more significant is the corresponding coefficient<sup>62,63</sup>. Small values of the coefficients of the terms  $X_1X_2$ ,  $X_1X_3$ ,  $X_2X_3$  and  $X_1X_2X_3$  in Eq. 4.4 and  $X_2X_3$  and  $X_1X_2X_3$  in Eq. 4.5 for PS and SS respectively implied that all these terms were least contributing in the preparation of the DAR-NS. The small values of coefficients were non-significant ( $p < 0.0500$ ) and hence neglected from the FM. Reduced model (RM) polynomial equations (Eq. 4.6 and Eq. 4.7, for PS and SS respectively) were obtained following MRA of PS and SS. Based on their p-value it implied that the quadratic main effects of  $X_1$ ,  $X_2$  and  $X_3$  were significant for both PS and SS.

RM equations for PS and SS are written below as Eq. 4.6 and Eq. 4.7, respectively.

RM for PS.

$$Y_1 = 196.18 - 11.19X_1 + 68.91X_2 - 73.87X_3 + 123.47X_1^2 + 99.87X_2^2 + 50.26X_3^2 \quad \text{Eq. 4.6}$$

RM for SS.

$$Y = 463.69 + 83.27X_1 - 60.43X_2 + 68.11X_3 - 29.12X_1X_2 + 28.86X_1X_3 - 96.95X_1^2 - 85.53X_2^2 - 47.07X_3^2 \quad \text{Eq. 4.7}$$

**Table 4.10** Results of model and coefficient estimation by ANOVA and Student's 't' test for responses  $Y_1$  (PS) and  $Y_2$  (SS) of DAR-NS.

Source	F-value		Coefficients		t-stat		p-value Prob>F	
	$Y_1$	$Y_2$	$Y_1$	$Y_2$	$Y_1$	$Y_2$	$Y_1$	$Y_2$
<b>Model</b>	93.94	23.86	-	-	-	-	<0.0001	<0.0001
<b>Intercept</b>	-	-	196.18	463.69	15.5870	21.7673	<0.0001	<0.0001
<b><math>X_1</math></b>	364.23	71.31	-111.19	83.27	-19.0849	8.4445	<0.0001	<0.0001
<b><math>X_2</math></b>	139.87	37.55	68.91	-60.43	11.8266	-6.1280	<0.0001	<0.0001
<b><math>X_3</math></b>	160.74	47.71	-73.87	68.11	-12.6781	6.9072	<0.0001	<0.0001
<b><math>X_1X_2</math></b>	0.012	5.81	0.78	-29.12	0.1098	-2.4112	0.9140	0.0283
<b><math>X_1X_3</math></b>	0.0001	5.71	0.17	28.86	0.0245	2.3893	0.9807	0.0295
<b><math>X_2X_3</math></b>	0.038	4.25	-1.39	-24.91	-0.1950	-2.0627	0.8478	0.0558
<b><math>X_1^2</math></b>	149.70	32.22	123.47	-96.95	12.2353	-5.6765	<0.0001	<0.0001
<b><math>X_2^2</math></b>	97.94	25.08	99.87	-85.53	9.8967	-5.0077	<0.0001	<0.0001
<b><math>X_3^2</math></b>	24.80	7.60	50.26	-47.07	4.9800	-2.7559	<0.0001	0.0141
<b><math>X_1X_2X_3</math></b>	2.09	1.37	12.63	-17.30	1.4446	-1.1694	0.1679	0.2594

The results of ANOVA of the FM and RM second order polynomial equation of PS and SS are tabulated in Table 4.11. Since the F-calculated value was less than the F-tabulated value for both PS and SS, it was concluded that the neglected terms did not significantly contribute in the prediction of PS and SS<sup>7</sup>. Hence, F-statistics of the results of ANOVA of full and reduced model justified the omission of non-significant terms of Eq. 4.4 and Eq.

4.5.

When the coefficients of three independent variables ( $X_1, X_2$  and  $X_3$ ) in Eq. 4.6 and Eq. 4.7 were compared, the value for the variable  $X_1$  ( $b_1= 111.19$  for PS and  $b_1=83.27$  for SS) was found to be maximum and hence  $X_1$  was considered to be a major contributing variable affecting the both PS and SS of the DAR-NS. The Fisher F test with a very low probability value ( $\text{Prob}>F \Rightarrow <0.0001$ ) for both the responses, PS and SS demonstrated a very high significance for the regression model. The goodness of fit of the selected model was checked by the squared correlation coefficient ( $R^2$ ). In this case, the values of the correlation coefficients ( $R^2=0.9833$  and  $0.9372$  for FM &  $0.9810$  and  $0.9151$  for RM, for PS and SS respectively) indicated that at least 91% of the total variation were explained by the model. High  $R^2$  values of the FM as compared to RM were due to large number of factors were included. More the number of factors more is the  $R^2$  value<sup>64</sup>. The values of adjusted  $R^2$  ( $0.9728$  and  $0.8979$  for FM &  $0.9753$  and  $0.8773$  for RM, for PS and SS respectively) were similar for FM and RM of both PS and SS, indicating the suitability of reducing the model. Moreover, the high values of the correlation coefficients ( $R=0.9916$  and  $0.9601$  for FM &  $0.9905$  and  $0.9566$  for RM, for PS and SS respectively) signifies an tremendous correlation between the independent variables<sup>65</sup>. All the above considerations indicated an outstanding competence of the developed regression model<sup>62,63,65</sup>.

**Table 4.11** ANOVA of full and reduced models for PS and SS of DAR-NS.

Source	Model	df	SS	MSS	F	R	R <sup>2</sup>	Adj. R <sup>2</sup>
<b>For Y<sub>1</sub></b>								
<b>Regression</b>	FM	10	574011.29	57401.12	93.94	0.9916	0.9833	0.9728
	RM	6	572705.19	95450.86	172.26	0.9905	0.9810	0.9753
<b>Residual</b>	FM	16	9776.39	611.02				
	RM	20	11082.49	554.12				
<b>For Y<sub>2</sub></b>								
<b>Regression</b>	FM	10	417641.48	41764.15	23.86	0.9601	0.9372	0.8979
	RM	8	407800.75	50795.09	24.24	0.9566	0.9151	0.8773
<b>Residual</b>	FM	16	28004.59	1750.29				
	RM	18	37845.31	2102.52				

Where; df: degree of freedom, SS: sum of square, MSS: mean sum of square, R: correlation coefficient, R<sup>2</sup>: squared correlation coefficient and Adj. R<sup>2</sup>: adjusted correlation coefficient.

For Y<sub>1</sub>,

$$SS(RM)_{Y_1} - SS(FM)_{Y_1} = 11082.49 - 9776.39 = 1306.10$$

Number of parameters omitted=04

MSS of error (FM)=611.02

$$F\text{-calculated } (Y_1) = [SS(RM)_{Y_1} - SS(FM)_{Y_1}] / \text{No. of parameters omitted} / \text{MSS of error (FM)}$$

$$= (1306.10)/(04)/(611.02)$$

$$= 0.5344$$

F-tabulated ( $Y_1$ )= 3.0069 ( $\alpha=0.05$ ,  $v_1=4$  and  $v_2=16$ )

For  $Y_2$ ,

$$SSE2_{Y_2} - SSE1_{Y_2} = 37845.31 - 28004.59 = 9840.72$$

Number of parameters omitted=02

MSS of error (FM)=1750.29

$$F\text{-calculated } (Y_2) = (SSE2_{Y_2} - SSE1_{Y_2}) / \text{No. of parameters omitted} / \text{MSS of error (FM)}$$

$$= (9840.72)/(02)/(1750.29)$$

$$= 2.8111$$

F-tabulated ( $Y_2$ )= 3.6337 ( $\alpha=0.05$ ,  $v_1=2$  and  $v_2=16$ )

#### 4.3.6.1.2.1 Contour Plots

Two-dimensional contour plots were established between  $X_1$  vs  $X_2$ ,  $X_1$  vs  $X_3$  and  $X_2$  vs  $X_3$  at fixed level (0) of third variable for PS (Fig. 4.4) and SS (Fig. 4.5), which are very useful to study the interaction effects of two factors on the responses at one time. Plots showed that PS and SS were greatly dependent on stabilizer concentration ( $X_1$ ), drug concentration ( $X_2$ ) and milling time ( $X_3$ ). Fig. 4.4(a) exhibited that PS was found maximum with highest level of  $X_2$  and lowest level of  $X_1$  whereas PS was dropped with increase in  $X_1$  and decrease in  $X_2$ . As per the Fig. 4.4(b), when  $X_1$  and  $X_3$  were at their maximum levels, PS was found to be minimum. However, the contour of  $X_2$  and  $X_3$  (Fig. 4.4(c)) showed higher PS with increase in  $X_2$  and lower PS with increase in  $X_3$ . Fig. Fig. 4.4(c), also described that maximum level of  $X_3$  and middle level of  $X_2$ , gave the desired PS of about 200 nm. Highest SS was observed at 0.00 to +1 level of  $X_1$  and -1 to 0.00 level of  $X_2$  (Fig. 4.5(a)). Fig. 4.5(b) illustrated the pattern of increase in SS with increase in  $X_1$  and  $X_3$ . Whereas Fig. 4.5(c) depicted that lowest SS was found at maximum  $X_2$  and minimum  $X_3$  and increased with increase in  $X_3$  and decrease in  $X_2$ . It was concluded from the expression of contours that low concentration of drug with high stabilizer concentration with high milling time was required for lowest PS and highest SS in preparation of optimized DAR-NS.

#### 4.3.6.1.2.2 Response Surface Plots

Response surface plots which are very helpful in learning about both the main and interaction effects of the independent variables at any given time, were plotted between  $X_1$  vs  $X_2$ ,  $X_1$  vs  $X_3$  and  $X_2$  vs  $X_3$  at fixed level (0) of third variable as shown in Fig. 4.6 and Fig. 4.7 for each PS and SS respectively. By analysing the Fig. 4.6 and 4.7, we can say, that all the three independent variables ( $X_1$ -surfactant concentration,  $X_2$ -drug

concentration and  $X_3$ -milling time) showed their significant effect on PS and SS of the nanosuspension when varied alone as well as simultaneous. Fig. 4.6(a) showed the optimum decrease in PS when  $X_1$  was increased from -1 to +1 and  $X_2$  was decreased from +1 to -1. Fig. 4.6(b) illustrated the desirable decrease in PS with simultaneous increase in  $X_2$  and  $X_3$  from -1 to +1. Response surface plot between  $X_2$  and  $X_3$  (Fig. 4.6(c)) explained that PS was decreased with decrease in  $X_2$  from +1 to 0 and again increased with further decrease in  $X_2$  from 0 to -1, while PS was surprisingly decreased with increase in  $X_3$  from -1 to +1 but showed the same pattern as written above with variation in  $X_2$  from -1 to +1.

Response surface plot for SS between  $X_1$  and  $X_2$  (Fig. 4.7(a)) demonstrated increase in SS with increase in  $X_1$  from -1 to +1 and decrease in  $X_2$  from +1 to 0. On the other hand Fig. 4.7(b) showed increase in SS with simultaneous increase in  $X_1$  and  $X_3$  from -1 to +1 and predicted the range of  $X_1$  and  $X_3$  from 0 to +1 for desired SS. Fig. 4.7(c) gave an idea about increase in SS when  $X_2$  was increased from -1 to 0 simultaneously with increase in  $X_3$  from -1 to +1.

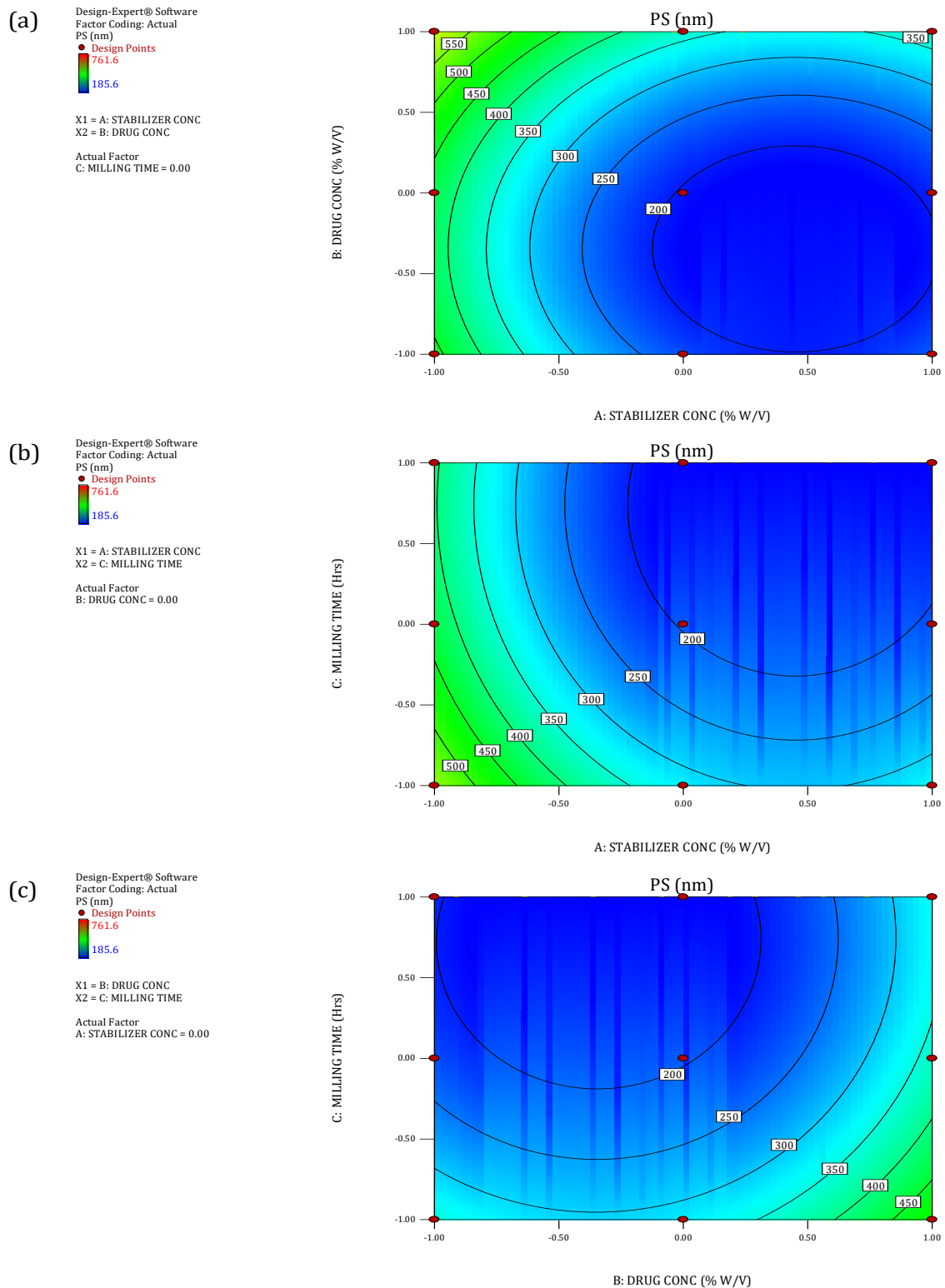


**Fig. 4.4** Contour plots showing effect of (a)  $X_1$  vs  $X_2$  (at 0 level of  $X_3$ ), (b)  $X_1$  vs  $X_3$  (at 0 level of  $X_2$ ) and (c)  $X_2$  vs  $X_3$  (at 0 level of  $X_1$ ) on PS of DAR-NS.

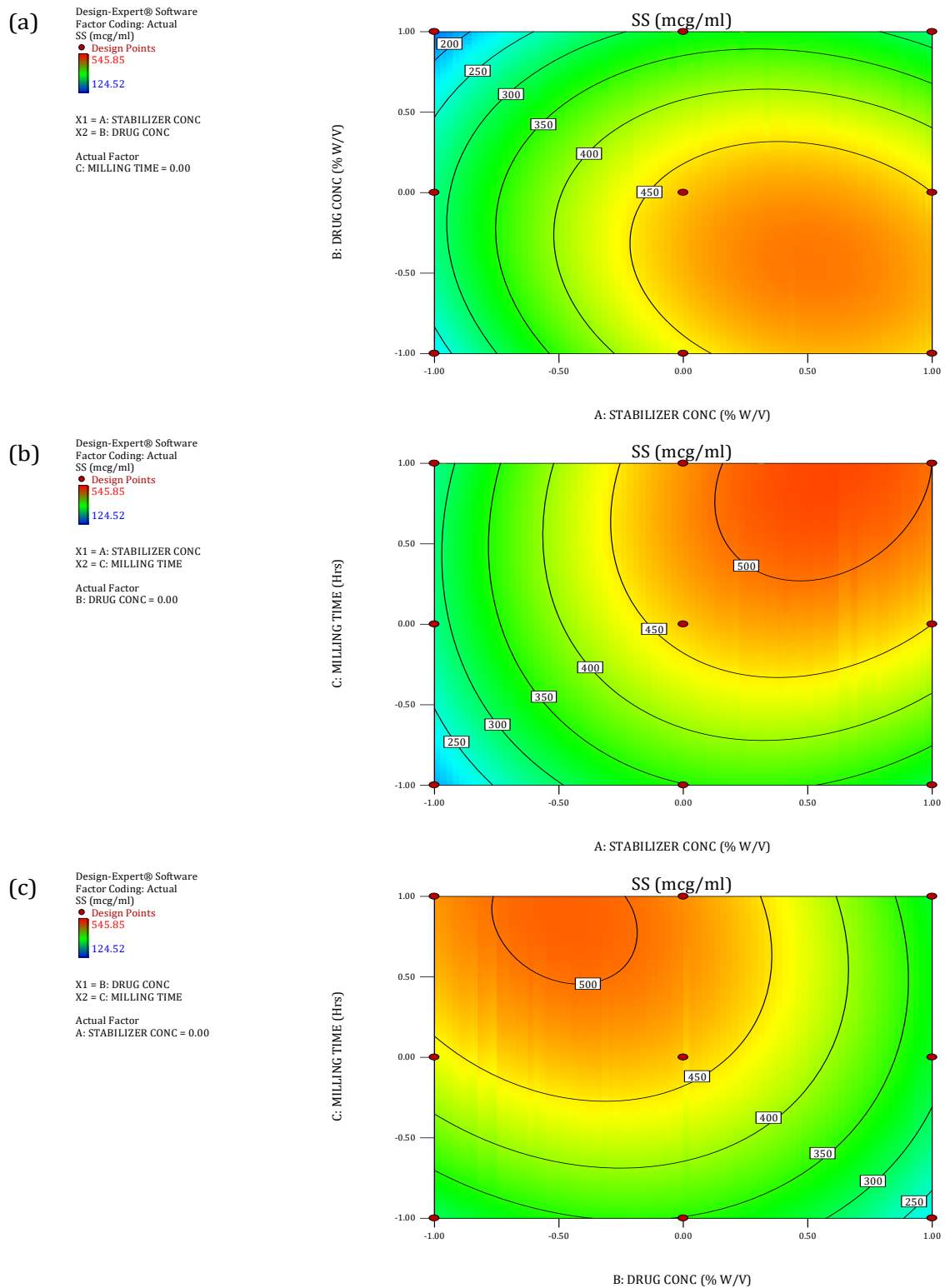


**Fig. 4.5** Contour plots showing effect of (a)  $X_1$  vs  $X_2$  (at 0 level of  $X_3$ ), (b)  $X_1$  vs  $X_3$  (at 0 level of  $X_2$ ) and (c)  $X_2$  vs  $X_3$  (at 0 level of  $X_1$ ) on SS of DAR-NS.

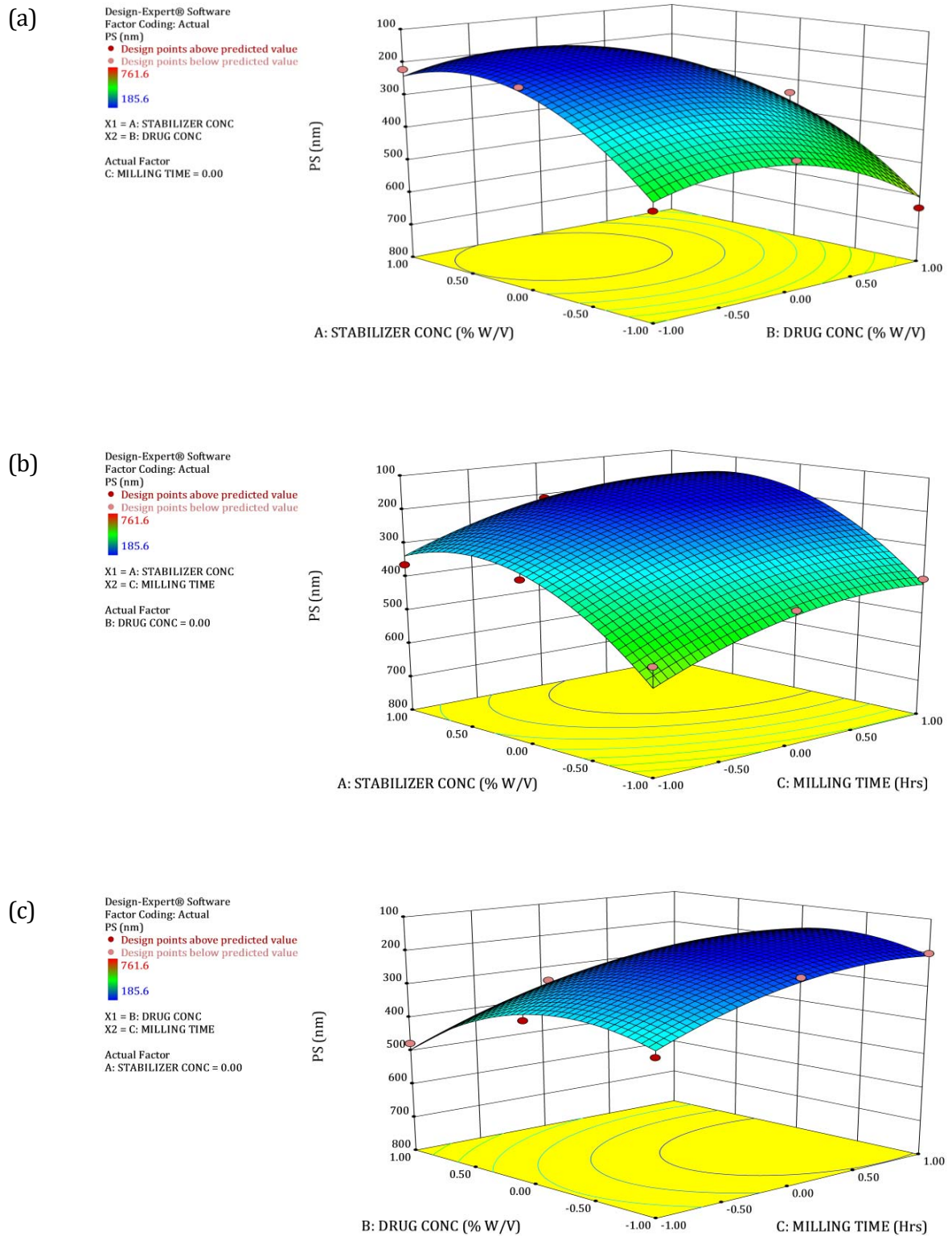


**Fig. 4.6** Response surface plots showing effect of (a)  $X_1$  vs  $X_2$  (at 0 level of  $X_3$ ), (b)  $X_1$  vs  $X_3$  (at 0 level of  $X_2$ ) and (c)  $X_2$  vs  $X_3$  (at 0 level of  $X_1$ ) on PS of DAR-NS.

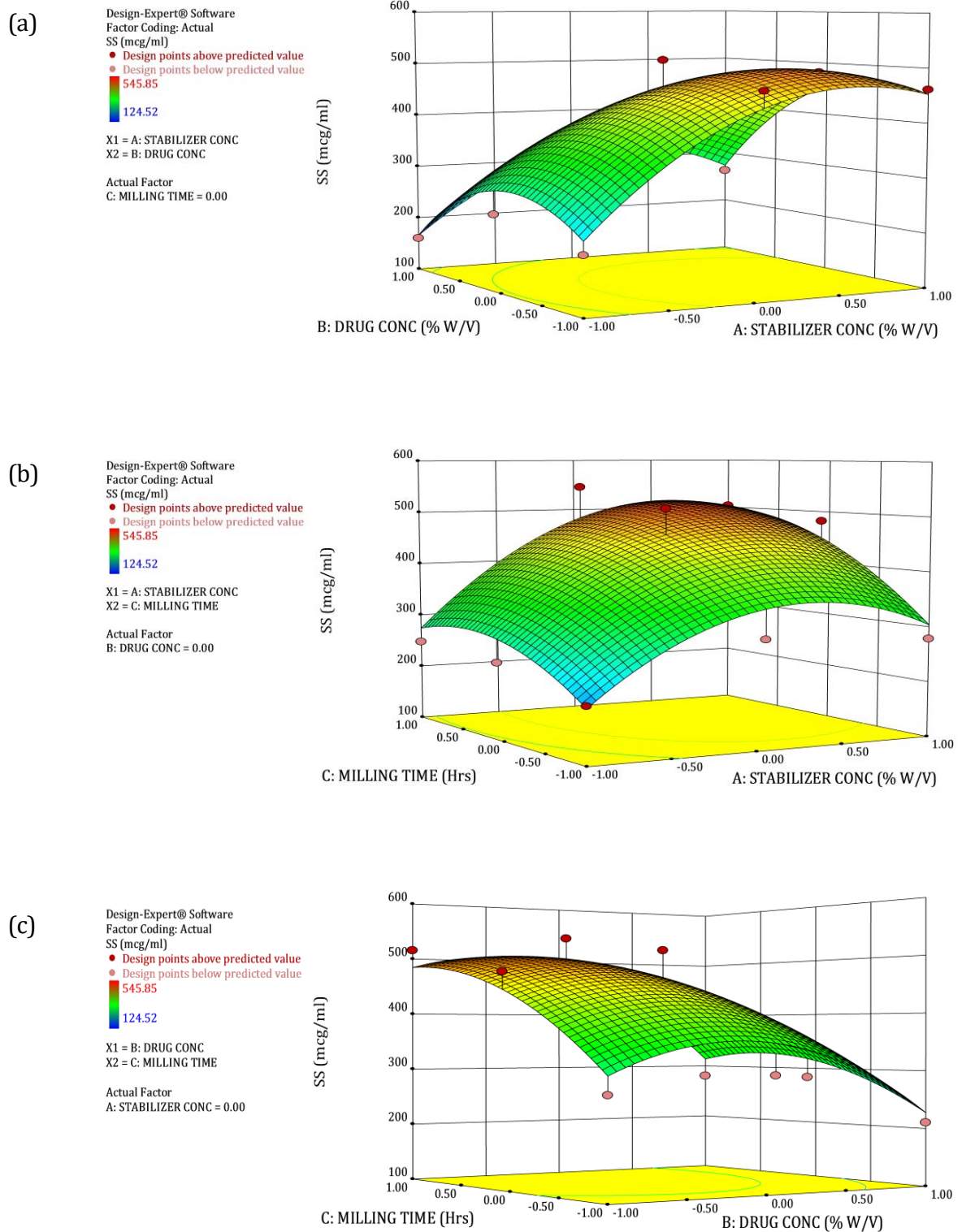


**Fig. 4.7** Response surface plots showing effect of (a)  $X_1$  vs  $X_2$  (at 0 level of  $X_3$ ), (b)  $X_1$  vs  $X_3$  (at 0 level of  $X_2$ ) and (c)  $X_2$  vs  $X_3$  (at 0 level of  $X_1$ ) on SS of DAR-NS.

#### 4.3.6.1.2.3 Check Point Analysis and Normalized Error Determination

Check point analysis was performed by preparing three formulation batches.  $Y_1$  and  $Y_2$  were evaluated and results were tabulated (Table 4.12). Results showed that there was no significant difference between experimentally measured values and predicted values of  $Y_1$  and  $Y_2$  ( $p < 0.05$ ). The lower calculated values of normalized error (NE) (0.01449 and 0.01042 for  $Y_1$  and  $Y_2$  of DAR NS respectively) explained and supported the precision of regression analysis in prediction of determined responses. Application of Student's t-test for data analysis between observed values and predicted values of  $Y_1$  and  $Y_2$  also proved the reliability of design of experiment as  $t_{\text{calculated}}$  values (0.5501 and 0.8989 for  $Y_1$  and  $Y_2$ , respectively) were significantly less than  $t_{\text{tabulated}}$  (2.9199 for both  $Y_1$  and  $Y_2$ ).

**Table 4.12** Check point analysis, Student's t-test and NE determination of PS and SS of DAR-NS.

Batch No.	$X_1$	$X_2$	$X_3$	PS		SS	
				Obs. (Avg)	Pred.	Obs. (Avg)	Pred.
1	-1 (50mg)	0.19 (1095mg)	0.49 (19.92 hrs)	301.21	298.37	351.58	353.17
2	0 (100mg)	-0.14 (930mg)	0.22 (17.76 hrs)	210.89	212.60	472.76	469.43
3	+1 (150mg)	-0.08 (960mg)	0.14 (17.12 hrs)	238.50	236.65	432.22	434.84
$t_{\text{calculated}}$				0.5501		0.8989	
$t_{\text{tabulated}}$				2.9199		2.9199	
Normalized Error (NE)				0.0145		0.0104	

#### 4.3.6.1.2.4 Desirability Criteria

From the previous results, the optimum levels of  $X_1$ ,  $X_2$  and  $X_3$  were selected by multiple regression analysis. Since PS and SS were taken into account simultaneously, the batch B15 exhibited smallest PS (185.6nm) with highest SS (545.9 $\mu$ g/ml) (at  $X_1=0$ ,  $X_2=0$  and  $X_3=+1$ ) whereas batch B14 showed PS (202.9nm) with SS (511.7 $\mu$ g/ml) (at  $X_1=0$ ,  $X_2=0$  and  $X_3=0$ ) which were not much different with batch B15. But our desirability criteria included PS of less than 250 nm and maximum SS with minimum concentration of surfactant, high concentration of drug and low stirring time. So the optimum formulation offered by software based on desirability was found at 0,0 and 0 for  $X_1$ ,  $X_2$  and  $X_3$  respectively. The calculated desirability factor for optimized formulation was 0.996, which was very near to 1, hence confirmed the suitability of designed factorial

model.

#### 4.3.6.1.3 Preparation of optimized DAR-NS

Using Design-Expert 8.0 software optimization process, selected values for  $X_1$ ,  $X_2$  and  $X_3$  were 2%w/v, 20%w/v and 16 hours respectively which gives theoretical values of PS (202.9nm) with SS (511.7 $\mu$ g/ml). For confirmation, fresh formulations in triplicate were prepared at optimum levels of independent variables.

DAR-NS was prepared by media milling technique. Weighed and transferred 100 mg of poloxamer 407 (i.e. 2% w/v) in a 20 ml flat bottom A-grade glass vial. 5 ml double distilled water was added in the vial and sonicated to dissolve the content. Subsequently, 1000 mg of DAR (i.e. 20% w/v) was incorporated to the stabilizer solution and sonicated for 5 minutes to disperse the drug in the medium. Then magnetic stirring bar (22mm x 8mm) and 5 gm of zirconium oxide beads were added in the dispersion and comminution was carried out on a high speed magnetic stirrer at 2000 rpm for 16 hours at room temperature. The diameter of zirconium oxide beads was in the range of 0.4 to 0.5 mm. After completion of comminution, NS was separated from milling beads by decanting the suspension, followed by washing of beads with double distilled water. The prepared DAR-NS was stored in a sealed glass vial at room temperature till the further processing.

The observed values of PS and SS were found to be 196.4 $\pm$ 1.4nm and 518.7 $\pm$ 2.5 $\mu$ g/ml, respectively, which were in close agreement with the theoretical values.

#### 4.3.6.1.4 Freeze drying of DAR-NS

Freeze drying or Lyophilization is very common and useful technique to get dry powder from solution of nanoparticles or nanosuspensions. The dried powder form of the NS enhanced its stability during storage. But freeze drying causes increase in PS due to agglomeration of particles during the process<sup>66</sup>. If these aggregates are not broken up during re-constitution, it may cause instability to the system. Therefore, to prevent the formation of aggregates and to stabilize the system, different cryoprotectants such as Sucrose, Trehalose dihydrate and Mannitol were tried in different ratios of total solid content of DAR-NS: cryoprotectant (i.e. 1:1% w/w, 1:2% w/w, 1:3% w/w and 1:4% w/w) and PS were evaluated as shown in Table 4.13. The PS of DAR-NS before freeze drying was 196.4nm. Dry powder was obtained in batches 2,3,5,6 and 10 whereas in batches 1,4,7,8,9,11 and 12, hard cake formation was found. It was observed that dry powders were easily redispersed in 5ml distilled water on manual shaking for 1-2 mins

but hard cakes need to be sonicated for 5 mins to reconstitute in the same conditions. The ratio of PS (after freeze drying,  $PS_{FD}$  and initial,  $PS_{initial}$ ) was found to be lowest (i.e. 1.11) for trehalose at 1:3 ratio, indicating its suitability in maintaining particle size of DAR-NS after freeze drying. This formulation was considered for further studies.

**Table 4.13** Effect of cryoprotectants and their concentration on PS of freeze dried DAR-NS after redispersion in distilled water.

Batch No.	Cryoprotectant	Ratio	Avg. PS in nm ( $PS_{FD}$ ) <sup>#</sup>	$PS_{FD}/PS_{initial}$
1	Trehalose	1:1	328.6±10.2	1.67
2		1:2	279.3±4.9	1.42*
3		<b>1:3</b>	<b>218.1±3.6</b>	<b>1.11*</b>
4		1:4	336.7±6.8	1.71
5	Mannitol	1:1	344.1±9.5	1.75*
6		1:2	286.4±7.1	1.46*
7		1:3	324.8±11.2	1.65
8		1:4	366.9±9.8	1.87
9	Sucrose	1:1	369.9±12.4	1.88
10		1:2	302.5±7.9	1.54*
11		1:3	336.7±8.3	1.71
12		1:4	375.5±11.5	1.91

Initial PS of DAR-NS ( $PS_{initial}$ ) = 196.4±1.4nm

<sup>#</sup> Data are shown as Mean±SD, n=3.

\* showed good redispersibility on manual shaking.

### 4.3.6.2 Characterization of DAR-NS

#### 4.3.6.2.1 Particle size determination

In wet media milling technique, collision of milling media with the drug particles generated a high energy, shear forces and turbulent environment which provides sufficient energy to produce drug nanoparticles from drug microparticles. DAR-NS formulation was optimized and successfully prepared by media milling, achieving the average particle size of 218.1±3.6nm with polydispersity index (PDI) of 0.145±0.007 (Fig. 4.8). The PDI measures the width of distribution. The PDI value of DAR-NS was below 0.2 indicating a narrow size distribution of the prepared nanosuspension. It can be observed that there was no significant difference in particle size before and after freeze drying indicating the suitability of freeze drying process. The particle size of plain DAR was evaluated by Malvern Mastersizer 2000 and it was found to be 37.91±0.65 μm (PDI= 0.528) (Fig. 4.9). Thus there was significant reduction in particle size of DAR from micron to nano range by nanosizing.

#### 4.3.6.2.2 Zeta potential

Zeta potential of prepared nanosuspension was evaluated to get the information about

surface properties of nanoparticles. The average zeta potential of DAR-NS was found to be  $-34.5 \pm 3$  mV (Fig. 4.10). It is considered that for a nanosuspension exhibiting good physical stability (stabilized by electrostatic repulsion), a minimum zeta potential of  $\pm 30$  mV is required.

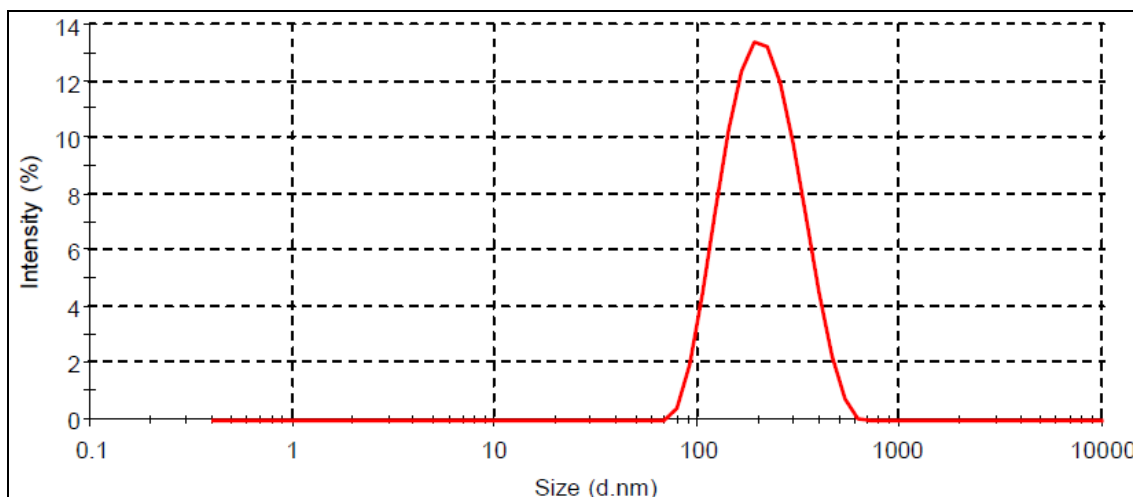


**Fig. 4.8** Particle size distribution of DAR-NS by Malvern Zetasizer.

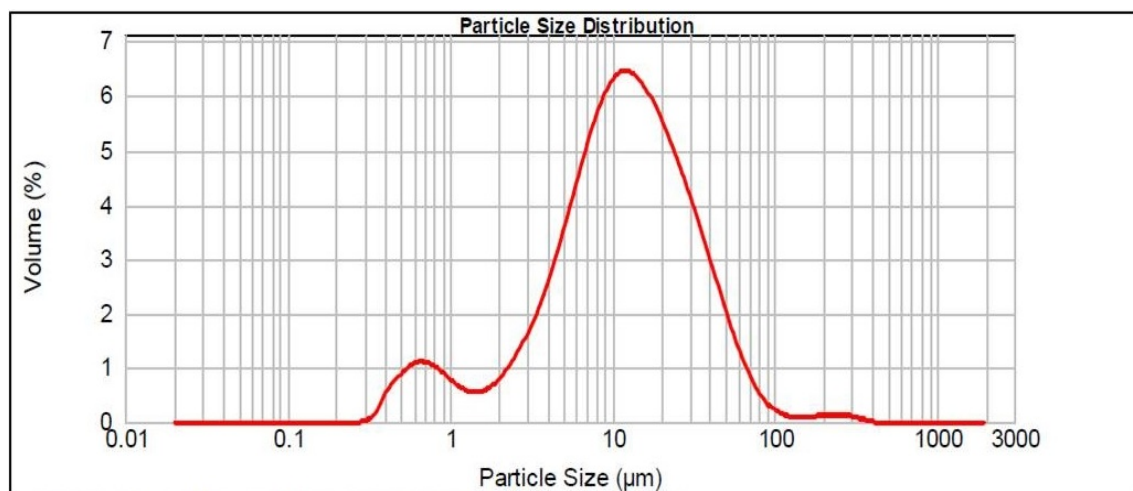


**Fig. 4.9** Particle size distribution of Plain DAR by Malvern Mastersizer

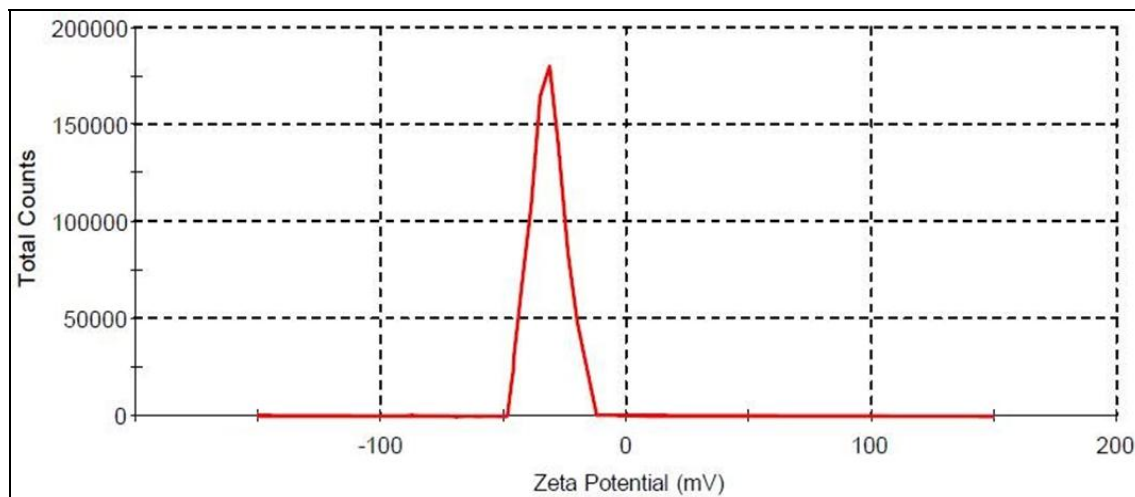


**Fig 4.10** Zeta potential report of DAR-NS by Malvern Zetasizer.

#### 4.3.6.2.3 Differential Scanning Calorimetry (DSC) Analysis

DSC is most widely used calorimetric technique for investigation of thermal parameters and physicochemical state of drug in various nano-formulations, which allow a better understanding of drug-exipient interactions. It is evident that if drug-exipients interaction took place, the elimination or shifting of one or more corresponding peaks to the involved components occurred in the thermogram of formulation while in case of no interaction, the peaks of individual components would be clearly visible<sup>67,68</sup>. The physical state of drug in a formulation could affect the *in-vitro* and *in-vivo* release of the drug from the system. If the compound is present in a molecular dispersion or solid solution state in a nanosuspension, no detectable endothermic peak will be observed<sup>69</sup>. DSC was performed for plain DAR, freeze dried DAR-NS, physical mixture (PM), poloxamer 407 and trehalose dihydrate. The DSC thermogram of plain DAR showed a single sharp endothermic peak at a temperature of 251.8°C corresponding to its melting point which indicates the crystalline nature of drug. DSC thermogram of poloxamer 407 exhibited an endothermic peak at 56.5°C while trehalose showed a melting peak at 99.8°C. Three endothermic peaks were observed in PM corresponding to the individual components of DAR-NS from 100°C to 300°C. There was no peak of DAR in the thermogram of DAR-NS, indicating that DAR lost its crystalline structure after nanosizing and present in amorphous form in the formulation matrix<sup>70</sup>. (Fig. 4.11)

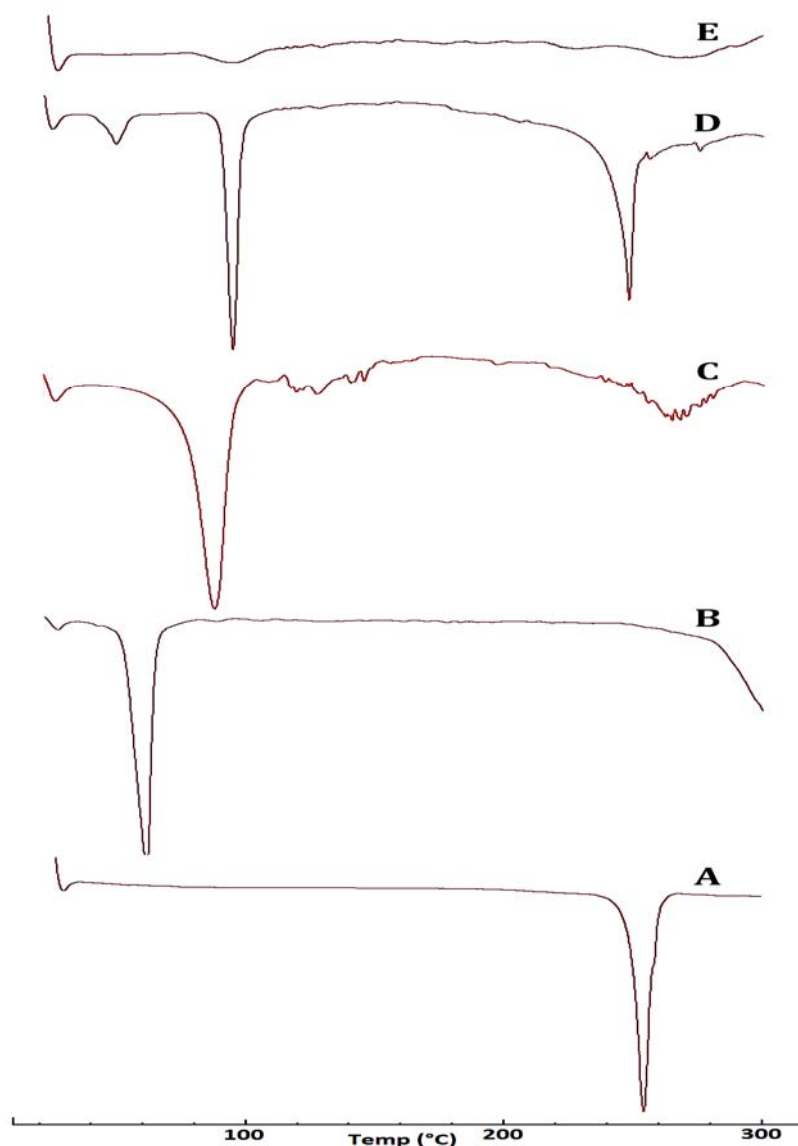


**Fig. 4.11** DSC thermograms of (A) Plain DAR, (B) Poloxamer 407, (C) Trehalose, (D) Physical Mixture for DAR-NS (PM) and (E) Freeze dried DAR-NS.

#### 4.3.6.2.4 X-Ray Diffraction (XRD) Study

XRD study was carried out to investigate the crystalline state of drug which is influencing the dissolution and stability behaviour of compound. The preservation of the crystal structure of the drug in the formulation is crucial for the sustained stability of the drug during its shelf-life. On the other hand, the drug in the amorphous state has better dissolution properties compared to the crystal form. Thus, decreasing the drug particle size to nanorange while preserving the crystal morphology, leads to improved dissolution profile while keeping the drug intact (*i.e.* sustained chemical stability). The crystalline state of the samples was evaluated to prove the effect of milling on the physical state of DAR. The XRD patterns of plain DAR, PM and DAR-NS were recorded

(Fig. 4.12). Upon XRD evaluation, it was observed that the specific peaks for DAR at specified  $2\theta$  diffraction angles 10.3, 17.4 and 27.7 were not observed in DAR-NS. This suggested that the crystallinity of DAR was not retained in DAR-NS formulation, indicating that the crystalline state of DAR was altered following milling. The absence of all major peaks of DAR in XRD pattern of the DAR-NS confirmed the formation of amorphous product which might leads to enhanced solubility of the drug in DAR-NS. But in case of PM, all the peaks of DAR were retained, indicating no change in crystallinity of DAR in physical mixing of drug with excipients. The results were in accordance with those of DSC studies, which also indicated loss of crystallinity due to nanosizing.

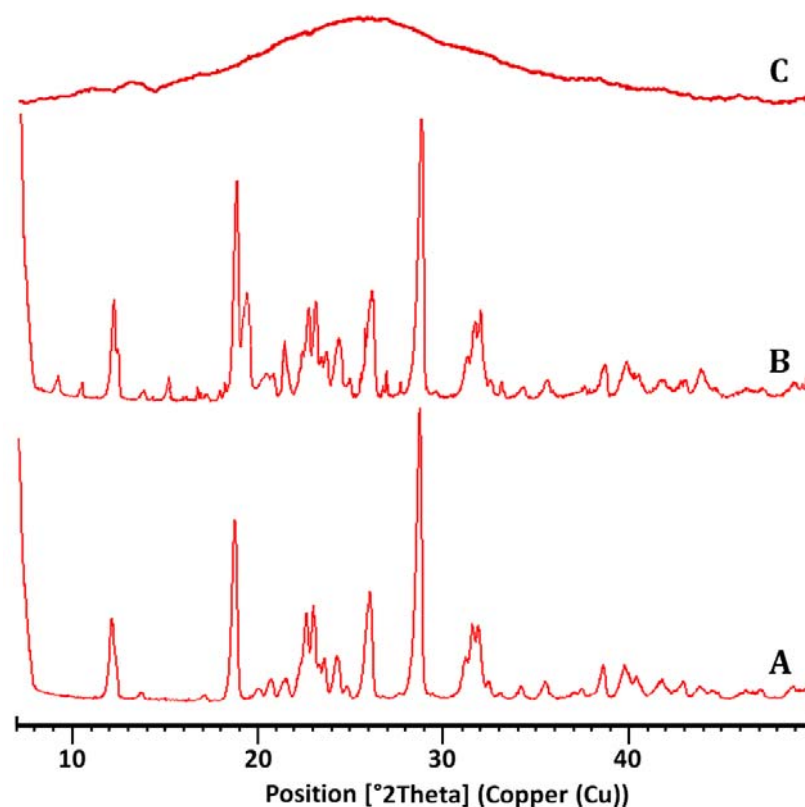


**Fig. 4.12** XRD spectra of (A) Plain DAR, (B) Physical Mixture for DAR-NS (PM) and (C) Freeze dried DAR-NS.

#### 4.3.6.2.5 Morphological analysis by SEM and TEM

Analysis by SEM has been performed to evaluate the morphology of drug particles in bulk drug and nano-formulations. It was observed in SEM images that there were distinct differences in morphologies of raw DAR and DAR-NS. SEM image of plain DAR exhibited large aggregates of irregular shaped crystals (Fig. 4.13). By evaluating the

SEM image of DAR-NS (Fig. 4.14), it can be predicted that media milling of DAR in presence of stabilizer (poloxamer 407) led to a change in morphology of drug particles and decrease in particle size from micron to nanometric range with relatively narrow size distribution. TEM image of DAR-NS demonstrate that the nanoformulation could be easily redispersed in water without forming any large aggregates. TEM image revealed that the particles of DAR were discrete, non-aggregated, homogenously dispersed, nearly spherical in shape and were in accordance with particle size obtained by DLS method (Fig. 4.15).

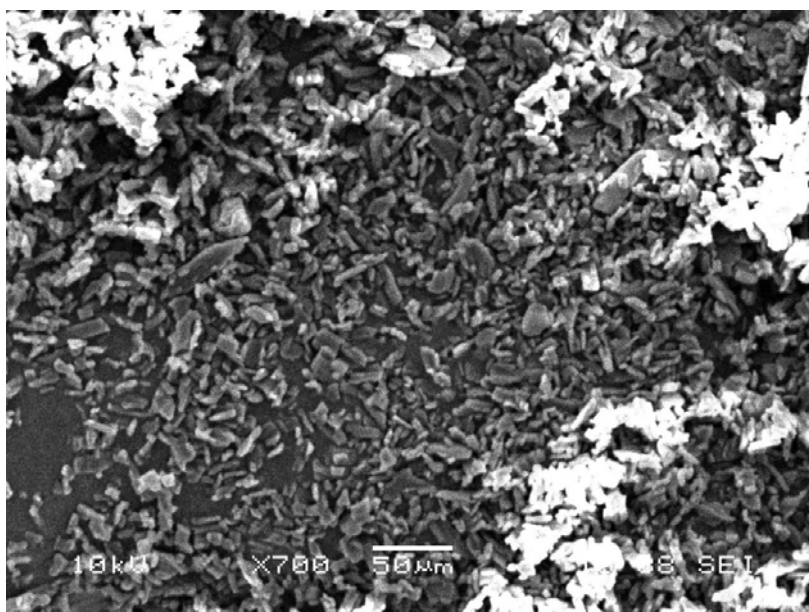


**Fig. 4.13** SEM image of plain DAR.

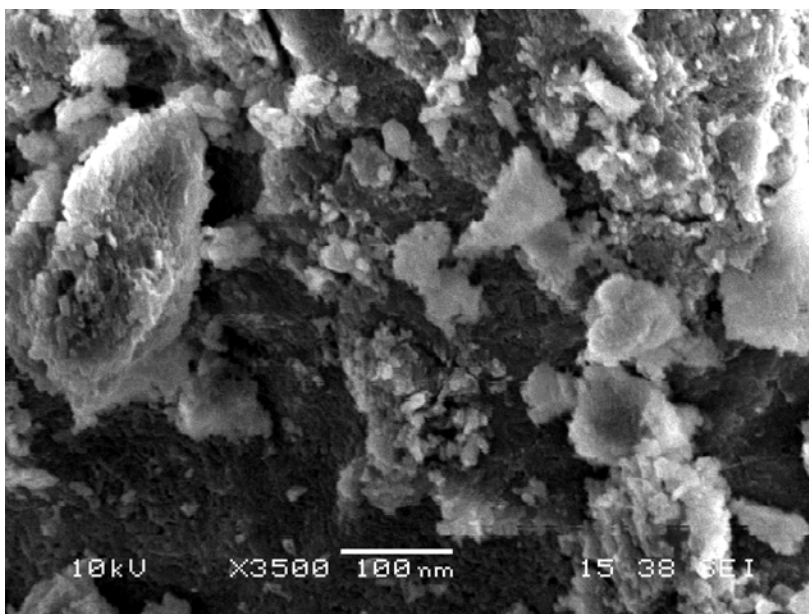


**Fig. 4.14** SEM image of DAR-NS.

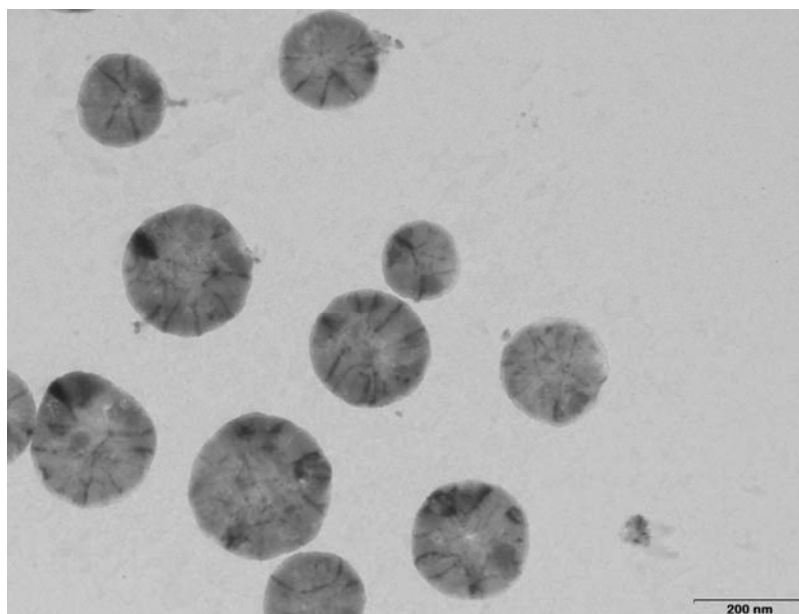


**Fig. 4.15** TEM image of DAR-NS

#### **4.3.6.2.6 Percentage drug content in DAR-NS**

Percentage drug content in DAR-NS was found to be  $99.58 \pm 0.79\%$ , indicating the suitability of media milling method for preparation of nanosuspension.

#### **4.3.6.2.7 Saturation solubility**

A wonderful attribute of nanosuspension is the increase in saturation solubility and consequently an increase in the dissolution velocity of the compound. Saturation solubility is defined as the maximum quantity of a compound (solute) that can be dissolved in a certain quantity of a specific solvent at a specified temperature<sup>71</sup>. Although it is a compound specific, temperature dependent constant, it also depends on particle size. The saturation solubility increases with decreasing particle size. The saturation solubility of plain DAR was compared with freeze dried DAR-NS. The saturation solubility of plain DAR was found to be  $16.48 \pm 0.42 \mu\text{g/ml}$  which is very low whereas DAR-NS showed enhanced saturation solubility of DAR  $509.47 \pm 2.28 \mu\text{g/ml}$ . It can be observed that DAR-NS enhanced the saturation solubility of DAR by about 30.91 folds than plain DAR, attributed to nanosizing of DAR particles.

#### **4.3.6.2.8 *In vitro* dissolution study**

The release profiles of capsules containing plain DAR (DAR-P), marketed formulation (DAR-M) and freeze dried DAR nanosuspension (DAR-NS) in phosphate buffer pH-6.8, acetate buffer pH-4.5, 0.1N HCl and water have been shown in Fig 4.16 and described in Table 4.14. The DAR-NS, DAR-M and DAR-P showed better dissolution profile in

phosphate buffer pH-6.8 and water as compared to acetate buffer pH-4.5 and 0.1N HCl which may be due to low solubility of drug in acidic medium<sup>72</sup>. The drug release was noticeably increased in phosphate buffer pH-6.8 and water for DAR-NS as more than 50% of DAR was dissolved in first 5 mins, as compared to 25.8-36.4% and 7.2-8.1% from DAR-M and DAR-P, respectively. The DAR-P did not achieve complete dissolution during 120 min time period and only 13.4-56.9% the DAR released over the test period of 120 mins, due to large crystal size of drug whereas DAR-NS showed 58.1-99.9% drug dissolved with significantly enhanced dissolution rate over the time period of 120 mins, in all the selected dissolution mediums. This improved dissolution rate can be due to the larger surface area of nanoparticles available for dissolution in comparison to microcrystals and presence of surfactant in nanosuspension which increased the wettability of drug<sup>73</sup>.

**Table 4.14:** Statistical representation of % Cumulative drug release versus sampling time of DAR-P, DAR-M and freeze dried DAR-NS in phosphate buffer pH-6.8 (PB), acetate buffer pH-4.5 (AB), 0.1N HCl and water.

Time (min) ⇒	0	5	10	15	30	45	60	120
<b>% Cumulative release from Phosphate Buffer, pH-6.8*</b>								
<b>DAR-NS</b>	0.0	90.1±0.7	94.7±0.5	96.4±0.2	98.1±0.3	99.1±0.1	99.7±0.3	99.9±0.2
<b>DAR-M</b>	0.0	36.4±0.5	54.6±0.3	64.2±0.7	80.7±0.2	89.4±0.2	93.5±0.5	95.4±0.6
<b>DAR-P</b>	0.0	8.1±0.2	13.9±0.1	18.6±0.5	32.4±0.2	43.5±0.4	49.8±0.3	56.9±0.1
<b>% Cumulative release from Acetate Buffer, pH-4.5*</b>								
<b>DAR-NS</b>	0.0	46.4±0.9	56.1±0.4	59.5±0.2	65.1±0.6	66.9±0.2	67.8±0.2	68.4±0.4
<b>DAR-M</b>	0.0	14.4±0.3	20.6±0.6	24.6±0.5	32.9±0.2	38.7±0.4	40.1±0.7	42.2±0.8
<b>DAR-P</b>	0.0	1.9±0.4	3.1±0.3	4.4±0.1	7.8±0.3	10.9±0.5	12.8±0.2	16.5±0.2
<b>% Cumulative release from 0.1N HCl*</b>								
<b>DAR-NS</b>	0.0	34.1±0.4	46.9±0.2	50.4±0.6	54.2±0.7	56.2±0.3	57.1±0.1	58.1±0.3
<b>DAR-M</b>	0.0	8.3±0.8	14.7±0.4	19.9±0.7	30.4±0.2	34.7±0.2	35.6±0.3	37.9±0.2
<b>DAR-P</b>	0.0	1.2±0.1	2.3±0.3	3.2±0.4	6.6±0.6	9.1±0.3	11.2±0.2	13.4±0.5
<b>% Cumulative release from water*</b>								
<b>DAR-NS</b>	0.0	80.7±0.3	88.1±0.2	91.4±0.4	96.1±0.5	97.5±0.1	98.3±0.5	99.2±0.2
<b>DAR-M</b>	0.0	25.8±0.2	42.4±0.4	53.1±0.6	70.8±0.2	79.9±0.3	85.6±0.2	91.2±0.1
<b>DAR-P</b>	0.0	7.2±0.5	12.2±0.7	16.9±0.2	30.4±0.4	40.6±0.3	44.1±0.5	47.2±0.2

\* Data are shown as Mean±SD, n=3.

Various dissolution parameters were calculated using DDSolver, an excel add-in program and reported in Table 4.15. The Dissolution efficiency (DE), Dissolution percentage at 5 min and 60 min (DP<sub>5</sub> and DP<sub>60</sub>) and Area under curve (AUC) values were increased in the following order: DAR-P<DAR-M<DAR-NS; while time required to release 50% and 90% of drug (t<sub>50</sub> and t<sub>90</sub>) and mean dissolution time (MDT) were increased in vice versa i.e. DAR-P>DAR-M>DAR-NS. Thus, it can be said that prepared

nanosuspension have superior characteristics to plain drug and marketed formulation, indicating a major prospect to enhance the bioavailability of such drugs by nanosuspensions for oral administration where solubility and dissolution are rate limiting factors in bioavailability in the body. Nanotechnology is therefore more effective in increasing solubility and dissolution velocity and offers economical process and formulation.

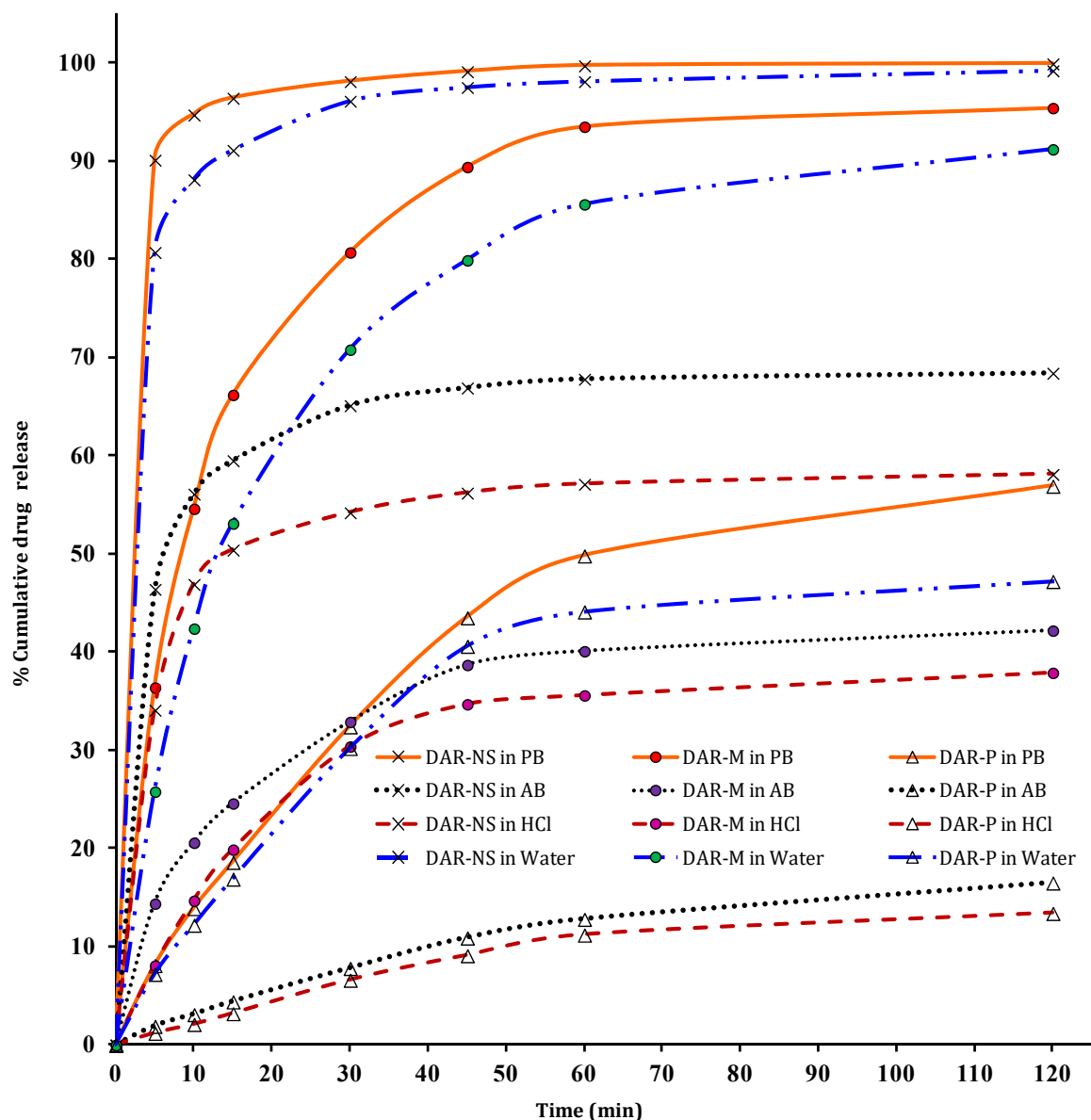


**Fig. 4.16** Graphical representation of % Cumulative drug release versus sampling time of DAR-P, DAR-M and freeze dried DAR-NS in phosphate buffer pH-6.8 (PB), acetate buffer pH-4.5 (AB), 0.1N HCl and water.

**Table 4.15** Comparison of various dissolution parameters of DAR-P, DAR-M and freeze dried DAR-NS in phosphate buffer pH-6.8 (PB), acetate buffer pH-4.5 (AB), 0.1N HCl and water.

	DE	DP <sub>5</sub>	DP <sub>60</sub>	t <sub>50</sub>	t <sub>90</sub>	MDT	AUC
<b>In Phosphate Buffer, pH-6.8*</b>							
DAR-NS	0.97±0.03	90.1±0.7	99.7±0.3	1.6±0.1	5.0±0.2	4.1±0.1	11581±48
DAR-M	0.84±0.04	36.4±0.5	93.5±0.5	9.7±0.4	48.3±0.7	14.8±0.2	10036±35
DAR-P	0.42±0.01	8.1±0.2	49.8±0.3	>60	>60	32.0±0.4	5009±28
<b>In Acetate Buffer, pH-4.5*</b>							
DAR-NS	0.64±0.04	46.4±0.9	67.8±0.2	9.3±0.5	>60	7.7±0.4	7682±23
DAR-M	0.36±0.02	14.4±0.3	40.1±0.7	>60	>60	18.9±0.7	4264±19
DAR-P	0.11±0.02	1.9±0.4	12.8±0.2	>60	>60	39.7±0.5	1324±25
<b>In 0.1N HCl*</b>							
DAR-NS	0.54±0.03	34.1±0.4	57.1±0.1	15.0±0.2	>60	9.0±0.2	6449±54
DAR-M	0.31±0.01	8.3±0.8	35.6±0.3	>60	>60	20.8±0.3	3761±29
DAR-P	0.09±0.05	1.2±0.1	11.2±0.2	>60	>60	37.5±0.6	1106±17
<b>In water*</b>							
DAR-NS	0.94±0.04	80.7±0.3	98.3±0.5	2.4±0.2	10.9±0.3	6.0±0.2	11313±39
DAR-M	0.76±0.03	25.8±0.2	85.6±0.2	14.8±0.7	>60	20.5±0.8	9078±31
DAR-P	0.37±0.04	7.2±0.5	44.1±0.5	>60	>60	26.8±0.3	4397±15

\* Data are shown as Mean±SD, n=3. DE: Dissolution efficiency, DP<sub>5</sub>: Dissolution percentage at 5 min, DP<sub>60</sub>: Dissolution percentage at 60 min, t<sub>50</sub>: time required to release 50% of drug (min), t<sub>90</sub>: time required to release 90% of drug (min), MDT: Mean dissolution time (min), AUC: Area under curve.

#### 4.3.6.2.9 Stability studies

The stability of DAR-NS was monitored for physical stability (i.e. PS, PDI and zeta potential) and chemical stability (i.e. percentage drug content), carried out for 6 months at different time intervals (i.e. 1<sup>st</sup>, 2<sup>nd</sup>, 3<sup>rd</sup> and 6<sup>th</sup> month) stored at 5°C±3°C and at room temperature. It was observed that there was no significant difference in the PS, PDI, ZP and % DAR content at both conditions for 6 months (Table 4.16 and Table 4.17) so it can be concluded that formulation is physically and chemically stable for a period of 6 months and indicating its suitability for storage at both the conditions.

**Table 4.16** Physical stability (i.e. PS, PDI and ZP) of DAR-NS at different time intervals stored at 5°C±3°C and room temperature.

Sr. No.	Time	At 5°C±3°C*			At Room Temperature*		
		PS (nm)	PDI	ZP (mV)	PS (nm)	PDI	ZP (mV)
1	Initial	218.1±3.6	0.145±0.007	-34.5±3	218.8±06	0.145±0.007	-34.5±3
2	1 <sup>st</sup> Month	218.4±4.1	0.146±0.005	-34.8±2	219.3±3.1	0.147±0.002	-35.1±3
3	2 <sup>nd</sup> Month	218.9±4.8	0.148±0.002	-33.3±4	219.9±2.7	0.150±0.005	-33.8±2
4	3 <sup>rd</sup> Month	219.5±2.3	0.151±0.006	-33.9±3	220.1±2.5	0.145±0.004	-34.2±2
5	6 <sup>th</sup> Month	218.7±2.9	0.149±0.005	-34.8±4	220.6±3.4	0.149±0.003	-33.5±4

\* Data are shown as Mean±SD, n=3.

**Table 4.17** Chemical stability (i.e. percentage drug content) of DAR-NS at different time intervals, stored at 5°C±3°C and room temperature.

Sr. No.	Time	At 5°C±3°C*	At Room Temperature*
		% content of DAR in DAR-NS	% content of DAR in DAR-NS
1	Initial	99.58±0.79	99.58±0.79
2	1 <sup>st</sup> Month	99.37±0.45	99.25±0.81
3	2 <sup>nd</sup> Month	99.21±0.63	99.32±0.72
4	3 <sup>rd</sup> Month	99.44±0.92	99.54±0.95
5	6 <sup>th</sup> Month	99.35±0.88	99.08±0.59

\* Data are shown as Mean±SD, n=3.

### 4.3.6.3 Cell Line Studies using Caco-2 cell line model

#### 4.3.6.3.1 *In vitro* Cell Cytotoxicity Studies (MTT Assay)

Cytotoxicity study of DAR-NS and DAR-P was accomplished in Caco2 cells by mitochondrial activity (MTT assay) to assess the safety/tolerability of prepared formulation on viability of cells. As Caco2 cells were used as absorption model, biocompatibility and tolerability of DAR-P and DAR-NS on absorption barrier was necessary. At initial 4 hr and 24 hr, the % cell viability is more than 80% at the 250 µg/ml concentration of DAR-P and DAR-NS. Hence for permeability studies, the drug and formulation concentration was fixed at 250 µg/ml. It can be observed that the DAR-NS showed very less cytotoxicity than the plain DAR upto 48 hours at all the concentrations. (Table 4.18) This confirms the biocompatibility of DAR-NS and explains that composition of nanosuspension did not contribute to toxicity of Caco2 cells<sup>74</sup>. At initial 4 hours, 24 hours and 48 hours, DAR-NS was found to have less cytotoxicity with more than 80% cell viability as compared to DAR-P at all the concentrations except at 1000µg/ml in 48 hours condition. This could be attributed to protective effect of poloxamer 407. Cytotoxicity graphs at 4 hours, 24 hours and 48 hours were constructed (Fig. 4.17, 4.18 and 4.19) and IC<sub>50</sub> values were calculated for DAR-P and DAR-NS (Table 4.19). The higher IC<sub>50</sub> values for DAR-NS than DAR-P at all the incubation time conditions concluded to lack of cytotoxicity due to formulation of a biocompatible nanosuspension.

**Table 4.18** In vitro cytotoxicity studies of DAR-P and DAR-NS in Caco2 cell lines at 4 hours, 24 hours and 48 hours.

Conc. (µg/ml)	%Cell Viability at 4 Hrs.*		%Cell Viability at 24 Hrs.*		%Cell Viability at 48 Hrs.*	
	DAR-P	DAR-NS	DAR-P	DAR-NS	DAR-P	DAR-NS
0.1	99.25±0.92	99.99±0.74	94.32±0.66	98.45±0.97	90.14±0.69	94.62±0.56
1	98.59±0.61	99.23±0.81	90.62±0.53	97.23±0.28	86.90±0.75	93.26±0.52
10	96.13±0.89	98.55±0.26	86.24±0.88	94.12±0.67	83.64±0.39	92.82±0.83
100	94.61±0.58	97.89±0.86	82.43±0.64	92.23±0.51	80.86±0.84	88.46±0.49
250	91.45±0.62	93.56±0.98	80.42±0.93	90.41±0.39	75.63±0.85	84.15±0.39
500	86.58±0.45	88.56±0.52	79.49±0.46	85.54±0.42	70.26±0.46	80.98±0.86
1000	83.16±0.94	86.89±0.68	70.60±0.91	82.99±0.64	62.43±0.28	75.12±0.61

\* Data are shown as Mean±SD, n=3.

**Table 4.19** IC<sub>50</sub> values of DAR-P and DAR-NS in Caco2 cell lines at 4 hours, 24 hours and 48 hours.

Conditions	IC <sub>50</sub> Values (µg/ml)*	
	DAR-P	DAR-NS
At 4 hours	3010.96±19.62	3571.54±11.25
At 24 hours	1878.42±14.11	3192.61±17.58
At 48 hours	1408.16±15.18	2248.07±10.34

\* Data are shown as Mean±SD, n=3.

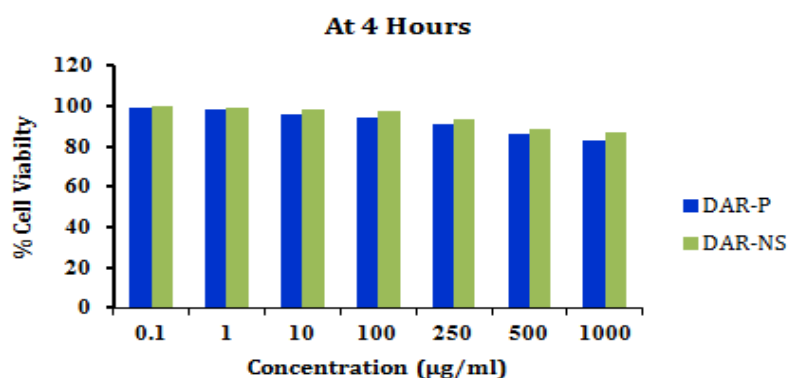


**Fig. 4.17** In vitro cytotoxicity studies of DAR-P and DAR-NS in Caco2 cell lines at 4 hours.

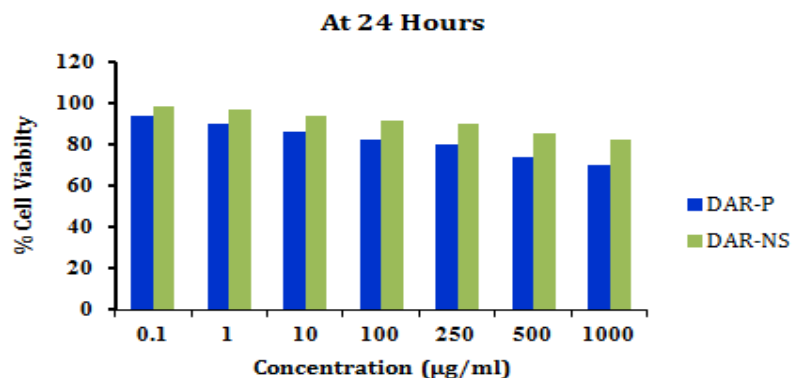


**Fig. 4.18** In vitro cytotoxicity studies of DAR-P and DAR-NS in Caco2 cell lines at 24 hours.

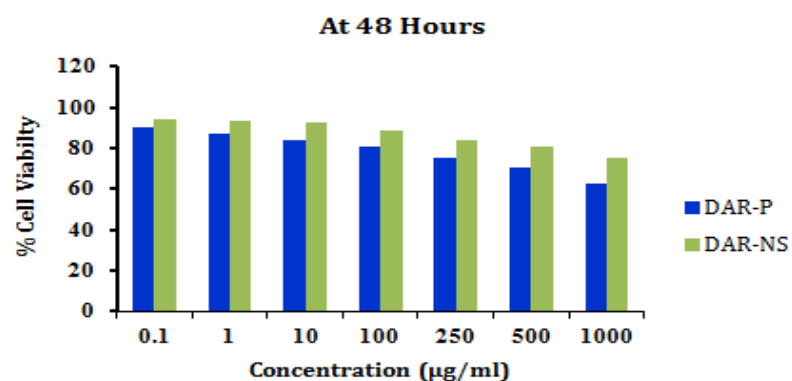


**Fig. 4.19** In vitro cytotoxicity studies of DAR-P and DAR-NS in Caco2 cell lines at 48 hours.

#### 4.3.6.3.2 *In vitro* cell permeability assessment of DAR-NS

Caco-2 monolayer model is a wonderful tool for *in vitro* assessment of gastrointestinal permeability of drug as it provides better prediction of the human absorption of the drug which show active uptake or efflux or pass through the membrane via paracellular route. Additionally, because use of this model can decrease the number of animals needed for experimental studies. In this study, *in vitro* permeability assessment of DAR-NS, plain DAR (DAR-P) and marketed formulation (DAR-M) was done by calculating apparent permeability coefficient ( $P_{app}$ ) from apical to basolateral. Transepithelial permeability of DAR was measured at concentration of 250 µg/ml, as negligible toxicity towards Caco-2 cells was found at this concentration during MTT assay of the same. The average  $P_{app}$  for Lucifer yellow with Caco-2 cells was found  $(0.87 \pm 0.07) \times 10^{-6}$  cm/sec, confirmed the integrity of monolayers and suitability of monolayers for further experiment. The  $P_{app}$  for DAR-P and DAR-M were calculated and found to be  $(5.95 \pm 0.24)$

$\times 10^{-6}$  cm/sec and  $(8.73 \pm 0.82) \times 10^{-6}$  cm/sec respectively while the  $P_{app}$  for DAR-NS was observed at  $(39.44 \pm 0.59) \times 10^{-6}$  cm/sec which is about 6.63 fold and 4.52 fold higher than the DAR-P and DAR-M, respectively. The found results were very much satisfactory and matching with the aim of the project. It can be concluded that the higher  $P_{app}$  for DAR-NS was because of small particle size of DAR in nanosuspension and additionally the hydrophilic and lipophilic nature of poloxamer-407 present in the formulation. Whereas the lower permeability coefficient of DAR can be attributed to hydrophobicity and low permeation ( $\log P$  2.47) of drug. If the  $P_{app}$  value of a compound is less than  $1 \times 10^{-6}$  cm/sec, in between  $1-10 \times 10^{-6}$  cm/sec, and more than  $10 \times 10^{-6}$  cm/sec can be classified as poorly (0-20%), moderately (20-70%) and well (70-100%) absorbed compounds, respectively<sup>19,75</sup>.

**Table 4.20** Apparent permeability coefficient ( $P_{app}$ ) from apical to basolateral for DAR-P, DAR-M and DAR-NS using Caco-2 cells model.

Drug/Formulation	Apparent permeability coefficient ( $P_{app}$ ) $\pm$ SD ( $10^{-6}$ cm/sec)*
DAR-P	5.95 $\pm$ 0.24
DAR-M	8.73 $\pm$ 0.82
DAR-NS	39.44 $\pm$ 0.59

\* Data are shown as Mean $\pm$ SD, n=3.

#### 4.3.6.4 Pharmacokinetic evaluation of DAR-NS using *in vivo* animal model

*In vivo* animal study was performed to evaluate the oral bioavailability and other pharmacokinetic parameters of prepared formulation (DAR-NS) with respect to plain drug (DAR-P) and commercial formulation (DAR-M). DAR is completely metabolized in rhein before entering in the systemic blood circulation, after oral dosing.

The mean drug plasma concentration versus time after oral administration of DAR-P, DAR-M and DAR-NS are reported in Table 4.21 whereas Fig 4.20 illustrate the same graphically. The pharmacokinetic parameters for all the three orally administered forms of DAR were determined using PKsolver add-in in microsoft excel. Non-compartmental analysis of drug-plasma concentration with linear trapezoidal method after extravascular administration in rabbits was performed and obtained parameters are represented in Table 4.22. Plasma rhein concentration profile of DAR-NS showed significant improvement in drug absorption compared to DAR-P and DAR-M. Area under concentration-time curve ( $AUC_{0-t}$ ) of rhein was found  $30.90 \pm 0.56 \mu\text{g}^*\text{h/ml}$  for DAR-NS which was 3.95 fold and 2.41 fold higher with that of DAR-P ( $7.83 \pm 0.19 \mu\text{g}^*\text{h/ml}$ ) and DAR-M ( $12.81 \pm 0.62 \mu\text{g}^*\text{h/ml}$ ), respectively. The area under moment curve ( $AUMC_{total}$ )

showed significantly higher value for DAR-NS ( $227.45 \pm 4.87 \mu\text{g} \cdot \text{h}^2/\text{ml}$ ), compared to DAR-P ( $50.47 \pm 2.31 \mu\text{g} \cdot \text{h}^2/\text{ml}$ ) and DAR-M ( $89.95 \pm 2.59 \mu\text{g} \cdot \text{h}^2/\text{ml}$ ). The maximum peak plasma concentration ( $C_{\text{max}}$ ) of DAR-NS was about 2.93 fold and 2.48 fold greater than that of DAR-P and DAR-M, respectively. The enhancement in AUC and  $C_{\text{max}}$  of DAR-NS compared to DAR-P and DAR-M could be due to the quick absorption of drug molecule by gastrointestinal wall due to the reduced particle size and increased surface area followed by significantly improved dissolution rate and increase in adhesion surface area between nanoparticle and intestinal epithelium of villi which provides a direct contact with the absorbing membrane of the gut wall<sup>76</sup>. Mean residence time (MRT) for DAR-P, DAR-M and DAR-NS were  $6.16 \pm 0.14$  h,  $7.12 \pm 0.09$  h and  $7.06 \pm 0.10$  h, respectively. Time to reach maximum plasma concentration ( $T_{\text{max}}$ ) for DAR-NS, DAR-M and DAR-P was found to be 2.0, 3.0 and 3.5 h, respectively. The shortest  $T_{\text{max}}$  for DAR-NS may be due to fastest dissolution rate and the highest  $T_{\text{max}}$  of DAR-P could be attributed to crystalline nature of drug<sup>1</sup>.

When half life ( $t_{1/2}$ ) of DAR-NS was compared with DAR-P and DAR-M, the  $t_{1/2}$  for DAR-NS ( $13.62 \pm 0.38$  h) was not found much higher than that of DAR-P ( $7.94 \pm 0.42$  h) and DAR-M ( $10.65 \pm 0.57$  h). The elimination rate constant ( $K_{\text{elimination}}$ ) for DAR-P, DAR-M and DAR-NS were found to be  $0.12 \pm 0.02 \text{ h}^{-1}$ ,  $0.07 \pm 0.01 \text{ h}^{-1}$  and  $0.05 \pm 0.01 \text{ h}^{-1}$ , respectively. No significant difference in  $t_{1/2}$  and  $K_{\text{elimination}}$  of all three was observed which indicated that their elimination was comparable.

Relative bioavailability or bioequivalence is the most important criteria for comparing the bioavailabilities of different formulations of same drug. The relative bioavailability (F) of DAR-NS and DAR-M were found to be 394.64% and 163.60%, respectively, with respect to DAR-P. Thus there was 3.94 and 2.41 fold increase in bioavailability of DAR from DAR-NS with respect to DAR-P and DAR-M, respectively. These results could be explained by greater dissolution rate, increased wettability, reduced particle size and increased surface area of DAR in DAR-NS when compared to DAR-P and DAR-M. So it can be observed easily that these results may lead to economical benefits by reduction in dose of DAR. Additionally, dose related side effects of drug will also minimize when administered in multiple dose regimens.

**Table 4.21** Statistical representation of rhein plasma profile for DAR-P, DAR-M and DAR-NS in Albino rabbits following oral administration.

Time (Hour)	Rhein mean plasma concentration $\pm$ SD*		
	DAR-P ( $\mu\text{g/ml}$ )	DAR-M ( $\mu\text{g/ml}$ )	DAR-NS ( $\mu\text{g/ml}$ )
0.0	0	0	0
0.5	0.04 $\pm$ 0.02	0.10 $\pm$ 0.06	1.54 $\pm$ 0.25
1.0	0.09 $\pm$ 0.07	0.28 $\pm$ 0.12	3.37 $\pm$ 0.36
1.5	0.22 $\pm$ 0.19	1.17 $\pm$ 0.17	6.52 $\pm$ 0.47
2.0	0.68 $\pm$ 0.14	2.08 $\pm$ 0.29	8.54 $\pm$ 0.59
2.5	1.06 $\pm$ 0.18	2.96 $\pm$ 0.11	6.98 $\pm$ 0.21
3.0	1.89 $\pm$ 0.36	3.44 $\pm$ 0.21	4.94 $\pm$ 0.19
3.5	2.91 $\pm$ 0.27	2.41 $\pm$ 0.23	3.46 $\pm$ 0.41
4.0	1.32 $\pm$ 0.17	1.64 $\pm$ 0.12	2.03 $\pm$ 0.18
4.5	0.98 $\pm$ 0.24	1.01 $\pm$ 0.12	1.46 $\pm$ 0.17
8.0	0.21 $\pm$ 0.11	0.35 $\pm$ 0.09	0.68 $\pm$ 0.14
12.0	0.10 $\pm$ 0.05	0.14 $\pm$ 0.05	0.31 $\pm$ 0.11
24.0	0.03 $\pm$ 0.01	0.06 $\pm$ 0.03	0.19 $\pm$ 0.10
48.0	ND	0.02 $\pm$ 0.01	0.07 $\pm$ 0.05

\* Data are shown as Mean $\pm$ SD, n=3, ND: Not detected

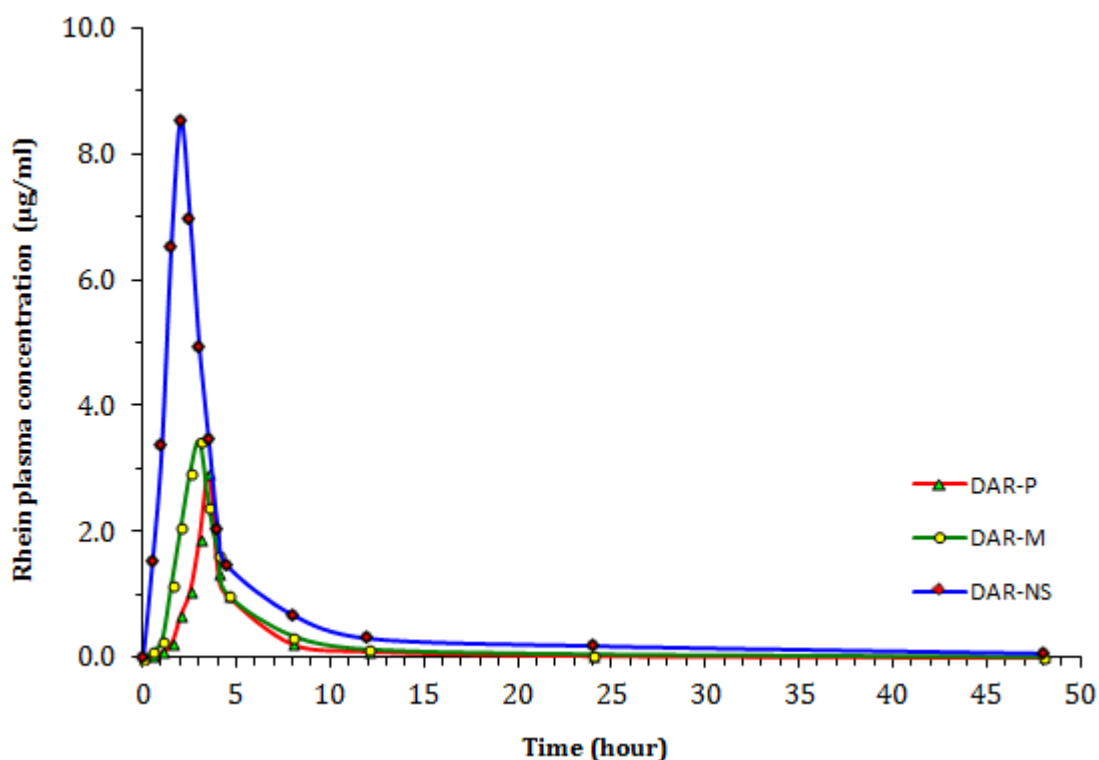


**Fig. 4.20** Graphical representation of rhein plasma profile for DAR-P, DAR-M and DAR-NS in Albino rabbits following oral administration.

**Table 4.22** Pharmacokinetic parameters after oral administration of DAR-P, DAR-M and DAR-NS in Albino rabbits.

Pharmacokinetic parameters*	DAR-P	DAR-M	DAR-NS
$C_{max}$ ( $\mu\text{g/ml}$ )	2.91 $\pm$ 0.26	3.44 $\pm$ 0.31 <sup>†</sup>	8.54 $\pm$ 0.23 <sup>†#</sup>
$T_{max}$ (h)	3.50 $\pm$ 0.23	3.00 $\pm$ 0.17 <sup>†</sup>	2.00 $\pm$ 0.14 <sup>†#</sup>
$AUC_{0-t}$ ( $\mu\text{g}\cdot\text{h/ml}$ )	7.83 $\pm$ 0.19	12.81 $\pm$ 0.62 <sup>†</sup>	30.90 $\pm$ 0.56 <sup>†#</sup>
$AUC_{0-\infty}$ ( $\mu\text{g}\cdot\text{h/ml}$ )	8.09 $\pm$ 0.36	13.19 $\pm$ 0.91 <sup>†</sup>	32.59 $\pm$ 0.97 <sup>†#</sup>
$AUMC_{total}$ ( $\mu\text{g}\cdot\text{h}^2/\text{ml}$ )	50.47 $\pm$ 2.31	89.95 $\pm$ 2.59 <sup>†</sup>	227.45 $\pm$ 4.87 <sup>†#</sup>
MRT (h)	6.16 $\pm$ 0.14	7.12 $\pm$ 0.09 <sup>†</sup>	7.06 $\pm$ 0.10 <sup>†#</sup>
$T_{1/2}$ (h)	7.94 $\pm$ 0.42	10.65 $\pm$ 0.57 <sup>†</sup>	13.62 $\pm$ 0.38 <sup>†#</sup>
$K_{elimination}$ ( $\text{h}^{-1}$ )	0.12 $\pm$ 0.02	0.07 $\pm$ 0.01 <sup>†</sup>	0.05 $\pm$ 0.01 <sup>†#</sup>
F (%) w.r.t DAR-P	100	163.60 <sup>†</sup>	394.64 <sup>†#</sup>

\* Data are shown as Mean $\pm$ SD, n=3, <sup>†</sup>P<0.05 compared with DAR-P, <sup>#</sup>P<0.05 compared with DAR-M.

### 4.3.7 Conclusion

The oral administration of drug is the most convenient way to transport the drug in body. But the poor water solubility of drugs leads to low dissolution rate, less transportation and influencing the absorption of drug in GIT. All these factors finally resulted in low bioavailability of drug which is the major problem in pharmaceutical field. Recently, drug delivery research mainly focusses on nanotechnology based approach for poorly water soluble drugs to increase their solubility and bioavailability. In nanoparticulate technology, nanosuspension has confirmed its importance and suitability for various classes of drugs with low solubility in order to improve their BA/BE performance. In addition to that, improvement in bioavailability leads to minimize the dose related side effects and increase in economical benefits.

The aim of the present study was to enhance the bioavailability of poorly water soluble drug Diacerein (DAR) by developing an orally administrable and efficient nanosuspension. DAR-NS was prepared by media milling method using Zirconium oxide beads. Preliminary optimization of formulation parameters was done systematically and critical variables were selected. The significant parameters such as drug concentration, stabilizer concentration and milling time were optimized by factorial design. Study revealed that the particle size can be greatly influenced by these factors. The optimized formulation contained 20% w/v of DAR, 2% w/v poloxamer 407 and 100% milling media in 5 ml double distilled water and comminution was carried out for 16 hours at room temperature. Efficient particle size (218.1 $\pm$ 3.6 nm) with low PDI (0.145 $\pm$ 0.007) by media milling was achieved using suitable excipients that provide physical stabilization (zeta potential-34.5 $\pm$ 0.3 mV) (steric and electrostatic) and improved saturation

solubility ( $509.47 \pm 2.28$   $\mu\text{g/ml}$ ) of water insoluble drug, DAR. Completely dried and fluffy powder was obtained by successful freeze drying of prepared DAR-NS with cryoprotectant, trehalose. The lyophilized powder was completely and easily re-dispersed in water.

DSC and XRD studies supported each other that DAR lost its crystallinity after nanosizing leads to better dissolution properties and sustained stability of the drug during its shelf life. The SEM images confirmed that the media milling process in presence of poloxamer 407 was effective in converting large aggregates of irregular shaped crystals of bulk DAR into submicron to nanometric range with relatively narrow size distribution. TEM photograph of DAR-NS revealed that the particles of DAR were discrete, non-aggregated, homogenously dispersed, nearly spherical in shape and were in accordance with particle size obtained by DLS method. Drug content of DAR-NS was found to be  $99.58 \pm 0.79\%$  which again proved the suitability of method for particle size reduction. The dissolution profiles of DAR-P, DAR-M and DAR-NS were checked in phosphate buffer pH-6.8, acetate buffer pH-4.5, 0.1N HCl and water over the test period of 120 mins. DAR-NS was found superior to DAR-P and DAR-M in terms of % cumulative release of DAR, dissolution efficiency and mean dissolution time. The prepared DAR-NS was found physically and chemically stable over a time period of 6 months.

*In vitro* Cell Cytotoxicity Studies (MTT Assay) confirmed the biocompatibility of DAR-NS and explains that composition of nanosuspension did not contribute to toxicity of Caco2 cells. *In vitro* assessment of permeability using Caco-2 cell line model demonstrated that DAR-NS was successfully enhanced the permeability of DAR by 6.63 and 4.52 fold to DAR-P and DAR-M respectively. *In vivo* assessment demonstrated that DAR-NS exhibited better pharmacokinetic properties compared to DAR-P and DAR-M. The relative oral bioavailability of DAR in Albino rabbits resulted from DAR-NS was found 3.94 and 2.41 fold greater than DAR-P and DAR-M, respectively. Thus it can be inferred that media milling is efficient method for nanosizing of DAR with poloxamer 407 which further leads to improved dissolution properties and excellent oral bioavailability of DAR from DAR-NS.

### 4.3.8 References

- 1 Sigfridsson, K., Forssén, S., Holländer, P., Skantze, U. & de Verdier, J. A formulation comparison, using a solution and different nanosuspensions of a poorly soluble compound. *Eur J Pharm Biopharm.* **67**, 540-547 (2007).
- 2 Van Eerdenbrugh, B. *et al.* Characterization of physico-chemical properties and pharmaceutical performance of sucrose co-freeze-dried solid nanoparticulate powders of the anti-HIV agent loviride prepared by media milling. *Int J Pharm.* **338**, 198-206 (2007).
- 3 Bhavsar, M. D., Tiwari, S. B. & Amiji, M. M. Formulation optimization for the nanoparticles-in-microsphere hybrid oral delivery system using factorial design. *J Control Release.* **110**, 422-430 (2006).
- 4 Zhang, X. *et al.* Formulation optimization of dihydroartemisinin nanostructured lipid carrier using response surface methodology. *Powder technology* **197**, 120-128 (2010).
- 5 Huang, Y.-B., Tsai, Y.-H., Lee, S.-H., Chang, J.-S. & Wu, P.-C. Optimization of pH-independent release of nifedipine hydrochloride extended-release matrix tablets using response surface methodology. *Int J Pharm.* **289**, 87-95 (2005).
- 6 Gupta, P., Hung, C. & Lam, F. Factorial design based optimization of the formulation of albumin microspheres containing adriamycin. *J Microencap* **6**, 147-160 (1989).
- 7 Bolton S & Bon C. *Pharmaceutical statistics: practical and clinical applications.* third edn, (Marcel Dekker Inc, 1997).
- 8 Box, G. E. & Wilson, K. On the experimental attainment of optimum conditions. *J Roy Stat Soc. Series B (Methodological)* **13**, 1-45 (1951).
- 9 Mak, K. W., Yap, M. G. & Teo, W. K. Formulation and optimization of two culture media for the production of tumour necrosis factor- $\beta$  in Escherichia coli. *J Chem Tech Biotech* **62**, 289-294 (1995).
- 10 Del Castillo, E., Montgomery, D. C. & McCarville, D. R. Modified desirability functions for multiple response optimization. *J Quality Tech* **28**, 337-345 (1996).
- 11 Derringer, G. Simultaneous optimization of several response variables. *J Quality Tech* **12**, 214-219 (1980).
- 12 Teeranachaideekul, V., Junyaprasert, V. B., Souto, E. B. & Müller, R. H. Development of ascorbyl palmitate nanocrystals applying the nanosuspension technology. *Int J Pharm.* **354**, 227-234 (2008).
- 13 Zhang, Y. *et al.* DDSolver: An Add-In Program for Modeling and Comparison of Drug Dissolution Profiles. *The AAPS Journal* **12**, 263-271 (2010).
- 14 Polli, J. E. In vitro studies are sometimes better than conventional human pharmacokinetic in vivo studies in assessing bioequivalence of immediate-release solid oral dosage forms. *The AAPS journal* **10**, 289-299 (2008).
- 15 Tavelin, S. *et al.* Prediction of the oral absorption of low-permeability drugs using small intestine-like 2/4/A1 cell monolayers. *Pharm Res* **20**, 397-405 (2003).
- 16 Press, B. & Di Grandi, D. Permeability for intestinal absorption: Caco-2 assay and related issues. *Curr Drug Metab.* **9**, 893-900 (2008).
- 17 Balimane, P. V., Han, Y.-H. & Chong, S. Current industrial practices of assessing permeability and P-glycoprotein interaction. *AAPS J* **8**, E1-E13 (2006).
- 18 Rubas, W. *et al.* Flux measurements across Caco-2 monolayers may predict transport in human large intestinal tissue. *J Pharm Sci.* **85**, 165-169 (1996).
- 19 Artursson, P. & Karlsson, J. Correlation between oral drug absorption in humans and apparent drug permeability coefficients in human intestinal epithelial (Caco-2) cells. *Biochem Biophys Res Commun.* **175**, 880-885 (1991).
- 20 Artursson, P. Cell cultures as models for drug absorption across the intestinal mucosa. *Crit Rev Ther Drug Carrier Syst.* **8**, 305-330 (1990).
- 21 Fogh J, Fogh JM & Orfeo T. One hundred and twenty seven cultured human tumor cell lines producing tumors in nude mice. *J Natl Cancer Inst.* **59**, 221-226 (1977).
- 22 Hidalgo, I. J., Raub, T. J. & Borchardt, R. T. Characterization of the human colon carcinoma cell line

- (Caco-2) as a model system for intestinal epithelial permeability. *Gastroenterology* **96**, 736-749 (1989).
- 23 Pinto M *et al.* Enterocyte-like differentiation and polarization of the human colon carcinoma cell line Caco-2 in culture. *Biol Cell*. **47**, 323-330 (1983).
- 24 Elsby, R., Surry, D., Smith, V. & Gray, A. Validation and application of Caco-2 assays for the in vitro evaluation of development candidate drugs as substrates or inhibitors of P-glycoprotein to support regulatory submissions. *Xenobiotica* **38**, 1140-1164 (2008).
- 25 Matsson, P. *et al.* Exploring the role of different drug transport routes in permeability screening. *J Med Chem*. **48**, 604-613 (2005).
- 26 Zhou, S. *et al.* Transport of the investigational anti-cancer drug 5, 6-dimethylxanthenone-4-acetic acid and its acyl glucuronide by human intestinal Caco-2 cells. *Eur J Pharm Sci*. **24**, 513-524 (2005).
- 27 Wang, Z., Hop, C. E., Leung, K. H. & Pang, J. Determination of in vitro permeability of drug candidates through a Caco-2 cell monolayer by liquid chromatography/tandem mass spectrometry. *J Mass Spectrom*. **35**, 71-76 (2000).
- 28 Alam, M. A., Mirza, M. A., Talegaonkar, S., Panda, A. K. & Iqbal, Z. Development of Celecoxib Complexes: Characterization and Cytotoxicity Studies in MCF-7. *Pharmaceut Anal Acta*. **4**, 1-8 (2013).
- 29 American Type Culture Collection. in *ATCC® 30-1010K* 1-6 (University Boulevard, Manassas, VA 20110 USA, 2011).
- 30 Spada, G., Gavini, E., Cossu, M., Rassu, G. & Giunchedi, P. Solid lipid nanoparticles with and without hydroxypropyl- $\beta$ -cyclodextrin: a comparative study of nanoparticles designed for colonic drug delivery. *Nanotechnology* **23**, 095101 (2012).
- 31 van Meerloo, J., Kaspers, G. L. & Cloos, J. in *Cancer Cell Culture Vol. 731 Methods in Molecular Biology* (ed Ian A. Cree) Ch. 20, 237-245 (Humana Press, 2011).
- 32 Khanavi, M. *et al.* Cytotoxic activity of some marine brown algae against cancer cell lines. *Biological research* **43**, 31-37 (2010).
- 33 Wang, X.-d. *et al.* Permeation of astilbin and taxifolin in Caco-2 cell and their effects on the P-gp. *Int J Pharm*. **378**, 1-8 (2009).
- 34 Sieuwerts, A. M., Klijjn, J. G., Peters, H. A. & Foekens, J. A. The MTT Tetrazolium Salt Assay Scrutinized: How to Use this Assay Reliably to Measure Metabolic Activity of Cell Cultures in vitro for the Assessment of Growth Characteristics, IC50-Values and Cell Survival. *Clin Chem Lab Med* **33**, 813-824 (1995).
- 35 Wallert and Provost Lab. 1-2 (Department of Chemistry and the Biochemistry and Biotechnology Program, University Moorhead, Minnesota 56563, Minnesota State, 2007).
- 36 Li, A. P. Screening for human ADME/Tox drug properties in drug discovery. *Drug Discov Today* **6**, 357-366 (2001).
- 37 Miret, S., Abrahamse, L. & de Groene, E. M. Comparison of in vitro models for the prediction of compound absorption across the human intestinal mucosa. *J Biomol Screen* **9**, 598-606 (2004).
- 38 Penzotti, J. E., Landrum, G. A. & Putta, S. Building predictive ADMET models for early decisions in drug discovery. *Curr Opinion Drug Discov Develop* **7**, 49-61 (2004).
- 39 van de Waterbeemd, H. & Jones, B. C. Predicting oral absorption and bioavailability. *Prog Med Chem* **41**, 1-59 (2003).
- 40 Avdeef, A. Physicochemical profiling (solubility, permeability and charge state). *Curr Top Med Chem*. **1**, 277-351 (2001).
- 41 Lipinski, C. A., Lombardo, F., Dominy, B. W. & Feeney, P. J. Experimental and computational approaches to estimate solubility and permeability in drug discovery and development settings. *Adv Drug Deliv Rev*. **46**, 3-26 (2001).
- 42 Hidalgo, I. J. Assessing the absorption of new pharmaceuticals. *Curr Top Med Chem*. **1**, 385-401 (2001).
- 43 Balimane, P. V., Chong, S. & Morrison, R. A. Current methodologies used for evaluation of intestinal permeability and absorption. *J Pharmacol Toxicol Methods*. **44**, 301-312 (2000).
- 44 Hillgren, K. M., Kato, A. & Borchardt, R. T. In vitro systems for studying intestinal drug absorption.

- Med Res Rev.* **15**, 83-109 (1995).
- 45 Hubatsch, I., Ragnarsson, E. G. & Artursson, P. Determination of drug permeability and prediction of drug absorption in Caco-2 monolayers. *Nature protocols* **2**, 2111-2119 (2007).
- 46 Stenberg, P., Norinder, U., Luthman, K. & Artursson, P. Experimental and computational screening models for the prediction of intestinal drug absorption. *J Med Chem.* **44**, 1927-1937 (2001).
- 47 Thiessen, J. J. in *The IUPHAR Compendium of Basic Principles For Pharmacological Research in Humans* Vol. 3 (eds Souich PD, Orme M, & Erill S) Ch. 8, 55-66 (IUPHAR, Department of Pharmacology, College of Medicine, University of California, Irvine, CA, USA, 2009).
- 48 Toutain, P.-L. & BOUSQUET-MÉLOU, A. Bioavailability and its assessment. *J Vet Pharmacol Therap.* **27**, 455-466 (2004).
- 49 Shin, S.-C., Bum, J.-P. & Choi, J.-S. Enhanced bioavailability by buccal administration of triamcinolone acetonide from the bioadhesive gels in rabbits. *Int J Pharm.* **209**, 37-43 (2000).
- 50 Zhang, Y., Huo, M., Zhou, J. & Xie, S. PKSolver: An add-in program for pharmacokinetic and pharmacodynamic data analysis in Microsoft Excel. *Comput Meth Prog Biomed* **99**, 306-314 (2010).
- 51 Liversidge, G. G. & Cundy, K. C. Particle size reduction for improvement of oral bioavailability of hydrophobic drugs: I. Absolute oral bioavailability of nanocrystalline danazol in beagle dogs. *Int J Pharm.* **125**, 91-97 (1995).
- 52 Reagan-Shaw S, Nihal M & Ahmad N. Dose translation from animal to human studies revisited. *The FASEB Journal\*Life Sciences Forum* **22**, 659-661 (2007).
- 53 Center for Drug Evaluation and Research-Center for Biologics Evaluation and Research. (U.S. Food and Drug Administration, Rockville, Maryland, USA, 2002).
- 54 Moghimi, S. M. & Hunter, A. C. Poloxamers and poloxamines in nanoparticle engineering and experimental medicine. *Trends in Biotech* **18**, 412-420 (2000).
- 55 Li, J.-T., Caldwell, K. D. & Rapoport, N. Surface Properties of Pluronic-Coated Polymeric Colloids. *Langmuir* **10**, 4475-4482 (1994).
- 56 Storm, G., Belliot, S. O., Daemen, T. & Lasic, D. D. Surface modification of nanoparticles to oppose uptake by the mononuclear phagocyte system. *Adv Drug Del Rev* **17**, 31-48 (1995).
- 57 Moghimi, S. M., Muir, I. S., Illum, L., Davis, S. S. & Kolb-Bachofen, V. Coating particles with a block copolymer (poloxamine-908) suppresses opsonization but permits the activity of dysopsonins in the serum. *Biochimica et biophysica acta* **1179**, 157-165 (1993).
- 58 Li, J.-T. & Caldwell, K. D. Plasma protein interactions with Pluronic™-treated colloids. *Coll Surf B: Biointerfaces* **7**, 9-22 (1996).
- 59 Ploehn, H. J. & Russel, W. B. in *Advances in Chemical Engineering* Vol. Volume 15 (ed Wei James) 137-228 (Academic Press, 1990).
- 60 Ali, H. S. M., York, P. & Blagden, N. Preparation of hydrocortisone nanosuspension through a bottom-up nanoprecipitation technique using microfluidic reactors. *Int J Pharm* **375**, 107-113 (2009).
- 61 Patravale, V. B., Date, A. A. & Kulkarni, R. M. Nanosuspensions: a promising drug delivery strategy. *J Pharm Pharmacol* **56**, 827-840 (2004).
- 62 Adinarayana, K. & Ellaiah, P. Response surface optimization of the critical medium components for the production of alkaline protease by a newly isolated *Bacillus* sp. *J Pharm Pharm Sci* **5**, 272-278 (2002).
- 63 Joyce, R. M. Experiment optimization in chemistry and chemical engineering, S. Akhnazarova and V. Kafarov, Mir Publishers, Moscow and Chicago, 1982, 312 *J Poly Sci: Poly Lett Edition* **22**, 372-372 (1984).
- 64 Montgomery, D. C. Using fractional factorial designs for robust process development. *Quality Engineering* **3** (1990).
- 65 George E P Box, J. S. H., William G Hunter *Statistics for Experimenters: Design, Innovation, and Discovery, 2nd Edition.* (John Wiley and Sons, 1978).
- 66 Abdelwahed, W., Degobert, G., Stainmesse, S. & Fessi, H. Freeze-drying of nanoparticles: formulation, process and storage considerations. *Adv Drug Deliv Rev* **58**, 1688-1713 (2006).
- 67 Jain NK., R., A. Development and characterization of nanostructured lipid carriers of oral

- hypoglycemic agent: selection of surfactants. *Int J Pharm Sci Rev Res* **7**, 125-130 (2011).
- 68 Nanjwade, B., Manjappa, AS, Murthy, RSR, Pol, YD. A novel pH-triggered in situ gel for sustained ophthalmic delivery of ketorolac tromethamine. *Asian J Pharm Sci* **4**, 189-199 (2009).
- 69 Dubernet, C. Pharmaceuticals and Thermal AnalysisThermoanalysis of microspheres. *Thermochimica Acta* **248**, 259-269 (1995).
- 70 Kashi, T. S. *et al.* Improved drug loading and antibacterial activity of minocycline-loaded PLGA nanoparticles prepared by solid/oil/water ion pairing method. *Int J Nanomed* **7**, 221-234 (2012).
- 71 Pardeike, J. *et al.* Nanosuspensions as advanced printing ink for accurate dosing of poorly soluble drugs in personalized medicines. *Int J Pharm* **420**, 93-100 (2011).
- 72 Jain, A., Singh, S. K., Singh, Y. & Singh, S. Development of lipid nanoparticles of diacerein, an antiosteoarthritic drug for enhancement in bioavailability and reduction in its side effects. *J Biomed Nanotech* **9**, 891-900 (2013).
- 73 Hintz, R. J. & Johnson, K. C. The effect of particle size distribution on dissolution rate and oral absorption. *Int J Pharm* **51**, 9-17 (1989).
- 74 Semete, B. *et al.* In vivo evaluation of the biodistribution and safety of PLGA nanoparticles as drug delivery systems. *Nanomed : Nanotech, Bio Med* **6**, 662-671 (2010).
- 75 Yee, S. In vitro permeability across Caco-2 cells (colonic) can predict in vivo (small intestinal) absorption in man--fact or myth. *Pharm Res* **14**, 763-766 (1997).
- 76 Xia, D. *et al.* Preparation of stable nitrendipine nanosuspensions using the precipitation-ultrasonication method for enhancement of dissolution and oral bioavailability. *Eur J Pharm Sci* **40**, 325-334 (2010).

#### 4.4 Part-2: Formulation of Diacerein inclusion complex with cyclodextrins

##### 4.4.1 Introduction

This chapter of the thesis has been aimed to develop and prepare a stable and efficient inclusion complex of poorly water soluble drug Diacerein (DAR) with cyclodextrin and derivatives to enhance the solubility, dissolution and bioavailability of DAR. The additional advantages of this technique include low hygroscopicity, less toxicity, high fluidity, excellent compatibility and compressibility of cyclodextrin complexation improves the stability of drugs in a formulation, resulting in longer shelf life. The objective of the study was achieved in following manner:

- a) To characterize the inclusion complexation of DAR in the liquid state i.e. Phase solubility studies of DAR with four different Cyclodextrins ( $\beta$ -cyclodextrin, hydroxypropyl- $\beta$ -cyclodextrin, methyl- $\beta$ -cyclodextrin and  $\gamma$ -cyclodextrin) were conducted and stability rate constants of the complexes were calculated.
- b) The inclusion complexes were prepared by different methods (i.e. physical mixing, kneading methods and slurry method followed by freeze drying) in different molar ratios and inclusion efficiencies were estimated.
- c) Solid state characterization of inclusion complex of DAR with Cyclodextrin was carried out by Differential Scanning Calorimetry (DSC), X-ray Diffraction (XRD) and Fourier Transform Infra-red spectroscopy (FTIR) analysis.
- d) Dissolution profile and % content of DAR in DAR inclusion complexes were checked.
- e) Stability studies of prepared inclusion complexes were carried out at  $5^{\circ}\text{C}\pm 3^{\circ}\text{C}$  (refrigerator) and at room temperature (RT) for a period of 6 months.
- f) *In-vitro* Cell Cytotoxicity Studies (MTT Assay) and *in-vitro* permeability assessment of DAR and its inclusion complex were attained using Caco-2 cell line model.
- g) Pharmacokinetic study was performed to evaluate the bioavailability and other pharmacokinetic parameters of DAR and its inclusion complex *in-vivo* animal model.

##### 4.4.2 Preparation of Diacerein inclusion complexes

The Cyclodextrins (CDs) used for the preparation of inclusion complexes were  $\beta$ -CD, HP- $\beta$ -CD, M- $\beta$ -CD and  $\gamma$ -CD. The DAR-CDs inclusion complexes were prepared in 1:1, 1:2 and 1:3 molar ratios by using two different methods (1) Kneading method and (2)

Freeze drying method and compared with the Physical mixtures of CDs and DAR in the respective molar ratios.

#### **4.4.2.1 Physical Mixture**

The physical mixture was prepared by mixing of pulverized powder of DAR and selected CDs ( $\beta$ -CD, HP- $\beta$ -CD, M- $\beta$ -CD and  $\gamma$ -CD) in 1:1, 1:2 and 1:3 drug-CD molar ratios individually. The specified quantities of DAR and CD were accurately weighed individually according to the molar ratio and transferred in a glass vial and sealed. The vial was shaken vigorously to mix the content completely. The mixture then passed through sieve (mesh # 100) and stored in dessicator containing activated silica gel until further evaluation.

#### **4.4.2.2 Kneading Method**

Inclusion complexes of DAR with various cyclodextrins (i.e.  $\gamma$ -CD,  $\beta$ -CD, HP- $\beta$ -CD and M- $\beta$ -CD) in different molar ratios like 1:1, 1:2 and 1:3 were prepared using Kneading method. First of all, a specified and accurately weighed quantity of cyclodextrin as per the pre-decided molar ratio was added to the mortar and small quantity of water was added while triturating to get slurry like consistency. Then accurately weighed quantity of DAR was slowly incorporated in the small parts into the slurry with continuous trituration. Trituration was continued for 1 hour. The viscosity of the mixture increased indicating the formation of the complex. Finally the mixture was dried in an oven at 45°C. The mixture was ground to get a fine powder and passed through sieve (mesh # 100). All the prepared inclusion complexes were stored in dessicator containing activated silica until further evaluation.

#### **4.4.2.3 Freeze drying method**

Inclusion complexes of DAR with various cyclodextrins (i.e.  $\gamma$ -CD,  $\beta$ -CD, HP- $\beta$ -CD and M- $\beta$ -CD) in different molar ratios like 1:1, 1:2 and 1:3 were prepared using freeze drying method. In this method, the specified quantity of cyclodextrin (as per the DAR:CD molar ratio) was transferred in a glass vial containing 10 ml of distilled water and sonicated to dissolve. Then the corresponding quantity of DAR was added and stirred at a high speed magnetic stirrer for 24 hrs at 25°C. Afterwards, the mixture was centrifuged at 5000 rpm for 15mins and clear solution was separated. The obtained solution was freeze-dried immediately after preparation. The acquired solution was filled into glass vials and frozen at -70°C for 24 hr using an ultra cold deep freezer; later the samples were freeze-dried using a Lyophilizer (Heto Dry Winner, Germany) for 24 hr to yield dry

powder.

#### **4.4.3 Selection of Inclusion Complex**

The best suitable carrier (i.e. CD) and DAR:CD molar ratio were selected on the basis of phase solubility experiment and inclusion efficiency.

##### **4.4.3.1 Phase solubility Study**

Higuchi and Connors, presented a very successful technique, 'phase solubility method' to study the cyclodextrin inclusion complexation which examines the effect of complexing agents on the compound being solubilized<sup>1</sup>. The practical and phenomenological implications of phase-solubility analysis were developed by Higuchi and Connors in their pioneering work published in 1964<sup>1</sup> and as later reviewed by Connors<sup>2</sup>.

Based on the shape of the generated phase-solubility relationships, several types of behaviors can be identified<sup>3</sup>. Phase solubility diagrams are categorized into A and B types; A type curves indicate the formation of soluble inclusion complexes while B type suggest the formation of inclusion complexes with poor solubility. A B<sub>S</sub> type response denotes complexes of limited solubility and a B<sub>I</sub> curve indicates insoluble complexes. A-type curves are subdivided into A<sub>L</sub> (linear increases of drug solubility as a function of CD concentration), A<sub>P</sub> (positively deviating isotherms), and A<sub>N</sub> (negatively deviating isotherms) subtypes. The complex formation with 1:1 stoichiometry gives the A<sub>L</sub> type diagrams, where as the higher order complex formation in which more than one cyclodextrin molecules are involved in the complexation gives the A<sub>P</sub> type. The interaction mechanism for the A<sub>N</sub> type is complicated, because of a significant contribution of solute-solvent interaction to the complexation<sup>4</sup>. Less soluble natural cyclodextrin (e.g. β-CD) often gives rise to B-type curves due to their poor water solubility whereas the more soluble chemically modified CDs (like HP-β-CD and SBE-β-CD) usually produce soluble complexes and thus give A-type systems. The most common type of cyclodextrin complex is the 1:1 drug-cyclodextrin complex (D-CD) where one drug molecule (D) forms a complex with one cyclodextrin molecule.

Under such conditions an A<sub>L</sub>-type phase-solubility diagram, with slope less than unity, would be observed and the equilibrium/binding/association/stability constant (K<sub>S</sub>) of the complex can be calculated from the slope of the linear portion of curve and the intrinsic solubility (S<sub>0</sub>) of the drug in the aqueous complexation media (i.e. drug solubility when no cyclodextrin is present):

$$\text{Stability constant (K}_s\text{)} = \frac{\text{Slope}}{S_o(1 - \text{Slope})}$$

The value of stability constant ( $K_s$ ) is most often between 50 and 2000  $M^{-1}$  with a mean value of 129, 490 and 355  $M^{-1}$  for  $\alpha$ -,  $\beta$ - and  $\gamma$ -cyclodextrin, respectively<sup>5</sup>.

### Experiment

An excess amount of plain DAR (50mg) was introduced into several 15ml stoppered glass tubes and 5ml of aqueous vehicle of containing successively larger concentrations (5-30mM/L) of the CDs (i.e.  $\beta$ -CD, HP- $\beta$ -CD, M- $\beta$ -CD and  $\gamma$ -CD) were added separately. The tubes were shaken for 48 hours at 80cycles/min at room temperature using Rotospin Test tube Rotator (Tarsons Products Pvt. Ltd. New Delhi, India). At equilibrium after 48 hours, aliquots were withdrawn, filtered with 0.45  $\mu\text{m}$  Nylon filters and suitably diluted, if needed. Concentrations of DAR in solutions were determined using UV spectrophotometer (UV-1700, Shimadzu, Japan) at 257nm (Refer Section 3.1.2). The phase solubility studies were further also carried out in HCl pH-1.2 and Phosphate buffer pH-6.8 instead of water.

The phase-solubility profiles were then constructed between the concentrations of DAR (at Y-axis) and different mM concentrations of CDs (i.e.  $\beta$ -CD, HP- $\beta$ -CD, M- $\beta$ -CD and  $\gamma$ -CD) at X-axis. The stability constants ( $K_s$ ) were calculated and types of phase solubility graphs were predicted.

#### 4.3.3.2 Inclusion efficiency estimation

All Freeze dried inclusion complexes, kneaded mixtures and physical mixtures of DAR with cyclodextrins (i.e.  $\beta$ -CD, HP- $\beta$ -CD, M- $\beta$ -CD and  $\gamma$ -CD) prepared in the selected molar ratios of DAR:CD (1:1, 1:2 and 1:3) were weighed accurately (50 mg) and transferred in 50 ml volumetric flasks individually. 10 mL of DMSO was added, mixed thoroughly and sonicated for 10 min to dissolve the content at ambient temperature. The volume was made up to mark with methanol and resulting solution was suitably diluted with methanol for further analysis. Concentration of DAR in solutions was determined using UV spectrophotometer (UV-1700, Shimadzu, Japan) at 257nm (Refer Section 3.1.2). Inclusion efficiency was calculated using the formula<sup>6</sup>:-

$$\% \text{ Inclusion Efficiency (\% IE)} = \frac{\% \text{ Drug Content}_{\text{Experimental}}}{\% \text{ Drug Content}_{\text{Theoretical}}} \times 100$$

Where;

$$\% \text{ Drug Content}_{\text{Theoretical}} = \frac{\text{Actual amount of drug added}}{\text{Total weight of (Drug + carrier)}} \times 100$$

and

$$\% \text{ Drug Content}_{\text{Experimental}} = \frac{\text{Amount of drug extracted}}{\text{Amount of inclusion complex taken}} \times 100$$

#### 4.4.4 Characterization of selected Inclusion complex

The Physical mixture, Kneaded mixture and Freeze dried solid of selected inclusion complex in defined molar ratio were further characterized for FTIR Spectroscopy, DSC Study and XRD analysis. The final product was analyzed for % drug content. The inclusion complex was subjected to *in-vitro* dissolution study and compared with marketed formulation ((Dycerin, Label claim-50mg) and plain DAR. Stability studies of lyophilized inclusion complex was performed. Comparative *in-vitro* cytotoxicity study (MTT Assay) and *in-vitro* permeability study of freeze dried inclusion complex and plain DAR were carried out using Caco-2 cell lines. Finally relative bioavailability of finalized inclusion complex was evaluated by comparing with bioavailabilities of plain DAR and marketed formulation.

##### 4.4.4.1 FTIR Spectroscopy

The FTIR spectra for plain DAR, pure HP- $\beta$ -CD, physical mixture of DAR:HP- $\beta$ -CD, Kneaded mixture of DAR:HP- $\beta$ -CD and freeze dried inclusion complexes of DAR:HP- $\beta$ -CD in defined molar ratio were obtained using a Bruker ALPHA FT-IR spectrometer equipped with DTGS detector and OPUS/Mentor software (Bruker Optics, Germany). The samples were prepared in KBr disc (2 mg sample in 200 mg KBr). Data were collected over a spectral region from 4000  $\text{cm}^{-1}$  to 600  $\text{cm}^{-1}$  with resolution 4  $\text{cm}^{-1}$  and 100 scans.

##### 4.4.4.2 Differential Scanning Calorimetric (DSC) Analysis

The plain DAR, pure HP- $\beta$ -CD, physical mixture of DAR:HP- $\beta$ -CD, Kneaded mixture of DAR:HP- $\beta$ -CD and freeze dried inclusion complexes of DAR:HP- $\beta$ -CD in selected molar ratio were investigated for their thermal properties, physical state and recognition of inclusion complex using Differential Scanning Calorimeter (DSC 60-A, Shimadzu, Japan). When the drug molecules were encapsulated in CD cavity, their melting, boiling or sublimation points generally shifted to a different temperatures which indicate some interaction between host and guest molecule<sup>7</sup>. Accurately weighed samples (4-7 mg) were placed in hermetically sealed aluminium pans and empty pan was used as a

reference. Heating scans by heat runs for each sample was set from 30 °C to 300 °C at 10 °C min<sup>-1</sup> in a nitrogen atmosphere.

#### **4.4.4.3 Powder X-Ray Diffraction (XRD) Study**

The XRD spectra of plain DAR, pure HP-β-CD, physical mixture of DAR:HP-β-CD, Kneaded mixture of DAR:HP-β-CD and freeze dried inclusion complexes of DAR:HP-β-CD in selected molar ratio were obtained using X-Ray Diffractometer (X-Pert-PRO, PANalytical, Netherland). The samples were mounted on a sample holder and XRD patterns were recorded in the range of  $3^\circ < 2\theta < 50^\circ$  at the speed of 5° min<sup>-1</sup>.

#### **4.4.4.4 Percentage drug content in lyophilized inclusion complex**

Accurately weighed lyophilized powder of DAR:HP-β-CD inclusion complex in selected molar ratio (equivalent to 25 mg of DAR) was transferred in a 25 ml volumetric flask and 5 ml DMSO was added. Content was sonicated to dissolve and volume was made up to the mark with diluent. The sample solution was centrifuged at 15,000 rpm for 10 minutes (Sigma centrifuge, Osterode, Germany) and supernatant was filtered with 0.22 μm pore size disposable filter (Millipore India, Bangalore). Filtrate was suitably diluted with diluent to get the sample concentration at 10 μg/ml. Standard solution of DAR (10 μg/ml) was also prepared and both the solutions were injected into the HPLC system (Shimadzu, Japan). (For instrumentation, chromatographic conditions and method refer Section 3.1.3) Each determination was performed in triplicate, chromatograms were recorded and average % content of DAR in the formulation and standard deviation was calculated.

#### **4.4.4.5 In vitro dissolution study**

*In vitro* release studies of lyophilized powder of DAR:HP-β-CD inclusion complex in selected molar ratio, marketed formulation ((Dycerin, Label claim-50mg) and plain DAR were carried out in different dissolution mediums (i.e. Distilled water, Phosphate Buffer pH-6.8, Acetate Buffer pH-4.5 and 0.1N HCl) using USP dissolution apparatus II (paddle method). Dissolution studies were carried out using clear hard gelatin capsules (Size 0) filled with an accurately weighed quantity of lyophilized powder of DAR:HP-β-CD inclusion complex (equivalent to 50 mg of DAR). The experiments were performed on 900mL media at 37°C at a rotation speed of 75 rpm. At preselected time intervals, 5 mL samples were withdrawn, filtered immediately and replaced with 5 mL of pre-thermostated fresh dissolution medium. Quantitative determination was performed by UV spectrophotometer at 257 nm. Dissolution tests were performed in triplicate and

graph of percent cumulative drug release vs time was plotted. Dissolution profiles were further evaluated on the basis of Dissolution efficiency (DE), Dissolution percentage at 5 min and 60 min (DP<sub>5</sub> and DP<sub>60</sub>), time required to release 50% and 90% of drug (t<sub>50</sub> and t<sub>90</sub>), Mean dissolution time (MDT) and Area under curve (AUC). The DDSolver, an Excel add-in software package, which is designed to analyze data obtained from dissolution experiments was used to calculate different dissolution parameters<sup>8</sup>.

#### **4.4.4.6 Stability Studies**

Stability studies of lyophilized DAR:HP-β-CD inclusion complex in selected molar ratio was carried out at 5°C±3°C (refrigerator) and at room temperature (RT) for a period of 6 months. Periodically, samples were withdrawn at 1<sup>st</sup>, 3<sup>rd</sup> and 6<sup>th</sup> month and subjected to examined for chemical stability. Chemical stability was checked by assessing the percentage content of DAR in stored formulations.

#### **4.4.5 Cell Line Studies of DAR and its Inclusion complex with HP-β-CD using Caco-2 cell line model**

In the present research scenario, in-vitro cytotoxicity study and permeability assessment using Caco-2 cell line, are essential experiment for the drug development and discovery. Caco-2 cell lines have been extensively used for such types of experiments due to their wide acceptability and applicability. In this section, we studied the cytotoxicity and intestinal permeability of developed DAR: HP-β-CD inclusion complex and plain DAR, using Caco-2 cell lines as best fitted model.

##### **4.4.5.1 Cell Culture**

Same as described in Section 4.6.1.

##### **4.4.5.2 *In vitro* Cell Cytotoxicity Studies (MTT Assay)**

###### **Experiment**

MTT stock solution (1 mg/ml) was prepared by dissolving accurately weighed 10 mg of MTT reagent powder with 10 ml phosphate buffered saline (PBS) in an amber colored 10 ml volumetric flask. The stock solution was stored in dark place at 4°C till the further use.

The *in vitro* cytotoxicity of lyophilized DAR:HP-β-CD inclusion complex and plain DAR was evaluated for Caco-2 cells using MTT assay. The cells were cultured in 96-well plates (prelabelled as 4 hour, 24 hour and 48 hour) at a seeding density of 1.0×10<sup>4</sup> cells/well for 48 hours. Samples were dissolved in DMSO and different dilutions were made with DMEM culture medium so that the concentration of DMSO did not exceed

more than 1% v/v in any diluted sample. Experiments were initiated by replacing the culture medium in each of 96 well of each plate with 100µl of sample solutions (0.1, 1, 10, 100, 250, 500 & 1000 µg/ml) and incubated at 37°C in ~85% relative humidity and ~5% CO<sub>2</sub> environment. After 4 hour of incubation, prelabelled 4 hour-96 well plate was removed from incubator into laminar flow hood area, sample solution was discarded and 100µl of MTT reagent (1 mg/ml) in phosphate buffered saline (PBS) was added aseptically. The plate was again incubated at 37°C in ~5% CO<sub>2</sub> environment for another 4 hours. At the end of incubation period, medium was removed carefully and intracellular formazan was solubilized with 100µl DMSO by agitating cells on orbital shaker for 15 mins. Absorbance was measured at 590 nm with a reference filter of 620 nm using Micro plate multi detection instrument (680-XR, Bio-Rad Laboratories, France). The medium treated cells were used as controls. Same procedure was followed for 24 hour and 48 hour plates.

### **Statistical analysis**

All calculations, graph preparations and statistical analysis were performed using Microsoft Excel. Percentage of cell viability was calculated based on the absorbance measured relative to the absorbance of cells exposed to the negative control. To compare the sensitivity of cells to the DAR and its formulation, IC<sub>50</sub> values (concentration of the drug that leads to 50% inhibition in cell proliferation) were calculated.

#### **4.4.5.3 *In vitro* cell permeability assessment of DAR:HP-β-CD inclusion complex**

Among the various techniques available for the prediction of intestinal permeability, the Caco-2 cell lines has been widely used and referred as identical model of the intestinal barrier<sup>9,10</sup>. These human cells are capable to grow into differentiated monolayers with well established tight junctions and brush border membrane as well as to express several membrane transporters and metabolizing enzymes, allowing the measurement of functional permeability (both passive diffusion and active transport)<sup>11,12</sup>. As a result, this assay is widely accepted by both the pharmaceutical industry and regulatory bodies as the permeability determined using Caco-2 cell lines associates well with oral absorption in humans<sup>13-15</sup>.

### **Experiment**

Caco-2 cell passage 40-45 cultured in 12 well cell culture inserts (pore size-0.4µm, diameter-12/18 mm, area-1.13 cm<sup>2</sup>, Product code 12565009, NUNC™, Roskilde,

Denmark), were used for *in vitro* permeability assessment of lyophilized DAR:HP- $\beta$ -CD inclusion complex and plain DAR after 21 days post seeding. Prior to the experiment, the inserts were washed twice and equilibrated for 30 mins with pre-warmed transport medium (Hank's balanced salt solution-HBSS containing 25 mM of HEPES, pH-7.4). Accurate quantity of samples were dispersed in transport medium to prepare the solutions having DAR concentration at 250  $\mu$ g/ml and sonicated. The integrity of the monolayers were checked by monitoring the permeability of paracellular leakage marker (Lucifer Yellow) across the monolayer. Quantification of Lucifer yellow was performed using a Spectrofluorimeter using excitation wavelength at 485 nm and emission wavelength at 530 nm. The cell monolayers were considered tight enough for the transport experiment enough when the apparent permeability coefficient ( $P_{app}$ ) for Lucifer Yellow was less than  $0.5 \times 10^{-6}$  cm/s. All Transport studies were conducted aseptically at 37°C in an atmosphere of ~85% relative humidity and ~5% CO<sub>2</sub>. The 150  $\mu$ l of transport buffer containing 250  $\mu$ g/ml test compounds was added to the apical side while the basolateral side of the inserts contained 1.5 ml of transport medium. After the incubation 30, 60, 120, 180, 240 and 480 mins, aliquot of 100  $\mu$ l was withdrawn from the receiver chamber and was immediately replenished with an equal volume of pre-warmed transport medium. The samples were stored at -20°C until analyzed. The concentration of the test compounds in the transport medium were analyzed using developed RP-HPLC method as described in Section 3.1.4. The apical to basolateral permeability coefficient ( $P_{app}$  in cm/sec) was calculated according to following equation:

$$P_{app} = \frac{dQ/dt}{A \times C_0 \times 60}$$

where, dQ/dt (flux) is the amount of drug transported across the monolayer from apical to basolateral compartment as a function of time (mg/min), A is the monolayer membrane surface area (cm<sup>2</sup>) and C<sub>0</sub> is the initial concentration of drug on the apical compartment (mg/ml).

#### **4.4.6 Pharmacokinetic evaluation of lyophilized DAR:HP- $\beta$ -CD inclusion complex using *in vivo* animal model**

In this study, pharmacokinetic behaviors of the prepared lyophilized DAR:HP- $\beta$ -CD inclusion complex, plain DAR and marketed formulation were investigated to know the outcome of complexation of DAR with HP- $\beta$ -CD on oral bioavailability of DAR. The plots

of drug plasma concentration vs time were plotted for DAR after oral administration of lyophilized inclusion complex and compared it with plain DAR and marketed formulation (Dycerin). Non compartmental pharmacokinetic analysis was performed<sup>16</sup>. Various pharmacokinetic parameters were calculated using the computer based statistical package PKsolver add-in for microsoft excel<sup>17</sup>. The calculated parameters are Maximum plasma concentration ( $C_{max}$ ), Time to achieve maximum plasma concentration ( $T_{max}$ ), Area under the plasma concentration-time curve from time zero to t ( $AUC_{0-t}$ ), Elimination rate constant ( $-K_{elimination}$ ), Elimination half life ( $t_{1/2}$ ), Area under the plasma concentration-time curve from time zero to infinity ( $AUC_{0-\infty}$ ), Area under momentum curve (AUMC), Mean residence time (MRT) and Relative bioavailability (%F)<sup>18</sup>.

#### 4.4.6.1 Animals

Same as described in Section 4.7.1.

#### 4.4.6.2 Experimental: Dosing and sampling

Relative bioavailability of lyophilized DAR:HP- $\beta$ -CD inclusion complex was evaluated by comparing the bioavailability of DAR-inclusion complex with bioavailabilities of plain DAR and marketed formulation. The maximum dose of DAR that can be given to a adult human in a single day is 100 mg. So as described in section 4.3.5.2, the dose of DAR for rabbits was calculated to be 5.14 mg/kg. In this study, the DAR dose given to the rabbits is 9.25 mg/1.8 kg rabbit weight.

Animals were divided in three treatment groups and each group contained 9 rabbits. The animals were fasted over night prior to the experiment with free access of water. The lyophilized DAR:HP- $\beta$ -CD inclusion complex, plain DAR and marketed formulation (equivalent to 9.250 mg of DAR) were filled in hard gelatin capsule (Capsugel®#size 5) and administered orally. Blood samples (1.5 ml) were collected through marginal ear vein using fresh sterilized disposable needles and syringes in heparinized tubes at 0, 0.5, 1, 1.5, 2, 2.5, 3, 3.5, 4, 4.5, 8, 12, 24 and 48 hours after administration. Collected blood samples were vortexed for 1 min and centrifuged at 20,000 rpm for 10 mins at 4°C (Ultra-centrifuge, 3K 30 Sigma Laboratory Centrifuge, Osterode, Germany). Separated plasma samples were withdrawn and stored at -20°C until further processing.

#### 4.4.6.3 Instrumental and statistical analysis

Collected plasma samples were extracted and analyzed by using developed RP-HPLC method (Chapter 3, Section 3.2.5). The drug plasma concentrations were determined from the calibration curve. Non-compartmental trapezoidal method was employed to

calculate the area under the curve (AUC) of plasma concentration as a function of time (t). All data were reported as mean  $\pm$  SD. The statistical significance of the differences between the groups was tested by one-way ANOVA followed by Bonferroni multiple comparison test.

#### 4.4.7 Result and Discussion

##### 4.4.7.1 Selection of Inclusion complex

##### 4.4.7.1.1 Phase solubility Analysis

Phase solubility analysis has been the very important and initial requirement for optimizing the development process of an inclusion complex of a drug as it allows the assessment of affinity between CD and drug molecule in aqueous phase. Phase solubility study provides the stability constant for drug-cyclodextrin inclusion complex as well as it also present the insight into stoichiometry of the complex at equilibrium<sup>19</sup>. The phase-solubility profiles were constructed between the apparent equilibrium concentrations of DAR (at Y-axis) and defined concentrations of CDs (i.e.  $\beta$ -CD, HP- $\beta$ -CD, M- $\beta$ -CD and  $\gamma$ -CD) at X-axis in water, phosphate buffer pH-6.8 and HCl pH-1.2 as shown in the Fig 4.21, 4.22 and 4.23 respectively. The slopes, intercepts,  $R^2$  and calculated stability constants ( $K_s$ ) were tabulated and types of phase solubility graphs were predicted (Table 4.23).

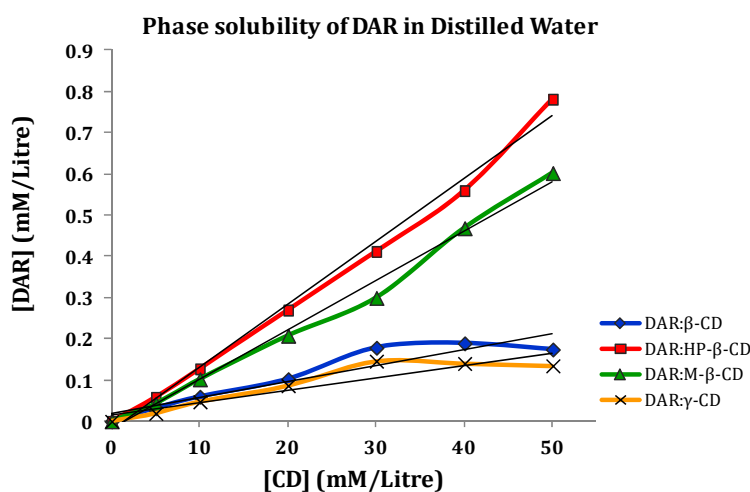


**Fig. 4.21** Phase solubility studies of DAR with CDs in distilled water.

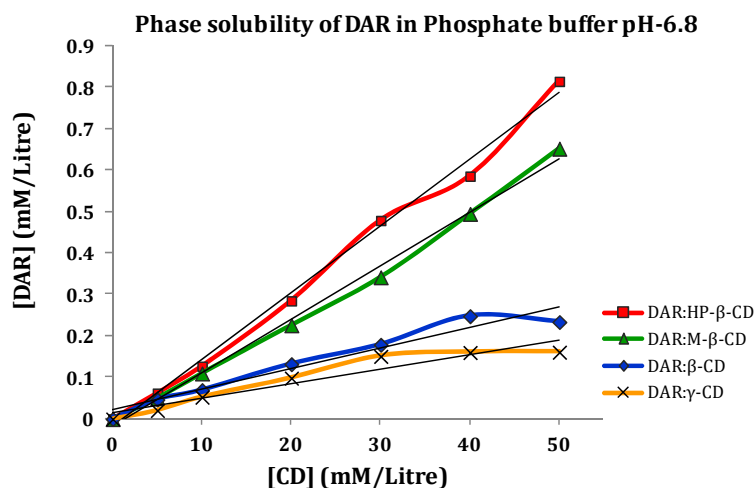


**Fig. 4.22** Phase solubility studies of DAR with CDs in Phosphate Buffer pH6.8.

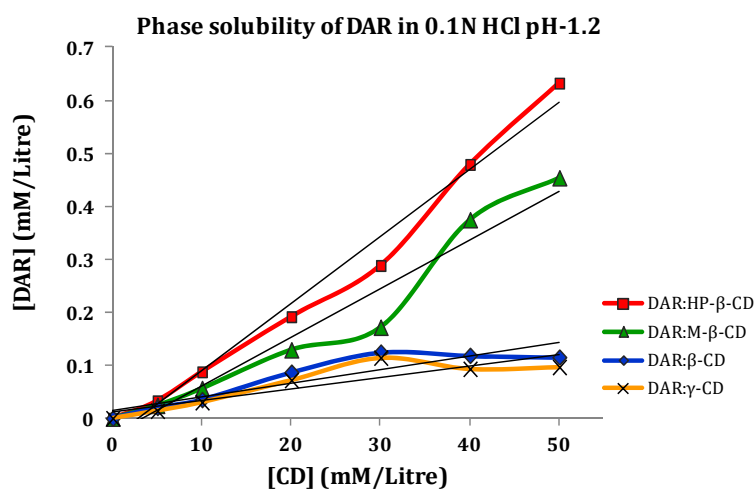


**Fig. 4.23** Phase solubility studies of DAR with CDs in 0.1N HCl pH-1.2.

**Table 4.23** Comparison of slopes, intercepts, R<sup>2</sup> and K<sub>s</sub> of phase solubility studies in water, phosphate buffer pH-6.8 and HCl pH-1.2 for DAR with CDs.

Drug:CD	Slope	Intercept	R <sup>2</sup>	K <sub>s</sub> (M <sup>-1</sup> )	Type of Graph
<b>In Distilled Water*</b>					
DAR: HP-β-CD	0.015±0.001	0.022±0.002	0.992±0.002	<b>711.5±6.9</b>	A <sub>L</sub> -Type
DAR: M-β-CD	0.012±0.002	0.019±0.003	0.989±0.009	629.3±9.2	A <sub>L</sub> -Type
DAR: β-CD	0.004±0.001	0.019±0.002	0.887±0.005	207.2±8.4	A <sub>N</sub> -Type
DAR: γ-CD	0.003±0.001	0.015±0.004	0.860±0.005	196.7±3.7	A <sub>N</sub> -Type
<b>In Phosphate Buffer, pH-6.8*</b>					
DAR: HP-β-CD	0.016±0.002	0.021±0.001	0.994±0.002	<b>806.1±11.7</b>	A <sub>L</sub> -Type
DAR: M-β-CD	0.013±0.003	0.018±0.002	0.984±0.003	726.0±8.6	A <sub>L</sub> -Type
DAR: β-CD	0.005±0.001	0.020±0.002	0.950±0.008	255.01±6.5	A <sub>N</sub> -Type
DAR: γ-CD	0.004±0.002	0.015±0.001	0.915±0.006	242.2±6.1	A <sub>N</sub> -Type
<b>In HCl pH-1.2*</b>					
DAR: HP-β-CD	0.013±0.001	0.035±0.003	0.986±0.005	<b>366.7±7.4</b>	A <sub>L</sub> -Type
DAR: M-β-CD	0.009±0.001	0.032±0.002	0.952±0.003	294.8±5.8	A <sub>L</sub> -Type
DAR: β-CD	0.003±0.002	0.015±0.002	0.840±0.008	173.8±8.9	A <sub>N</sub> -Type
DAR: γ-CD	0.002±0.001	0.013±0.003	0.794±0.004	168.4±9.7	A <sub>N</sub> -Type

\* Data are shown as Mean±SD, n=3

The results indicated that the low solubility of DAR was increased linearly with all the CDs in all the mediums and the value of K<sub>s</sub> for inclusion complex increased in the order of (DAR:HP-β-CD)>(DAR:M-β-CD)>(DAR:β-CD)>(DAR:γ-CD). The smaller values of K<sub>s</sub> (less than 200 M<sup>-1</sup>) indicate a weak interaction between drug and CD, while larger values of K<sub>s</sub> (more than 1000 M<sup>-1</sup>) are symptomatic of an incompatible drug release from the inclusion complex<sup>20</sup>. The resultant values of K<sub>s</sub> predicted that HP-β-CD and M-β-CD formed sufficiently stable inclusion complex with DAR where as the stability of DAR:β-CD and DAR:γ-CD were not found good, comparatively. The linear increase in solubility of DAR with increase in CDs concentration, giving rise to A<sub>L</sub>-type phase solubility diagram for DAR:HP-β-CD and DAR:M-β-CD while DAR:β-CD and DAR:γ-CD showed A<sub>N</sub>-type of solubility curves at different pH values. The R<sup>2</sup> values were also increased in the order of (DAR:HP-β-CD)>(DAR:M-β-CD)>(DAR:β-CD)>(DAR:γ-CD). It can be seen that DAR:HP-β-CD and DAR:M-β-CD possess good stability but K<sub>s</sub> for DAR:HP-β-CD was greater in all the mediums and found highest in phosphate buffer pH-6.8. This may be due to acidic nature of DAR which was completely unionized at this pH and lead to formation of a stable complex with HP-β-CD. The pH value has significant influence on the interaction mode between drug and CDs, indicating the different affinity of acidic, neutral and basic drugs for the inclusion complex formation and additionally the increase in drug ionization at particular pH resulted in decrease of the

complex stability constant<sup>21,22</sup>. On the basis of phase solubility study, it can be concluded that DAR:HP- $\beta$ -CD formed most stable inclusion complex with highest solubility, among the four.

#### 4.4.7.1.2 Inclusion efficiency estimation

Inclusion efficiencies of all Freeze dried inclusion complexes, kneaded mixtures and physical mixtures of DAR with cyclodextrins (i.e.  $\beta$ -CD, HP- $\beta$ -CD, M- $\beta$ -CD and  $\gamma$ -CD) in the selected molar ratios of DAR:CD (1:1, 1:2 and 1:3) were determined and results were presented in Table 4.24. The results clearly showed that the %IE of DAR: HP- $\beta$ -CD inclusion complex in molar ratio of 1:2 was found higher for physical mixture (72.39% $\pm$ 2.87%), kneaded mixture (84.61% $\pm$ 1.28%) and freeze dried inclusion complex (99.32% $\pm$ 1.41%) than the other inclusion complexes prepared by respective mode of preparation. It indicated that DAR was uniformly distributed in DAR:HP- $\beta$ -CD inclusion complex in molar ratio of 1:2 and others did not show satisfactory drug incorporation.

**Table 4.24** Inclusion efficiency values of all Freeze dried inclusion complexes, kneaded mixtures and physical mixtures of DAR with cyclodextrins ( $\beta$ -CD, HP- $\beta$ -CD, M- $\beta$ -CD and  $\gamma$ -CD) in 1:1, 1:2 and 1:3 molar ratios of DAR:CD.

DAR:CD	% Inclusion Efficiency (% IE)*		
	For molar ratio (1:1)	For molar ratio (1:2)	For molar ratio (1:3)
<b>Physical Mixtures</b>			
DAR: HP- $\beta$ -CD	40.18 $\pm$ 1.52	<b>46.39<math>\pm</math>2.87</b>	32.44 $\pm$ 1.63
DAR: M- $\beta$ -CD	31.98 $\pm$ 3.66	35.21 $\pm$ 2.54	29.21 $\pm$ 1.92
DAR: $\beta$ -CD	22.27 $\pm$ 4.12	28.36 $\pm$ 2.96	29.15 $\pm$ 2.03
DAR: $\gamma$ -CD	25.68 $\pm$ 0.98	27.57 $\pm$ 2.74	31.62 $\pm$ 1.28
<b>Kneaded Mixtures</b>			
DAR: HP- $\beta$ -CD	57.63 $\pm$ 2.51	<b>64.61<math>\pm</math>1.28</b>	53.29 $\pm$ 1.92
DAR: M- $\beta$ -CD	51.64 $\pm$ 1.97	56.23 $\pm$ 3.02	49.89 $\pm$ 2.14
DAR: $\beta$ -CD	40.14 $\pm$ 1.75	45.35 $\pm$ 1.84	50.98 $\pm$ 1.98
DAR: $\gamma$ -CD	43.56 $\pm$ 1.58	48.87 $\pm$ 1.76	50.25 $\pm$ 2.31
<b>Freeze dried inclusion complex</b>			
DAR: HP- $\beta$ -CD	81.37 $\pm$ 1.03	<b>99.32<math>\pm</math>1.41</b>	71.18 $\pm$ 3.22
DAR: M- $\beta$ -CD	73.74 $\pm$ 4.08	91.59 $\pm$ 1.67	62.31 $\pm$ 1.53
DAR: $\beta$ -CD	46.28 $\pm$ 1.49	53.36 $\pm$ 2.28	57.96 $\pm$ 1.64
DAR: $\gamma$ -CD	51.63 $\pm$ 2.37	58.93 $\pm$ 2.16	60.19 $\pm$ 1.78

\* Data are shown as Mean $\pm$ SD, n=3

Based on the results obtained from phase solubility studies and inclusion efficiency estimation, DAR: HP- $\beta$ -CD in the molar ratio of 1:2 was selected as best suitable inclusion complex for further studies due to its superior solubilizing capacity and greater inclusion efficiency. Moreover, earlier reports suggest that the modified  $\beta$ -

cyclodextrins (HP- $\beta$ -CD) have enormous applicability in development of solid oral dosage forms due to their higher complexation efficiency and lower cytotoxicity than the  $\beta$ -cyclodextrin<sup>23-26</sup>.

#### **4.4.7.2 Characterization of selected Inclusion complex**

##### **4.4.7.2.1 FTIR Spectroscopy**

The FTIR Spectroscopy of Plain DAR, pure HP- $\beta$ -CD, physical mixture, kneaded mixture and freeze dried inclusion complex for DAR: HP- $\beta$ -CD::(1:2)M was carried out and result had been represented in Fig. 4.24.

The IR studies of DAR exhibited peaks at 3452.33  $\text{cm}^{-1}$  and 3071.08  $\text{cm}^{-1}$  were due to O-H and aromatic stretching. Peaks at 1768.81  $\text{cm}^{-1}$ , 1694.88  $\text{cm}^{-1}$  and 1211.30  $\text{cm}^{-1}$  were due to C=O stretching of carbonyl group, C=O stretching of keto group and C-O stretching of ester group, respectively. Aromatic bending was observed from 760.1  $\text{cm}^{-1}$  to 705.65  $\text{cm}^{-1}$ . These bands confirmed the structure of DAR. However, the FTIR spectra of HP- $\beta$ -CD showed a large and broad band at 3381.51  $\text{cm}^{-1}$  corresponding to absorption by hydrogen bonded O-H groups.

The IR spectrum of physical mixture of DAR:HP- $\beta$ -CD::1:2M had shown peaks at 1771.16  $\text{cm}^{-1}$ , 1676.74  $\text{cm}^{-1}$  and 1209.98  $\text{cm}^{-1}$  were due to C=O stretching of carbonyl group, C=O stretching of keto-group and C-O stretching of ester group, respectively. The intense appearance and little shifting of these peaks indicate weak interaction between drug and excipients.

The IR spectrum of kneaded mixture of DAR:HP- $\beta$ -CD::1:2M had shown peaks at 1770.86  $\text{cm}^{-1}$ , 1678.26  $\text{cm}^{-1}$  and 1210.95  $\text{cm}^{-1}$  were due to C=O stretching of carbonyl group, C=O stretching of keto-group and C-O stretching of ester group, respectively. The intense appearance and little shifting of these peaks indicate weak interaction between drug and excipients but more than the physical mixture. Whereas in the IR spectrum of freeze dried inclusion complex of DAR:HP- $\beta$ -CD::1:2M, all the characteristic peaks of DAR disappeared which indicate a good inclusion and interaction of DAR with HP- $\beta$ -CD at the selected molar ratio. Moreover this study also proved the efficiency of selected method of preparation.

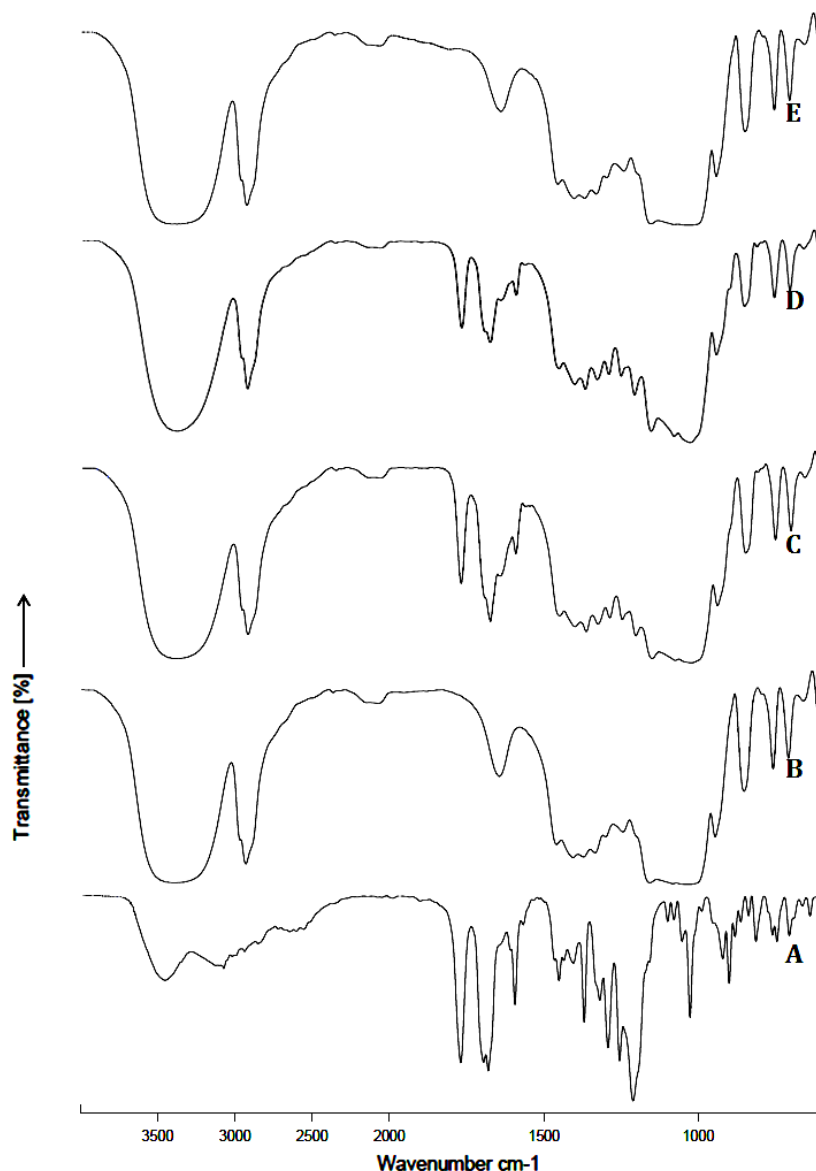


**Fig. 4.24** IR spectrums of (A) Plain DAR, (B) HP- $\beta$ -CD, (C) Physical Mixture for DAR: HP- $\beta$ -CD::(1:2)M, (D) Kneaded Mixture for DAR: HP- $\beta$ -CD::(1:2)M and (E) Freeze dried inclusion complex of DAR: HP- $\beta$ -CD::(1:2)M.

#### 4.4.7.2.2 Differential Scanning Calorimetric (DSC) Analysis

The thermal behavior of plain DAR, pure HP- $\beta$ -CD, physical mixture, kneaded mixture and freeze dried inclusion complex for DAR: HP- $\beta$ -CD::(1:2)M were studied using Differential Scanning Calorimetry (DSC) in order to confirm the formation of solid inclusion complexes (Fig. 4.25). When guest molecules are incorporated in the cyclodextrin cavity or in the crystal lattice, their melting, boiling and sublimation points usually shifted to a different temperature or disappear within the temperature range, where the cyclodextrin lattice is decomposed.

The DSC thermogram of DAR showed a sharp endothermic peak for at 251.8°C corresponding to its melting point. The DSC thermogram of HP-β-CD exhibited a broad endothermic peak at 88.7°C which corresponded to the loss of hydration water of the material. The HP-β-CD decomposed at the temperature of 300°C hence not showing any melting peak of HP-β-CD in between 30°C to 300°C.

In the DSC thermogram of physical mixture in DAR:HP-β-CD::1:2 molar ratio showed two sharp endothermic peaks, corresponding to HP-β-CD and DAR indicated that inclusion of drug within CD was not achieved. The DSC thermogram of kneaded mixture for DAR:HP-β-CD::1:2M also showed two endothermic peaks corresponding HP-β-CD and DAR but the height of DAR endothermic peak was reduced considerably in comparison with pure DAR and physical mixture indicating the interaction between DAR and HP-β-CD but true complex had not been formed. The occurrence of DAR peak also reflected the existence of few DAR crystals in the preparation.

The DSC thermogram of freeze dried inclusion complex of DAR:HP-β-CD::1:2M had shown an endothermic peak for HP-β-CD but the disappearance of characteristic endothermic peak due to DAR with this system, clearly indicated the formation of true inclusion complex. The absence of DAR peak might also be attributed to the amorphous form of the drug in the complex formation. After this study, it can be concluded that preparation of inclusion complex followed by freeze drying was the best suitable method for formation of inclusion complex of DAR.

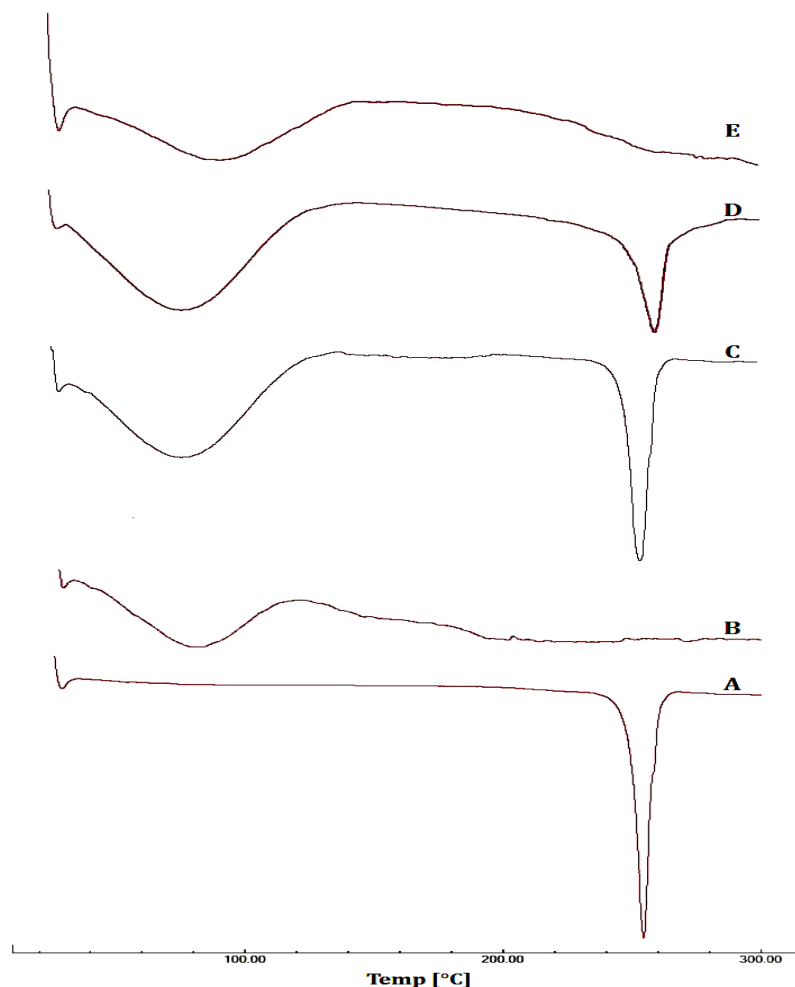


**Fig. 4.25** DSC thermograms of (A) Plain DAR, (B) HP-β-CD , (C) Physical Mixture for DAR: HP-β-CD::(1:2)M, (D) Kneaded Mixture for DAR: HP-β-CD::(1:2)M and (E) Freeze dried inclusion complex of DAR: HP-β-CD::(1:2)M.

#### 4.4.7.2.3 Powder X-Ray Diffraction (XRD) Study

The Powder X-Ray Diffraction (XRD) Study of Plain DAR, pure HP-β-CD, physical mixture, kneaded mixture and freeze dried inclusion complex for DAR: HP-β-CD::(1:2)M was carried out and result had been represented in Fig. 4.26.

XRD study was carried out to investigate the crystalline state of drug which is influencing the dissolution and stability behaviour of compound. The preservation of the crystal structure of the drug in the formulation is crucial for the sustained stability of the drug during its shelf-life. The peak position (diffraction angle) is an identification tool of a crystal structure, where as the number of peaks is a measure of sample crystallinity in a diffractogram<sup>27</sup>. The development of an amorphous form confirmed that the drug was dispersed completely in a molecular state with cyclodextrin. It had been investigated by several researchers that the occurrence of a difused diffraction

pattern, appearance of new peaks and elimination of characteristic peaks of the guest/drug molecule, evident for the formation of an inclusion complex of drug with cyclodextrins<sup>28-31</sup>.

The XRD pattern of pure DAR exhibited various diffraction peaks at 10.3, 17.2, 21.3, 24.9 and 27.6 °2θ indicating the crystalline nature of drug. No diffraction peaks were observed in the diffractogram of HP-β-CD, showed the amorphous form of HP-β-CD. The XRD patterns of physical mixture and kneaded mixture showed sufficiently visible characteristic peaks of DAR, pointing toward the insufficient inclusion or lack of inclusion of DAR in HP-β-CD. The XRD of freeze dried inclusion complex of DAR: HP-β-CD::(1:2)M showed a halo pattern, with the disappearance of all characteristic peaks of DAR which indicated the complete incorporation of DAR in HP-β-CD cavity and formation of complete and stable inclusion complex. The results obtained from XRD analysis were in good agreement with DSC observations.

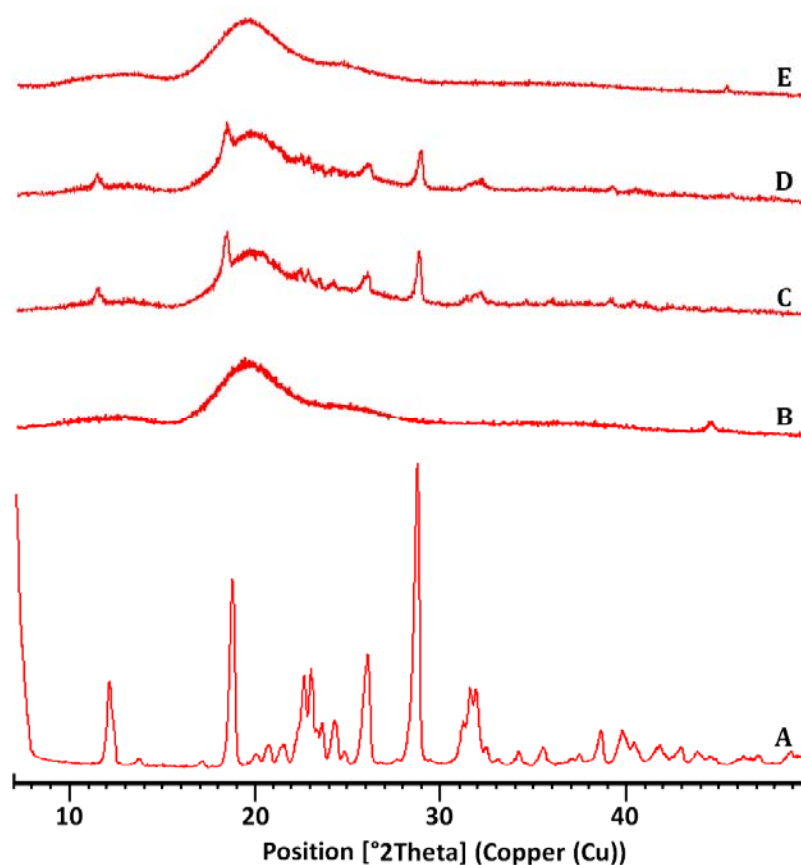


**Fig. 4.26** XRD patterns of (A) Plain DAR, (B) HP-β-CD, (C) Physical Mixture for DAR: HP-β-CD::(1:2)M, (D) Kneaded Mixture for DAR: HP-β-CD::(1:2)M and (E) Freeze dried inclusion complex of DAR: HP-β-CD::(1:2)M.

#### 4.4.7.2.4 Percentage DAR content in lyophilized inclusion complex of DAR: HP- $\beta$ -CD

Percentage DAR content in lyophilized inclusion complex of DAR:HP- $\beta$ -CD in (1:2) molar ratio was found to be  $100.02 \pm 1.62\%$ , indicating the suitability of freeze drying method for production of inclusion complex.

#### 4.4.7.2.5 *In vitro* dissolution study

The dissolution profiles for the plain DAR (DAR-P) marketed formulation (DAR-M) and Freeze dried inclusion complex of DAR:HP- $\beta$ -CD:(1:2)M (DAR-IC) in phosphate buffer pH-6.8 (PB), acetate buffer pH-4.5 (AB), 0.1N HCl and water are presented in Fig. 4.27. The values reported in Table 4.25 and 4.26 are arithmetic means of 3 determinations. It was evident from the data that optimized inclusion complex of DAR: HP- $\beta$ -CD in the molar ratio of 1:2 served better dissolution profile and drug release than the DAR-P and DAR-M in all the dissolution mediums. The DAR-IC, DAR-M and DAR-P showed better dissolution profile in phosphate buffer pH-6.8 and water as compared to acetate buffer pH-4.5 and 0.1N HCl which may be due to low solubility of drug in acidic medium<sup>32</sup>. The drug release was noticeably increased in phosphate buffer pH-6.8 and water for DAR-IC as about 90% of DAR was dissolved in 30 mins, as compared to 70.8-80.7% and 30.4-32.4% from DAR-M and DAR-P, respectively. The DAR-P did not achieve complete dissolution during 120 min time period and only 13.4-56.9% the DAR released over the test period of 120 mins, due to large crystal size of drug whereas DAR-IC showed 46.7-99.9% drug dissolved with significantly enhanced dissolution rate over the time period of 120 mins, in all the selected dissolution mediums. The significant improvement in dissolution characteristics of inclusion complexes may be due to the formation of readily soluble inclusion complex in the dissolution medium, increased drug particle wettability and reduction of the crystallinity of the drug product.

The Dissolution efficiency (DE), Dissolution percentage at 5 min and 60 min (DP5 and DP60) and Area under curve (AUC) values were increased in the following order: DAR-P < DAR-M < DAR-IC; while time required to release 50% and 90% of drug ( $t_{50}$  and  $t_{90}$ ) and mean dissolution time (MDT) were increased in vice versa i.e. DAR-P > DAR-M > DAR-IC. The  $t_{50}$  and  $t_{90}$  for DAR-IC were significantly reduced to 7.2-14.8 mins and 23.9-48.3 mins respectively as compared to DAR-M and DAR-P in all the dissolution mediums but these were found least in phosphate buffer pH-6.8. This may be due to acidic nature of DAR which was completely unionized at this pH.

All the results indicated that the DAR-IC prepared by freeze drying technique was having superior characteristics to plain drug and marketed formulation, indicating a major prospect to enhance the bioavailability of such drugs by inclusion complexation for oral administration where solubility and dissolution are rate limiting factors in bioavailability in the body. Thus inclusion complexation of poor soluble drug with hydrophilic cyclodextrin is an effective and successful technique in order to improve their biopharmaceutical properties.

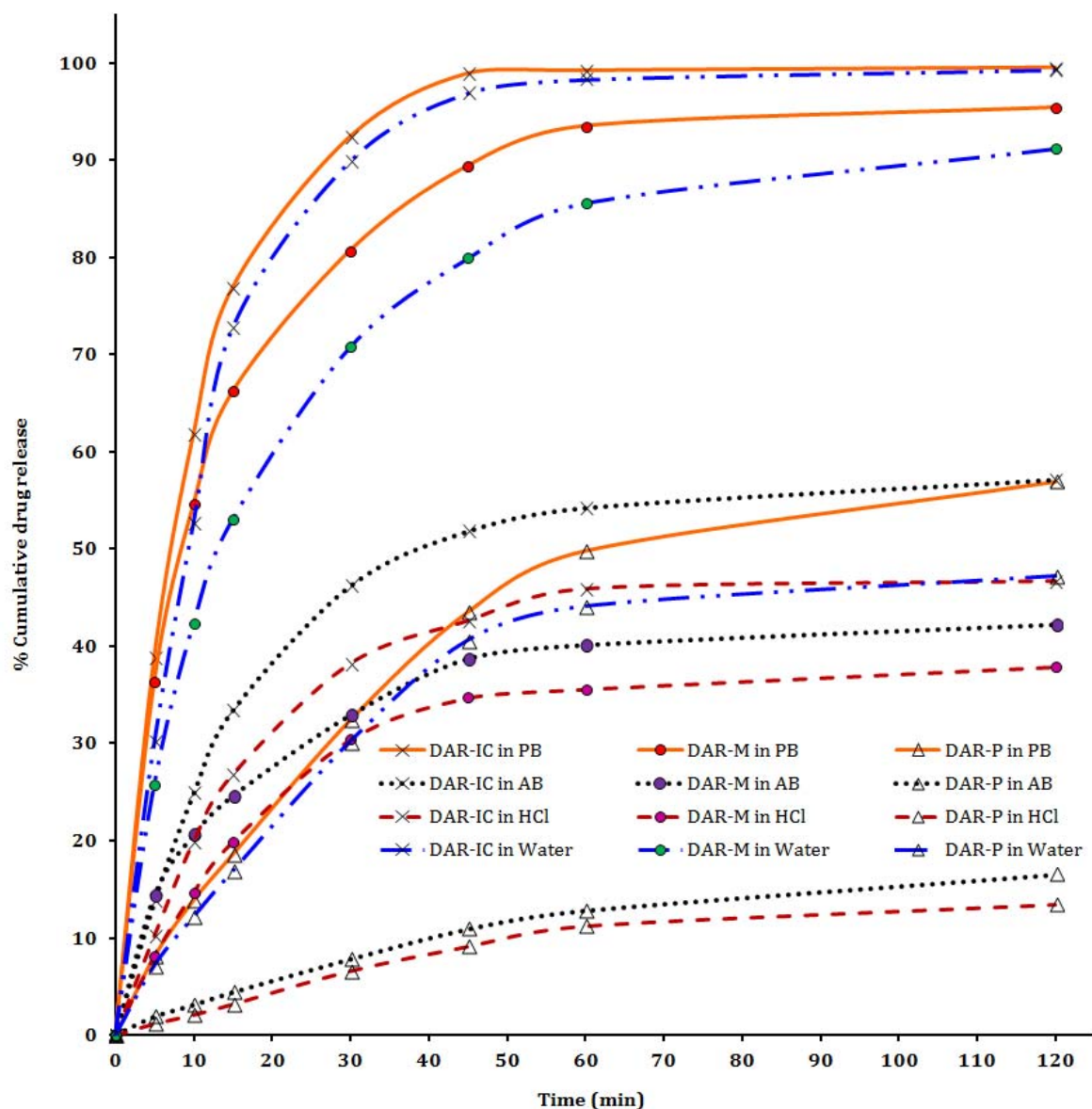


**Fig. 4.27** Graphical representation of % Cumulative drug release versus sampling time of DAR-P, DAR-M and Freeze dried DAR-IC in phosphate buffer pH-6.8 (PB), acetate buffer pH-4.5 (AB), 0.1N HCl and water.

**Table 4.25** Statistical representation of % Cumulative drug release versus sampling time of DAR-P, DAR-M and Freeze dried DAR-IC in phosphate buffer pH-6.8 (PB), acetate buffer pH-4.5 (AB), 0.1N HCl and water.

Time (min) ⇒	0	5	10	15	30	45	60	120
<b>% Cumulative release from Phosphate Buffer, pH-6.8*</b>								
DAR-IC	0.0	38.9±0.3	61.8±0.7	76.9±0.3	92.4±0.5	98.9±0.4	99.2±0.4	99.5±0.6
DAR-M	0.0	36.4±0.5	54.6±0.3	66.2±0.7	80.7±0.2	89.4±0.2	93.5±0.5	95.4±0.6
DAR-P	0.0	8.1±0.2	13.9±0.1	18.6±0.5	32.4±0.2	43.5±0.4	49.8±0.3	56.9±0.1
<b>% Cumulative release from Acetate Buffer, pH-4.2*</b>								
DAR-IC	0.0	13.8±0.5	24.9±0.2	33.4±0.7	46.2±0.3	51.8±0.4	54.2±0.6	57.1±0.5
DAR-M	0.0	14.4±0.3	20.6±0.6	24.6±0.5	32.9±0.2	38.7±0.4	40.1±0.7	42.2±0.8
DAR-P	0.0	1.9±0.4	3.1±0.3	4.4±0.1	7.8±0.3	10.9±0.5	12.8±0.2	16.5±0.2
<b>% Cumulative release from 0.1N HCl*</b>								
DAR-IC	0.0	10.2±0.3	19.9±0.5	26.8±0.5	38.2±0.4	42.6±0.6	45.9±0.3	46.7±0.5
DAR-M	0.0	8.3±0.8	14.7±0.4	19.9±0.7	30.4±0.2	34.7±0.2	35.6±0.3	37.9±0.2
DAR-P	0.0	1.2±0.1	2.3±0.3	3.2±0.4	6.6±0.6	9.1±0.3	11.2±0.2	13.4±0.5
<b>% Cumulative release from water*</b>								
DAR-IC	0.0	30.1±0.2	52.7±0.5	72.8±0.3	89.9±0.4	96.9±0.4	98.3±0.3	99.3±0.7
DAR-M	0.0	25.8±0.2	42.4±0.4	53.1±0.6	70.8±0.2	79.9±0.3	85.6±0.2	91.2±0.1
DAR-P	0.0	7.2±0.5	12.2±0.7	16.9±0.2	30.4±0.4	40.6±0.3	44.1±0.5	47.2±0.2

\* Data are shown as Mean±SD, n=3.

**Table 4.26** Comparison of various dissolution parameters of DAR-P, DAR-M and Freeze dried DAR-IC in phosphate buffer pH-6.8 (PB), acetate buffer pH-4.5 (AB), 0.1N HCl and water.

	DE	DP <sub>5</sub>	DP <sub>60</sub>	t <sub>50</sub>	t <sub>90</sub>	MDT	AUC
<b>In Phosphate Buffer, pH-6.8*</b>							
DAR-IC	0.90±0.06	38.9±0.9	99.2±0.5	7.2±0.1	23.9±0.7	11.0±0.4	10847±61
DAR-M	0.84±0.04	36.4±0.5	93.5±0.5	9.7±0.4	48.3±0.7	14.8±0.2	10036±35
DAR-P	0.42±0.01	8.1±0.2	49.8±0.3	>60	>60	32.0±0.4	5009±28
<b>In Acetate Buffer, pH-4.2*</b>							
DAR-IC	0.48±0.02	13.8±0.6	54.2±0.4	48.4±0.4	>60	19.4±0.7	5743±42
DAR-M	0.36±0.02	14.4±0.3	40.1±0.7	>60	>60	18.9±0.7	4264±19
DAR-P	0.11±0.02	1.9±0.4	12.8±0.2	>60	>60	39.7±0.5	1324±25
<b>In 0.1N HCl*</b>							
DAR-IC	0.40±0.05	10.2±0.6	45.9±0.5	>60	>60	18.2±0.4	4753±41
DAR-M	0.31±0.01	8.3±0.8	35.6±0.3	>60	>60	20.8±0.3	3761±29
DAR-P	0.09±0.05	1.2±0.1	11.2±0.2	>60	>60	37.5±0.6	1106±17
<b>In water*</b>							
DAR-IC	0.88±0.03	30.1±0.5	98.3±0.6	8.9±0.6	30.4±0.1	13.2±0.3	10609±52
DAR-M	0.76±0.03	25.8±0.2	85.6±0.2	14.8±0.7	>60	20.5±0.8	9078±31
DAR-P	0.37±0.04	7.2±0.5	44.1±0.5	>60	>60	26.8±0.3	4397±15

\* Data are shown as Mean±SD, n=3. DE: Dissolution efficiency, DP<sub>5</sub>: Dissolution percentage at 5 min, DP<sub>60</sub>: Dissolution percentage at 60 min, t<sub>50</sub>: time required to release 50% of drug (min), t<sub>90</sub>: time required to release 90% of drug (min), MDT: Mean dissolution time (min), AUC: Area under curve.

#### 4.4.7.2.6 Stability studies

The stability of DAR-IC was monitored for chemical stability (i.e. percentage drug content). The study was carried out for 6 months at different time intervals (i.e. 1<sup>st</sup>, 2<sup>nd</sup>, 3<sup>rd</sup> and 6<sup>th</sup> month) stored at 5°C±3°C and at room temperature. It was observed that no significant difference was found in % DAR content of stored formulations at both conditions for 6 months (Table 4.27) so it can be concluded that formulation was stable for a period of 6 months and indicating its suitability for storage at both the conditions.

**Table 4.27** Chemical stability (i.e. percentage drug content) of Freeze dried DAR-IC at different time intervals stored at 5°C±3°C and room temperature.

Sr. No.	Time	At 5°C±3°C*	At Room Temperature*
		% content of DAR in DAR-IC	% content of DAR in DAR-IC
1	Initial	100.02±1.62	100.02±1.62
2	1 <sup>st</sup> Month	99.65±0.72	99.84±0.46
3	2 <sup>nd</sup> Month	99.89±0.63	99.71±0.95
4	3 <sup>rd</sup> Month	99.29±0.55	99.38±0.86
5	6 <sup>th</sup> Month	99.76±1.13	99.45±0.98

\* Data are shown as Mean±SD, n=3.

#### 4.4.7.3 Cell Line Studies of DAR and it's Inclusion complex with HP-β-CD using Caco-2 cell line model

##### 4.4.7.3.1 *In vitro* Cell Cytotoxicity Studies (MTT Assay)

Cytotoxicity study of Freeze dried inclusion complex of DAR: HP-β-CD::(1:2)M (DAR-IC) and DAR-P was accomplished in Caco2 cells by mitochondrial activity (MTT assay) to assess the safety/tolerability of prepared formulation on viability of cells. As Caco2 cells were used as absorption model, biocompatibility and tolerability of DAR-P and DAR-IC on absorption barrier was necessary. At initial 4 hr and 24 hr, the % cell viability is more than 80% at the 250 µg/ml concentration of DAR-P and DAR-IC. Hence for permeability studies, the drug and formulation concentration was fixed at 250 µg/ml. It can be observed that the DAR-IC showed very less cytotoxicity than the plain DAR upto 48 hours at all the concentrations. (Table 4.28) This confirms the biocompatibility of DAR-IC and explains that composition of inclusion complex did not contribute to toxicity of Caco2 cells<sup>24,33</sup>. At initial 4 hours, 24 hours and 48 hours, DAR-IC was found to have less cytotoxicity with more than 80% cell viability as compared to DAR-P at all the concentrations except at 1000µg/ml in 48 hours condition. This could be attributed to protective action of HP-β-CD due to cavitization of drug molecule in CD. Cytotoxicity graphs at 4 hours, 24 hours and 48 hours were constructed (Fig. 4.28, 4.29 and 4.30)

and IC<sub>50</sub> values were calculated for DAR-P and DAR-IC (Table 4.29). The higher IC<sub>50</sub> values for DAR-IC than DAR-P at all the incubation time conditions concluded to lack of cytotoxicity due to formulation of a bio-tolerable inclusion complex.

**Table 4.28** In vitro cytotoxicity studies of DAR-P and freeze dried DAR-IC in Caco2 cell lines at 4 hours, 24 hours and 48 hours.

Conc. (µg/ml)	%Cell Viability at 4 Hrs.*		%Cell Viability at 24		%Cell Viability at 48 Hrs.*	
	DAR-P	DAR-IC	DAR-P	DAR-IC	DAR-P	DAR-IC
0.1	99.25±0.92	100.14±0.28	94.32±0.66	99.23±0.53	90.14±0.69	96.17±0.69
1	98.59±0.61	100.02±0.49	90.62±0.53	98.42±0.92	86.90±0.75	94.60±0.37
10	96.13±0.89	99.78±0.67	86.24±0.88	96.75±0.15	83.64±0.39	91.02±0.58
100	94.61±0.58	97.35±0.45	82.43±0.64	93.26±0.28	80.86±0.84	88.36±0.56
250	91.45±0.62	94.71±0.52	80.42±0.93	91.43±0.67	75.63±0.85	84.58±0.79
500	86.58±0.45	91.18±0.81	79.49±0.46	88.19±0.50	70.26±0.46	80.20±0.62
1000	83.16±0.94	88.63±0.32	70.60±0.91	85.61±0.46	62.43±0.28	75.05±0.54

\* Data are shown as Mean±SD, n=3.

**Table 4.29** IC<sub>50</sub> values of DAR-P and freeze dried DAR-IC in Caco2 cell lines at 4 hours, 24 hours and 48 hours.

Conditions	IC <sub>50</sub> Values (µg/ml)*	
	DAR-P	DAR-IC
At 4 hours	3010.96±19.62	4129.75±29.74
At 24 hours	1878.42±14.11	3646.95±35.17
At 48 hours	1408.16±15.18	2316.70±19.67

\* Data are shown as Mean±SD, n=3.

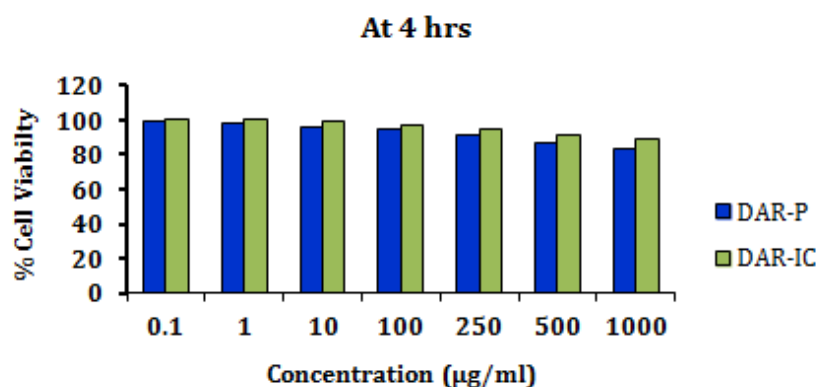


**Fig. 4.28** In vitro cytotoxicity studies of DAR-P and DAR-IC in Caco2 cell lines at 4 hours.

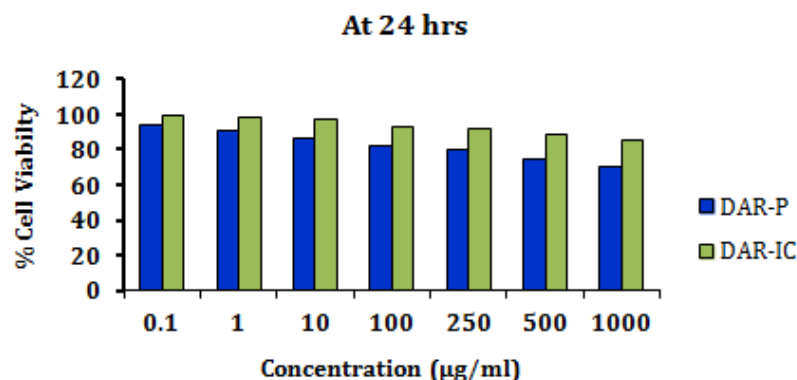


**Fig. 4.29** In vitro cytotoxicity studies of DAR-P and DAR-IC in Caco2 cell lines at 24 hours.

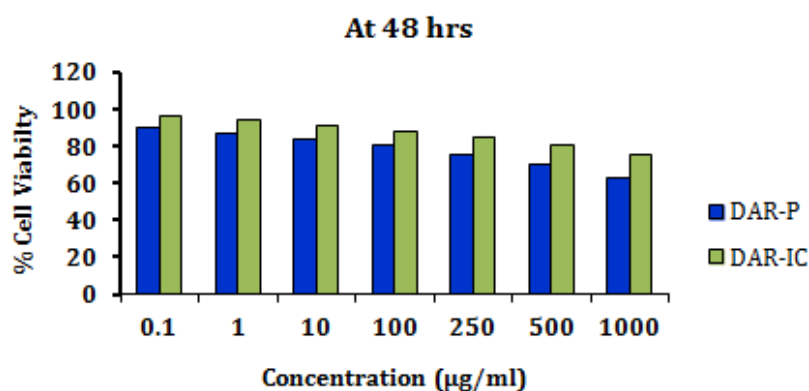


**Fig. 4.30** In vitro cytotoxicity studies of DAR-P and DAR-IC in Caco2 cell lines at 48 hours.

#### 4.4.7.3.2 In vitro assessment of permeability using Caco-2 cell line model

In this study, *in vitro* permeability assessment of Freeze dried inclusion complex of DAR: HP- $\beta$ -CD::(1:2)M (DAR-IC), plain DAR (DAR-P) and marketed formulation (DAR-M) was done by calculating apparent permeability coefficient ( $P_{app}$ ) from apical to basolateral (Table 4.30). Transepithelial permeability of DAR was measured at concentration of 250 $\mu$ g/ml, as negligible toxicity towards Caco-2 cells was found at this concentration during MTT assay of the same. The average  $P_{app}$  for Lucifer yellow with Caco-2 cells was found  $(0.87 \pm 0.07) \times 10^{-6}$  cm/sec, confirmed the integrity of monolayers and suitability of monolayers for further experiment. The  $P_{app}$  for DAR-P and DAR-M were calculated and found to be  $(5.95 \pm 0.24) \times 10^{-6}$  cm/sec and  $(8.73 \pm 0.82) \times 10^{-6}$  cm/sec respectively while the  $P_{app}$  for DAR-IC was observed at  $(30.26 \pm 0.38) \times 10^{-6}$  cm/sec which is about 5.09 fold and 3.47 fold higher than the DAR-P and DAR-M, respectively. The found results were very much satisfactory and matching with the aim of the project. It can be concluded that

the higher  $P_{app}$  for DAR-IC was because of molecular state of drug and presence of HP- $\beta$ -CD in the formulation<sup>34,35</sup>. Whereas the lower permeability coefficient of DAR-P can be attributed to hydrophobicity and low permeation ( $\log P$  2.47) of drug. If the  $P_{app}$  value of a compound is less than  $1 \times 10^{-6}$  cm/sec, in between  $1-10 \times 10^{-6}$  cm/sec, and more than  $10 \times 10^{-6}$  cm/sec can be classified as poorly (0-20%), moderately (20-70%) and well (70-100%) absorbed compounds, respectively<sup>36,37</sup>.

**Table 4.30** Apparent permeability coefficient ( $P_{app}$ ) from apical to basolateral for DAR-P, DAR-M and freeze dried DAR-IC using Caco-2 cells model.

Drug/Formulation	Apparent permeability coefficient ( $P_{app}$ ) $\pm$ SD ( $10^{-6}$ cm/sec)*
DAR-P	5.95 $\pm$ 0.24
DAR-M	8.73 $\pm$ 0.82
DAR-IC	30.26 $\pm$ 0.38

\* Data are shown as Mean $\pm$ SD, n=3.

#### 4.4.7.4 Pharmacokinetic evaluation of Freeze dried inclusion complex of DAR:HP- $\beta$ -CD in 1:2 molar ratio using *in vivo* animal model

*In vivo* animal study was carried out to estimate the oral bioavailability and other pharmacokinetic parameters of prepared Freeze dried inclusion complex of DAR:HP- $\beta$ -CD:(1:2)M (DAR-IC) with respect to plain drug (DAR-P) and commercial formulation (DAR-M). DAR is completely metabolized in rhein before entering in the systemic blood circulation, after oral dosing.

The mean drug plasma profile with respect to time is tabulated in Table 4.31, for DAR-P, DAR-M and DAR-IC. Fig. 4.31 represents the same plasma profile graphically. The pharmacokinetic parameters for all the three orally administered forms of DAR were determined using PKsolver add-in in microsoft excel. Non-compartmental analysis of plasma with linear trapezoidal method after extravascular administration in rabbits was performed and obtained parameters are represented in Table 4.32. Plasma rhein concentration profile of DAR-IC showed significant improvement in drug absorption compared to DAR-P and DAR-M. Area under concentration-time curve ( $AUC_{0-t}$ ) of rhein was found  $25.96 \pm 1.25 \mu\text{g} \cdot \text{h}/\text{ml}$  for DAR-IC which was 3.32 fold and 2.03 fold higher with that of DAR-P ( $7.83 \pm 0.19 \mu\text{g} \cdot \text{h}/\text{ml}$ ) and DAR-M ( $12.81 \pm 0.62 \mu\text{g} \cdot \text{h}/\text{ml}$ ), respectively. The area under momentum curve ( $AUMC_{total}$ ) showed significantly higher value for DAR-IC ( $194.75 \pm 7.83 \mu\text{g} \cdot \text{h}^2/\text{ml}$ ), compared to DAR-P ( $50.47 \pm 2.31 \mu\text{g} \cdot \text{h}^2/\text{ml}$ ) and DAR-M ( $89.95 \pm 2.59 \mu\text{g} \cdot \text{h}^2/\text{ml}$ ). The maximum peak plasma concentration ( $C_{max}$ ) of DAR-IC was about 2.68 fold and 2.27 fold greater than that of DAR-P and DAR-M,

respectively. The enhancement in AUC and  $C_{\max}$  of DAR-IC compared to DAR-P and DAR-M could be due to the quick absorption of drug molecule by gastrointestinal wall due to the tremendous increase in solubility and improved dissolution rate of DAR present in form of inclusion complex with HP- $\beta$ -CD<sup>38-40</sup>. Time to reach maximum plasma concentration ( $T_{\max}$ ) for DAR-IC, DAR-M and DAR-P was found to be 2.5, 3.0 and 3.5 hour, respectively. The shortest  $T_{\max}$  for DAR-IC may be due to fastest dissolution rate and amorphization of drug due to formation of inclusion complex and the highest  $T_{\max}$  of DAR-P could be attributed to crystalline nature of drug<sup>41</sup>. Mean residence time (MRT) for DAR-IC was found almost same as for DAR-P and DAR-M.

When half life ( $t_{1/2}$ ) of DAR-IC was compared with DAR-P and DAR-M, the  $t_{1/2}$  for DAR-IC ( $10.21 \pm 0.26$  h) was not found much different than that of DAR-P ( $7.94 \pm 0.42$  h) and DAR-M ( $10.65 \pm 0.57$  h). The elimination rate constant ( $K_{\text{elimination}}$ ) for DAR-P, DAR-M and DAR-IC were found to be  $0.12 \pm 0.02$  h<sup>-1</sup>,  $0.07 \pm 0.01$  h<sup>-1</sup> and  $0.07 \pm 0.01$  h<sup>-1</sup>, respectively. No significant difference in  $t_{1/2}$  and  $K_{\text{elimination}}$  of all three was observed which indicated that their elimination was comparable.

Relative bioavailability or bioequivalence is the most important criteria for comparing the bioavailabilities of different formulations of same drug. The relative bioavailability (F) of DAR-IC and DAR-M were found to be 331.55% and 163.60%, respectively, with respect to DAR-P. Thus there was 3.32 fold and 2.03 fold increase in bioavailability of DAR from DAR-IC with respect to DAR-P and DAR-M, respectively. These results could be explained by greater dissolution rate, increased wettability, increased hydrophilicity and reduced crystallinity of DAR in DAR-IC when compared to DAR-P and DAR-M. So it can be observed easily that these results may lead to economical benefits by reduction in dose of DAR. Additionally, dose related side effects of drug will also minimize when administered in multiple dose regimens.

**Table 4.31** Statistical representation of rhein plasma profile for DAR-P, DAR-M and freeze dried DAR-IC in Albino rabbits following oral administration.

Time (Hour)	Rhein mean plasma concentration $\pm$ SD*		
	DAR-P ( $\mu\text{g/ml}$ )	DAR-M ( $\mu\text{g/ml}$ )	DAR-IC ( $\mu\text{g/ml}$ )
0.0	0	0	0
0.5	0.04 $\pm$ 0.02	0.10 $\pm$ 0.06	0.62 $\pm$ 0.16
1.0	0.09 $\pm$ 0.07	0.28 $\pm$ 0.12	1.24 $\pm$ 0.28
1.5	0.22 $\pm$ 0.19	1.17 $\pm$ 0.17	3.15 $\pm$ 0.52
2.0	0.68 $\pm$ 0.14	2.08 $\pm$ 0.29	5.07 $\pm$ 0.34
2.5	1.06 $\pm$ 0.18	2.96 $\pm$ 0.11	7.81 $\pm$ 0.28
3.0	1.89 $\pm$ 0.36	3.44 $\pm$ 0.21	5.54 $\pm$ 0.26
3.5	2.91 $\pm$ 0.27	2.41 $\pm$ 0.23	3.27 $\pm$ 0.14
4.0	1.32 $\pm$ 0.17	1.64 $\pm$ 0.12	2.28 $\pm$ 0.31
4.5	0.98 $\pm$ 0.24	1.01 $\pm$ 0.12	1.75 $\pm$ 0.27
8.0	0.21 $\pm$ 0.11	0.35 $\pm$ 0.09	0.64 $\pm$ 0.09
12.0	0.10 $\pm$ 0.05	0.14 $\pm$ 0.05	0.27 $\pm$ 0.18
24.0	0.03 $\pm$ 0.01	0.06 $\pm$ 0.03	0.16 $\pm$ 0.16
48.0	ND	0.02 $\pm$ 0.01	0.05 $\pm$ 0.02

\* Data are shown as Mean $\pm$ SD, n=3, ND: Not detected

**Table 4.32** Pharmacokinetic parameters after oral administration of DAR-P, DAR-M and freeze dried DAR-IC in Albino rabbits.

Pharmacokinetic parameters*	DAR-P	DAR-M	DAR-IC
C <sub>max</sub> ( $\mu\text{g/ml}$ )	2.91 $\pm$ 0.26	3.44 $\pm$ 0.31 <sup>†</sup>	7.81 $\pm$ 0.42 <sup>†#</sup>
T <sub>max</sub> (h)	3.50 $\pm$ 0.23	3.00 $\pm$ 0.17 <sup>†</sup>	2.5 $\pm$ 0.04 <sup>†#</sup>
AUC <sub>0-t</sub> ( $\mu\text{g}\cdot\text{h/ml}$ )	7.83 $\pm$ 0.19	12.81 $\pm$ 0.62 <sup>†</sup>	25.96 $\pm$ 1.25 <sup>†#</sup>
AUC <sub>0-∞</sub> ( $\mu\text{g}\cdot\text{h/ml}$ )	8.09 $\pm$ 0.36	13.19 $\pm$ 0.91 <sup>†</sup>	27.02 $\pm$ 1.74 <sup>†#</sup>
AUMC <sub>total</sub> ( $\mu\text{g}\cdot\text{h}^2/\text{ml}$ )	50.47 $\pm$ 2.31	89.95 $\pm$ 2.59 <sup>†</sup>	194.75 $\pm$ 7.83 <sup>†#</sup>
MRT (h)	6.16 $\pm$ 0.14	7.12 $\pm$ 0.09 <sup>†</sup>	7.50 $\pm$ 0.09 <sup>†#</sup>
T <sub>1/2</sub> (h)	7.94 $\pm$ 0.42	10.65 $\pm$ 0.57 <sup>†</sup>	10.21 $\pm$ 0.26 <sup>†#</sup>
K <sub>elimination</sub> (h <sup>-1</sup> )	0.12 $\pm$ 0.02	0.07 $\pm$ 0.01 <sup>†</sup>	0.07 $\pm$ 0.01 <sup>†#</sup>
F (%) w.r.t DAR-P	100	163.60 <sup>†</sup>	331.55 <sup>†#</sup>

\* Data are shown as Mean $\pm$ SD, n=3, <sup>†</sup>P<0.05 compared with DAR-P, <sup>#</sup>P<0.05 compared with DAR-M.

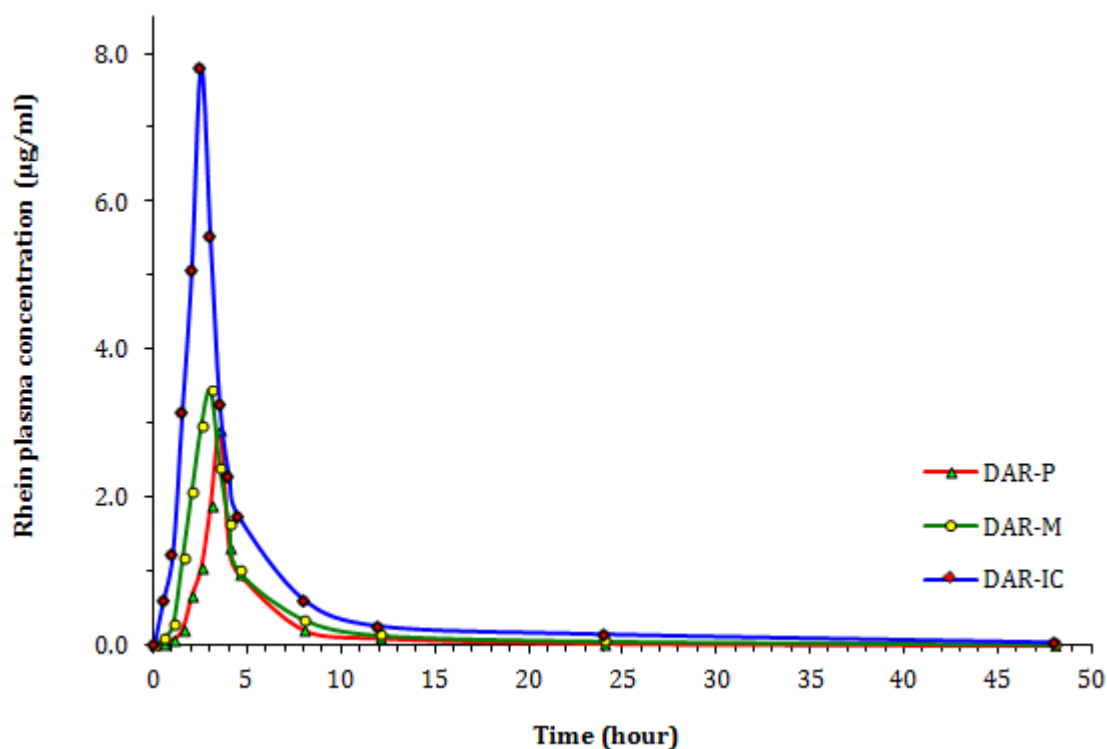


**Fig. 4.31** Graphical representation of rhein plasma profile for DAR-P, DAR-M and DAR-IC in Albino rabbits following oral administration.

#### 4.4.8 Conclusions

The objective of this study was to achieve significantly improved bioavailability of poorly water soluble drug, Diacerein (DAR) by developing an orally administrable and stable drug:cyclodextrin inclusion complex with enhanced solubility, dissolution and bio-tolerability. DAR:Cyclodextrin inclusion complexes were prepared with  $\beta$ -CD, HP- $\beta$ -CD, M- $\beta$ -CD and  $\gamma$ -CD in 1:1, 1:2 and 1:3 molar ratios. The modes of preparation employed were physical mixing, kneading method and freeze drying method. Phase solubility study was carried out in order to characterize the inclusion complexes in liquid state. Phase solubility study provides the stability constant for drug-cyclodextrin inclusion complex as well as it also present the insight into stoichiometry of the complex at equilibrium. The phase solubility studies of DAR with  $\beta$ -CD, HP- $\beta$ -CD, M- $\beta$ -CD and  $\gamma$ -CD were studied in water, phosphate buffer pH-6.8 and HCl pH-1.2 according to Higuchi and Connor's method. The DAR:HP- $\beta$ -CD showed highest stability constant at  $806.1 \pm 11.7 \text{ M}^{-1}$ ,  $711.5 \pm 6.9 \text{ M}^{-1}$  and  $366.7 \pm 7.4 \text{ M}^{-1}$  in phosphate buffer pH-6.8, water and HCl pH-1.2, respectively. The linear increase in solubility of DAR with increase in CDs concentration, giving rise to  $A_L$ -type phase solubility diagram for DAR:HP- $\beta$ -CD and

DAR:M- $\beta$ -CD while DAR: $\beta$ -CD and DAR: $\gamma$ -CD showed  $A_N$ -type of solubility curves at different pH values. The  $R^2$  values were also increased in the order of (DAR:HP- $\beta$ -CD)>(DAR:M- $\beta$ -CD)>(DAR: $\beta$ -CD)>(DAR: $\gamma$ -CD). Additionally, inclusion efficiencies (%IE) were estimated to finalize the best suitable CD and molar ratio. The results clearly showed that the %IE of DAR: HP- $\beta$ -CD inclusion complex in molar ratio of 1:2 was found higher for physical mixture ( $72.39\% \pm 2.87\%$ ), kneaded mixture ( $84.61\% \pm 1.28\%$ ) and freeze dried inclusion complex ( $99.32\% \pm 1.41\%$ ) than the other inclusion complexes prepared by respective mode of preparations. It indicated that DAR was uniformly distributed in DAR:HP- $\beta$ -CD inclusion complex in molar ratio of 1:2 and others did not show satisfactory drug incorporation. Based on the results obtained from phase solubility studies and inclusion efficiency estimation, DAR:HP- $\beta$ -CD in the molar ratio of 1:2 was selected as best suitable inclusion complex for further studies due to its superior solubilizing capacity and greater inclusion efficiency.

The results obtained by FTIR, DSC and XRD studies were in excellent agreement and confirmed the formation of true inclusion complex of DAR with HP- $\beta$ -CD in 1:2 molar ratio by freeze drying method. The IR spectrum of freeze dried inclusion complex of DAR:HP- $\beta$ -CD::1:2M showed disappearance of all the characteristic peaks of DAR disappeared which indicate a good inclusion and interaction of DAR with HP- $\beta$ -CD at the selected molar ratio. The DSC thermogram of freeze dried inclusion complex of DAR:HP- $\beta$ -CD::(1:2)M had shown an endothermic peak for HP- $\beta$ -CD but the disappearance of characteristic endothermic peak due to DAR with this system, clearly indicated the formation of true inclusion complex. The XRD of freeze dried inclusion complex of DAR:HP- $\beta$ -CD::(1:2)M showed a halo pattern, with the disappearance of all characteristic peaks of DAR which indicated the complete incorporation of DAR in HP- $\beta$ -CD cavity and formation of complete and stable inclusion complex. Moreover these studies also proved the efficiency of freeze drying method of preparation.

Percentage DAR content in lyophilized inclusion complex of DAR:HP- $\beta$ -CD in (1:2) molar ratio was found to be  $100.02 \pm 1.62\%$ , indicating the suitability of freeze drying method for production of inclusion complex. Stability studies concluded that inclusion complex of DAR with HP- $\beta$ -CD in (1:2) molar ratio was found physically and chemically stable for a period of 6 months and indicating its suitability for storage at  $5^\circ\text{C} \pm 3^\circ\text{C}$  and at room temperature.

The dissolution profiles of DAR-P, DAR-M and DAR-IC were checked in phosphate buffer pH-6.8, acetate buffer pH-4.5, 0.1N HCl and water over the test period of 120 mins. DAR-NS was found superior to DAR-P and DAR-M in terms of % cumulative release of DAR, dissolution efficiency and mean dissolution time in all the dissolution mediums.

Cytotoxicity study of Freeze dried inclusion complex of DAR: HP- $\beta$ -CD::(1:2)M and plain DAR was accomplished in Caco2 cells by mitochondrial activity (MTT assay) to assess the safety/tolerability of prepared formulation on viability of cells. The higher IC<sub>50</sub> values for freeze dried inclusion complex than plain DAR at all the incubation time conditions concluded to lack of cytotoxicity due to formulation of a bio-tolerable inclusion complex.

*In-vitro* permeability assessment of freeze dried inclusion complex of DAR:HP- $\beta$ -CD::(1:2)M, plain DAR and marketed formulation was done by calculating apparent permeability coefficient ( $P_{app}$ ) from apical to basolateral. The  $P_{app}$  for Freeze dried inclusion complex was observed at  $(30.26 \pm 0.38) \times 10^{-6}$  cm/sec which is about 5.09 fold and 3.47 fold higher than the plain DAR and marketed formulation, respectively. The found results were very much satisfactory and matching with the aim of the project.

*In vivo* assessment demonstrated that freeze dried inclusion complex of DAR:HP- $\beta$ -CD::(1:2)M exhibited better pharmacokinetic properties compared to plain DAR and commercial formulation. The relative oral bioavailability of DAR in Albino rabbits resulted from Freeze dried inclusion complex was found 3.32 and 2.03 fold greater than plain DAR and marketed formulation, respectively.

The obtained results justified the selection of cyclodextrin, molar ratio and method of preparation for the formulation of efficient and stable inclusion complex of DAR with cyclodextrin. The outcome was supported by FTIR, DSC and XRD studies which further lead to enhanced dissolution properties, low cytotoxicity and improved bioavailability of DAR in inclusion complex with HP- $\beta$ -CD.

#### 4.4.9 References

- 1 Higuchi T & Connors KA. in *Advances in Analytical Chemistry and Instrumentation* Vol. 4 (ed Reilly CN) 117-217 (Wiley-Interscience, 1965).
- 2 Connors KA. in *Comprehensive Supramolecular Chemistry* (eds Szejtli J & Osa T) 205-241 (Elsevier, 1996).
- 3 Brewster, M. & Loftsson, T. in *Injectable drug development—techniques to reduce pain and irritation* (eds Gupta P & Brazeau G) 307-336 (Interpharm Press, 1999).
- 4 K. P. R. Chowdary, K. R. S., Adinarayana Tanniru. Recent research on cyclodextrin complexation in formulation development- a review. *J Global Trend Pharm Sci* **5**, 1576-1583 (2014).
- 5 Connors, K. A. The Stability of Cyclodextrin Complexes in Solution. *Chem Rev* **97**, 1325-1358 (1997).

- 6 Patel, S. G. & Rajput, S. J. Enhancement of Oral Bioavailability of Cilostazol by Forming its Inclusion Complexes. *AAPS PharmSciTech* **10**, 660-669 (2009).
- 7 Sinha, V., Anitha, R., Ghosh, S., Nanda, A. & Kumria, R. Complexation of celecoxib with  $\beta$ -cyclodextrin: Characterization of the interaction in solution and in solid state. *J Pharm Sci* **94**, 676-687 (2005).
- 8 Zhang, Y. *et al.* DDSolver: An Add-In Program for Modeling and Comparison of Drug Dissolution Profiles. *The AAPS Journal* **12**, 263-271 (2010).
- 9 Press, B. & Di Grandi, D. Permeability for intestinal absorption: Caco-2 assay and related issues. *Current Drug Metabol* **9**, 893-900 (2008).
- 10 Balimane, P. V., Han, Y. H. & Chong, S. Current industrial practices of assessing permeability and P-glycoprotein interaction. *The AAPS journal* **8**, E1-13, (2006).
- 11 Hidalgo, I. J., Raub, T. J. & Borchardt, R. T. Characterization of the human colon carcinoma cell line (Caco-2) as a model system for intestinal epithelial permeability. *Gastroenterology* **96**, 736-749 (1989).
- 12 Kratz, J. M., Teixeira, M. R., Koester, L. S. & Simoes, C. M. An HPLC-UV method for the measurement of permeability of marker drugs in the Caco-2 cell assay. *Brazil J Med Biol Res* **44**, 531-537 (2011).
- 13 Artursson, P. & Karlsson, J. Correlation between oral drug absorption in humans and apparent drug permeability coefficients in human intestinal epithelial (Caco-2) cells. *Biochem Biophys Res Commun* **175**, 880-885 (1991).
- 14 Elsbj, R., Surry, D. D., Smith, V. N. & Gray, A. J. Validation and application of Caco-2 assays for the in vitro evaluation of development candidate drugs as substrates or inhibitors of P-glycoprotein to support regulatory submissions. *Xenobio; FateForeign Comp Biol Sys* **38**, 1140-1164 (2008).
- 15 Matsson, P. *et al.* Exploring the role of different drug transport routes in permeability screening. *Journal of medicinal chemistry* **48**, 604-613 (2005).
- 16 Shin, S.-C., Bum, J.-P. & Choi, J.-S. Enhanced bioavailability by buccal administration of triamcinolone acetonide from the bioadhesive gels in rabbits. *Int J Pharm.* **209**, 37-43 (2000).
- 17 Zhang, Y., Huo, M., Zhou, J. & Xie, S. PKSolver: An add-in program for pharmacokinetic and pharmacodynamic data analysis in Microsoft Excel. *Comput Meth Progr Biomed* **99**, 306-314 (2010).
- 18 Liversidge, G. G. & Cundy, K. C. Particle size reduction for improvement of oral bioavailability of hydrophobic drugs, *Int J Pharm.* **125**, 91-97 (1995).
- 19 Sathigari, S. *et al.* Physicochemical Characterization of Efavirenz-Cyclodextrin Inclusion Complexes. *AAPS PharmSciTech* **10**, 81-87 (2009).
- 20 Mukne, A. P. & Nagarsenker, M. S. Triamterene-beta-cyclodextrin systems: preparation, characterization and in vivo evaluation. *AAPS PharmSciTech* **5**, E19 (2004).
- 21 Jug, M., Kos, I. & Bećirević-Laćan, M. The pH-dependent complexation between risperidone and hydroxypropyl- $\beta$ -cyclodextrin. *J Inclu Phenom Macro Chem* **64**, 163-171 (2009).
- 22 Omari, M. M. A., Zughul, M. B., Davies, J. E. D. & Badwan, A. A. Effect of Buffer Species on the Inclusion Complexation of Acidic Drug Celecoxib with Cyclodextrin in Solution. *J Inclu Phenom Macro Chem* **55**, 247-254 (2006).
- 23 Zeng, J., Ren, Y., Zhou, C., Yu, S. & Chen, W.-H. Preparation and physicochemical characteristics of the complex of edaravone with hydroxypropyl- $\beta$ -cyclodextrin. *Carbohydr Poly* **83**, 1101-1105 (2011).
- 24 Kiss, T. *et al.* [Cytotoxic examinations of various cyclodextrin derivatives on Caco-2 cells]. *Acta Pharma Hung* **77**, 150-154 (2007).
- 25 Kiss, T. *et al.* Evaluation of the cytotoxicity of beta-cyclodextrin derivatives: evidence for the role of cholesterol extraction. *Eur J Pharm Sci* **40**, 376-380 (2010).
- 26 Kiss, T. *et al.* Cytotoxicity of different types of methylated beta-cyclodextrins and ionic derivatives. *Pharmazie* **62**, 557-558 (2007).
- 27 Veiga, M. D., Diaz, P. J. & Ahsan, F. Interactions of griseofulvin with cyclodextrins in solid binary systems. *J Pharm Sci* **87** (1998).
- 28 Nakai, Y., el-Said Aboutaleb, A., Yamamoto, K., Saleh, S. I. & Ahmed, M. O. Study of the interaction of clobazam with cyclodextrins in solution and in the solid state. *Chem Pharm Bull (Tokyo)* **38**, 728-732 (1990).

- 29 Okawara, M., Tokudome, Y., Todo, H., Sugibayashi, K. & Hashimoto, F. Enhancement of diosgenin distribution in the skin by cyclodextrin complexation following oral administration. *Biolog Pharm Bul* **36**, 36-40 (2013).
- 30 Taupitz, T., Dressman, J. B. & Klein, S. New formulation approaches to improve solubility and drug release from fixed dose combinations: case examples pioglitazone/glimepiride and ezetimibe/simvastatin. *Eur J Pharm Biopharm* **84** (2013).
- 31 Taupitz, T., Dressman, J. B., Buchanan, C. M. & Klein, S. Cyclodextrin-water soluble polymer ternary complexes enhance the solubility and dissolution behaviour of poorly soluble drugs. Case example: itraconazole. *Eur J Pharm Biopharm* **83** (2013).
- 32 Jain, A., Singh, S. K., Singh, Y. & Singh, S. Development of lipid nanoparticles of diacerein, an antiosteoarthritic drug for enhancement in bioavailability and reduction in its side effects. *J Biomed Nanotech* **9**, 891-900 (2013).
- 33 Codruța M. Șoica<sup>1</sup>, C. I. P., Sorina Ciurlea, Rita Ambrus, Cristina Dehelean Physico-chemical and toxicological evaluations of betulin and betulinic acid interactions with hydrophilic cyclodextrins. *FARMACIA* **58(5)** (2010).
- 34 Shen, Y. *et al.* Effects of hydroxypropyl-beta-cyclodextrin on cell growth, activity, and integrity of steroid-transforming *Arthrobacter simplex* and *Mycobacterium sp.* *Appl Micro Biotech* **90**, 1995-2003 (2011).
- 35 Shen, Y., Liang, J., Li, H. & Wang, M. Hydroxypropyl-beta-cyclodextrin-mediated alterations in cell permeability, lipid and protein profiles of steroid-transforming *Arthrobacter simplex*. *Appl Micro Biotech* **99**, 387-397 (2015).
- 36 Artursson, P. & Karlsson, J. Correlation between oral drug absorption in humans and apparent drug permeability coefficients in human intestinal epithelial (Caco-2) cells. *Biochem Biophys Res Commun.* **175**, 880-885 (1991).
- 37 Yee, S. In vitro permeability across Caco-2 cells (colonic) can predict in vivo (small intestinal) absorption in man--fact or myth. *Pharm Res* **14**, 763-766 (1997).
- 38 Lin, S.-Z., Wouessidjewe, D., Poelman, M.-C. & Duchêne, D. Indomethacin and cyclodextrin complexes. *Int J Pharm* **69**, 211-219 (1991).
- 39 Guyot, M., Fawaz, F., Bildet, J., Bonini, F. & Lagueny, A. M. Physicochemical characterization and dissolution of norfloxacin/cyclodextrin inclusion compounds and PEG solid dispersions. *Int J Pharm* **123**, 53-63 (1995).
- 40 Soliman, O. A. E. *et al.* Amorphous spironolactone-hydroxypropylated cyclodextrin complexes with superior dissolution and oral bioavailability. *Int J Pharm* **149**, 73-83 (1997).
- 41 Sigfridsson, K., Forssén, S., Holländer, P., Skantze, U. & de Verdier, J. A formulation comparison, using a solution and different nanosuspensions of a poorly soluble compound. *Eur J Pharm Biopharm.* **67**, 540-547 (2007).